# MICROGRID RELIABILITY MODELING AND OPTIMAL PLANNING OF BATTERY ENERGY STORAGE SYSTEMS

BY

**MOHAMMED ATTA AHMED ABDULGALIL**

A Thesis Presented to the

DEANSHIP OF GRADUATE STUDIES

**KING FAHD UNIVERSITY OF PETROLEUM & MINERALS**

DHAHRAN, SAUDI ARABIA

In Partial Fulfillment of the
Requirements for the Degree of

# MASTER OF SCIENCE

**In**

**ELECTRICAL ENGINEERING**

**MAY 2018**

KING FAHD UNIVERSITY OF PETROLEUM & MINERALS
DHAHRAN 31261, SAUDI ARABIA

## DEANSHIP OF GRADUATE STUDIES

This thesis, written by **MOHAMMED ATTA AHMED ABDULGALIL** under the direction of his thesis adviser and approved by his thesis committee, has been presented to and accepted by the Dean of Graduate Studies, in partial fulfillment of the requirements for the degree of **MASTER OF SCIENCE IN ELECTRICAL ENGINEERING**.

**Thesis Committee**

Dr. Muhammad Khalid (Adviser)

Dr. Ibrahim El-Amin (Member)

Dr. Fahad Al-Ismail (Member)

Dr. Ali Al-Shaikhi
Department Chairman

Dr. Salam A. Zummo
Dean of Graduate Studies

5/12/2018
Date

عمادة الدراسات العليا
DEANSHIP OF GRADUATE STUDIES

*Dedication*

*This thesis is wholeheartedly dedicated to my beloved parents, who have been my source of inspiration and gave me everything to finish this study. They continually provide their moral, spiritual, emotional, and financial support.*

*To my siblings for their moral support and encouragement.*

*To my relatives and friends for their words of advice.*

*To the person who gave me strength when I thought of giving up.*

# ACKNOWLEDGMENTS

*I would first like to thank my thesis advisor, Dr. Muhammad Khalid. He took me from the first step of the research ladder. The door to his office was always open whenever I ran into a trouble spot or had a question about my research or writing. He consistently steered me in the right direction whenever he thought I needed it. He always encouraged me to publish papers and shared his experience with me to save my time and effort. He continuously supported and guided me from the first day.*

*In addition, I would also like to thank my thesis committee members, Dr. Ibrahim El-Amin, and Dr. Fahad Al-Ismail. They helped me a lot with suggesting new ideas to enhance the quality of this thesis and make it better for readers.*

*Moreover, I must express my very profound gratitude to my friends and colleagues, especially Mr. Mohamad Khater, Mr. Ayman Amin, Mr. Abubakr Elsayed, and Mr. Hosam Alharbi who are coauthors in some of my publications. I am gratefully indebted to them for their contributions in our joint papers.*

*Finally, I would like to thank the Electrical Engineering Department at King Fahd University of Petroleum & Minerals (KFUPM) for their support and using their facilities. Also, I would like to thank the Deanship of Scientific Research at KFUPM for their support.*

# TABLE OF CONTENTS

# LIST OF TABLES

# LIST OF FIGURES

# LIST OF SYMBOLS

| | |
|---|---|
| $\lambda$ | Failure rate of a component or system |
| $D_t$ | Demand at hour $t$ |
| $EC_{ESS}$ | Energy cost of ESS per MWh |
| $E_{ESS_t}$ | Energy stored in ESS at hour $t$ |
| $E^R_{ESS}$ | Rated energy of ESS |
| $F_t$ | Fixed cost of unit $i$ |
| $i$ | Unit index |
| $I$ | Set of units |
| $IC_{ESS}$ | Investment cost of ESS |
| $MDT_i$ | Minimum down time of unit $i$ |
| $MTBF$ | Mean time between failures of a component or system |
| $\lambda_{LP}$ | Failure rate at load point LP |
| $MTTF$ | Mean time to fail of a component or system |
| $MTTR$ | Mean time to repair of a component or system |
| $MUT_i$ | Minimum up time of unit $i$ |
| $NI$ | Number of units |

| | |
|---|---|
| $NT$ | Number of hours |
| $P_{i,t}$ | Power generated by unit $i$ at hour $t$ |
| $P_i^{max}$ | Maximum power of unit $i$ |
| $P_i^{min}$ | Minimum power of unit $i$ |
| $PC_{ESS}$ | Power cost of ESS per MW |
| $P_{M_t}$ | Power exchanged with the main grid |
| $\mu$ | Repair rate of a component or system |
| $P_M^{max}$ | Maximum exchanged power |
| $P_{ESS_t}$ | Power produced by ESS at hour $t$ |
| $P_{ESS}^R$ | Rated Power of ESS |
| $RD_i$ | Ramp down rate of unit $i$ |
| $r_i$ | Restoration time for interruption event $i$ |
| $RU_i$ | Ramp up rate of unit $i$ |
| $SD_i$ | Shut down cost of unit $i$ |
| $SU_i$ | Start up cost of unit $i$ |
| $t$ | Hour index |
| $T$ | Set of hours |
| $\gamma$ | Price of exchanged power per MW |
| $T_{i,t}^{OFF}$ | OFF time of unit $i$ at hour $t$ |
| $T_{i,t}^{ON}$ | ON time of unit $i$ at hour $t$ |
| $u_{i,t}$ | Commitment state of unit $i$ at hour $t$ |

| | |
|---|---|
| $U$ | Unavailability of a component or system |
| $V_i$ | Variable cost of unit $i$ |
| $y_{i,t}$ | Start up indicator of unit $i$ at hour $t$ |
| $z_{i,t}$ | Shut down indicator of unit $i$ at hour $t$ |
| $z_{i,t}$ | Shut down indicator of unit $i$ at hour $t$ |
| $s$ | Scenario index |
| $S$ | Set of scenarios |
| $A$ | Availability of a component or system |
| $NS$ | Number of scenarios |
| $P_{W_{t,s}}$ | Wind power at hour $t$ in scenario $s$ |
| $\rho_s$ | Probability of scenario $s$ |
| $P_W^{max}$ | Rated wind power |
| $v_{t,s}$ | Wind speed at hour $t$ in scenario $s$ |
| $v_{CI}$ | Cut-in wind speed |
| $v_{CO}$ | Cut-out wind speed |
| $v_R$ | Rated wind speed |
| $g$ | Index of thermal generating units |
| $t$ | Index of time |
| $C_i$ | Number of interrupted customers for event $i$ |
| $w$ | Index of wind turbine units |
| $i, j$ | Index of network buses |

| | |
|---|---|
| $\Omega_G$ | Set of all thermal generating units |
| $\Omega_G^i$ | Set of all thermal generating units connected to bus $i$ |
| $\Omega_l^i$ | Set of all buses connected to bus $i$ |
| $\Omega_B$ | Set of network buses |
| $\Omega_l$ | Set of network branches |
| $L_{i,t}$ | Electric power demand in bus $i$ at time $t$ (MW) |
| $b_g$ | Fuel cost coefficient of thermal unit $g$ ($) |
| $P_g^{min}$ | Minimum limits of power generation of thermal unit $g$ (MW) |
| $CMG_{ex}$ | Cost of microgrid related to exchanged power |
| $P_g^{max}$ | Maximum limits of power generation of thermal unit $g$ (MW) |
| $P_{ij}^{max}$ | Maximum power flow limits of branch connecting bus $i$ to bus $j$ (MW) |
| $P_{ij,t}$ | Active power flow of branch connecting bus $i$ to bus $j$ at time $t$ (MW) |
| $P_{g,t}$ | Active power generated by thermal unit $g$ at time $t$ (MW) |
| $P_{i,t}^w$ | Active power generated by wind turbine connected to bus $i$ at time $t$ (MW) |
| $OC$ | Total operating costs ($) |
| $\delta_{i,t}$ | Voltage angle in bus $i$ at time $t$ (rad) |
| $P_{i,t}^c$ | Charging power of ESS in bus $i$ at time $t$ (MW) |
| $P_{i,t}^d$ | Discharging power of ESS in bus $i$ at time $t$ (MW) |
| $RU_g$ | Ramp-up rate of thermal unit $g$ (MW/hr) |
| $CMG_{units}$ | Cost of microgrid related to its units |

| | |
|---|---|
| $RD_g$ | Ramp-down rate of thermal unit $g$ (MW/hr) |
| $\eta_c$ | Charging efficiency of ESS |
| $\eta_d$ | Discharging efficiency of ESS |
| $\Delta_t$ | Time step (hr) |
| $SOC_{i,t}$ | State of charge of ESS in bus $i$ at time $t$ (MWh) |
| $P^c_{i,min}$ | Minimum charging power of ESS in bus $i$ (MW) |
| $P^c_{i,max}$ | Maximum charging power of ESS in bus $i$ (MW) |
| $P^d_{i,min}$ | Minimum discharging power of ESS in bus $i$ (MW) |
| $P^d_{i,max}$ | Maximum discharging power of ESS in bus $i$ (MW) |
| $SOC_{i,min}$ | Minimum state of charge of ESS in bus $i$ (MWh) |
| $C_T$ | Total number of customers served |
| $VOLL$ | Value of loss of load ($/MWh) |
| $LS_{i,t}$ | Load shedding in bus $i$ at time $t$ (MW) |
| $VWC$ | Value of loss of wind ($/MWh) |
| $SOC_{i,max}$ | Maximum state of charge of ESS in bus $i$ (MWh) |
| $w_{i,t}$ | Availability of wind turbine connected to bus $i$ at time $t$ |
| $\Lambda^w_i$ | Capacity of wind turbine connected to bus $i$ (MW) |
| $P^{wc}_{i,t}$ | Curtailed power of wind turbine connected to bus $i$ at time $t$ (MW) |
| $x_{ij}$ | Reactance of branch connecting bus $i$ to bus $j$ ($\Omega$) |

# LIST OF ABBREVIATIONS

| | |
|---|---|
| ASAI | Average System Availability Index |
| ASUI | Average System Unavailability Index |
| BESS | Battery Energy Storage System |
| CAES | Compressed Air Energy Storage |
| CAIDI | Customer Average Interruption Duration Index |
| DP | Dynamic Programming |
| ESS | Energy Storage System |
| GA | Genetic Algorithm |
| GAMS | General Algebraic Modelling System |
| GWO | Grey Wolf Optimization |
| HESS | Hybrid Energy Storage System |
| LOLE | Loss of Load Expectation |
| LP | Linear Programming |
| MG | Microgrid |
| MILP | Mixed-Integer Linear Programming |
| MINLP | Mixed-Integer Non-Linear Programming |

| | |
|---|---|
| MPC | Model Predictive Control |
| MTBF | Mean Time between Failures |
| MTTF | Mean Time to Fail |
| MTTR | Mean Time to Repair |
| OPF | Optimal Power Flow |
| PSO | Particle Swarm Optimization |
| RBD | Reliability Block Diagram |
| RDG | Renewable Distributed Generation |
| RES | Renewable Energy Sources |
| RTS | Reliability Test System |
| SAIDI | System Average Interruption Frequency Index |
| SAIFI | System Average Interruption Duration Index |
| SEMS | Smart Energy Management System |
| SMES | Superconducting Magnetic Energy Storage System |

# THESIS ABSTRACT


| | |
|---|---|
| **NAME:** | Mohammed Atta Ahmed Abdulgalil |
| **TITLE OF STUDY:** | Microgrid Reliability Modeling and Optimal Planning of Battery Energy Storage Systems |
| **MAJOR FIELD:** | Electrical Engineering |
| **DATE OF DEGREE:** | May 2018 |



*Many technologies are being developed to reduce power generation costs and emissions. One of those technologies is an energy storage system (ESS). An ESS is a device that can capture the energy and then deliver it a later time for use. ESSs have many features including reducing generation, operation and maintenance costs, keeping the environment green and enhancing the reliability of the microgrid. ESSs are getting more attention due to the rapid increase in integrating renewable energy sources. This thesis discusses the ESSs in different fields in the field of power systems. Those fields include power system planning, operation, and reliability. To integrate an ESS with a microgrid, it must be optimally sized. This thesis proposes a technique to optimally size an ESS in a microgrid whether it is integrated with renewable energy sources or not. Also, two optimization approaches are used to size the ESS which is the deterministic*

*and probabilistic approaches. The probabilistic approach is used when uncertainty matters. After sizing the ESS, its capacity must be allocated and distributed optimally among the microgrid buses. This thesis proposed a technique to optimally allocate the ESS capacity using the DC optimal power flow method. Moreover, the optimal dispatch and power flow of microgrid generation units are formulated and studied to investigate the effects of integrating an ESS to a microgrid. Finally, the microgrid reliability is assessed in different cases to observe how an optimally sized ESS enhances its reliability regarding availability and cost.*

# ملخص الرسالة

**الاسم:** محمد عطا أحمد عبد الجليل

**عنوان الدراسة:** نمذجة اعتمادية شبكة كهربائية صغيرة والتخطيط المثالي لأنظمة تخزين الطاقة

**التخصص:** الهندسة الكهربائية

**تاريخ الدرجة العلمية:** مايو/أيار 2018

يتم تطوير العديد من التقنيات لتقليل تكاليف توليد الطاقة والانبعاثات. واحدة من تلك التقنيات هي نظام تخزين الطاقة. إن نظام تخزين الطاقة هو جهاز يمكنه تخزين الطاقة ثم توصيلها في وقت لاحق للاستخدام. يتميز نظام تخزين الطاقة بالعديد من الميزات بما في ذلك خفض تكاليف التوليد والتشغيل والصيانة، مع الحفاظ على نظافة البيئة وتعزيز اعتمادية الشبكة الكهربائية. تحظى أنظمة تخزين الطاقة باهتمام كبير نظرًا للزيادة السريعة في دمج مصادر الطاقة المتجددة. تناقش هذه الرسالة أنظمة تخزين الطاقة في مختلف المجالات في مجال أنظمة الطاقة. وتشمل هذه المجالات تخطيط نظام الطاقة والتشغيل والاعتمادية. لدمج نظام تخزين الطاقة مع شبكة كهربائية صغيرة، يجب أن يكون بحجمه المثالي. تقترح هذه الأطروحة تقنية لتحديد حجم نظام تخزين الطاقة بشكل مثالي في الشبكة الكهربائية الصغيرة سواء تم دمجها مع مصادر الطاقة المتجددة أم لا. أيضا، يتم استخدام طريقتين للتحسين في حجم نظام تخزين الطاقة وهما النهج الحتمي والنهج الاحتمالي. يستخدم النهج الاحتمالي عندما تكون الأمور غير مؤكدة. بعد تحديد الحجم المثالي لنظام تخزين الطاقة، يجب توزيع قدرته على النحو المثالي بين نقاط التوزيع في الشبكة الكهربائية. اقترحت هذه الأطروحة تقنية لتوزيع قدرة نظام تخزين الطاقة على نحو مثالي باستخدام طريقة تدفق الطاقة المثالي. وعلاوة على ذلك، يتم صياغة ودراسة التدفق المثالي لوحدات توليد الشبكة الكهربائية ودراستها للتحقق من آثار دمج نظام تخزين الطاقة مع الشبكة. وأخيرًا، يتم تقييم اعتمادية الشبكة الكهربائية في حالات مختلفة لمراقبة كيف تم تحسين اعتمادية الشبكة الكهربائية من ناحية التوفر والتكلفة بعد توصيلها بنظام تخزين الطاقة ذو الحجم المثالي.

# CHAPTER 1

# INTRODUCTION

## 1.1 Background and Motivation

Power systems are considered as the largest systems in the entire world. Also, there are several sizes of power systems. Microgrids are considered as a smaller size of power systems with low or medium voltage. Microgrids are defined as distribution systems in which a network of loads and distributed energy resources can operate connected to the main grid or isolated which is called the islanded mode [5]. One of the most significant advantages of the microgrids that they allow broad penetration of renewable energy resources to become the central generation element in this small power system. Renewable energy resources include wind turbines, solar cells, and hydropower.

Moreover, energy storage systems play an essential role in the microgrids being considered as a second generation and control element. Also, energy storage systems have economic benefits since they contribute to reducing the costs of generation [6]. Also, they store energy when the electricity prices are low and discharge when the

prices are high to increase the profits [7].

Energy storage systems are essential in microgrids because they store energy and supply it when it is needed. In the grid-connected mode, the energy storage system helps to provide the load demand when it becomes higher than the generation. In the islanded mode, where the microgrid is disconnected from the main grid, the energy storage system beside the distributed energy resources operate as voltage controller to regulate the microgrid voltage and share the local load [8]. Sizing an energy storage system has high importance and priority because of its cost and operations. Energy storage systems must be sized efficiently and with high reliability to do their intended function with the required capacity at the least possible cost during the specified time [9].

To reach this objective, a mathematical problem should be formulated. This problem is an optimization problem which has an objective function and constraints. All constraints are defined well including the reliability constraints such as loss of load expectation. In the problem formulation, it is a must to know that the investment cost increases with the size of the energy storage system linearly. On the other hand, the operation cost decreases with the size exponentially. The optimal solution of the problem is the least cost where the balance between the reliability enhancement and the cost optimization has been made [9].

The outcomes of this research can be applied in the renewable energy fields where microgrids depend on the renewable resources in generating the needed energy. This research can be used to help to reach the Saudi Vision 2030 as Saudi Arabia is planning to reduce the dependence on oil and rely on alternatives. So, this research will help

to improve the effectiveness of microgrids and the renewable resources used.

## 1.2 Objectives of Thesis

This thesis aims at closing some research gaps in its field. Those research gaps under investigation have been identified already, and several objectives have been defined to contribute to closing the research gaps. The objectives of this thesis are listed below.

1. Optimal sizing of an energy storage system to plan a microgrid for enhancing its reliability using the following techniques.
   (a) Deterministic optimization.
   (b) Stochastic optimization.
2. Optimal allocation of the optimally sized storage system.
3. Optimal dispatch of distributed generation units, wind farms and energy storage systems in power system operation.
4. Reliability assessment of microgrids with multiple distributed generations and hybrid energy storage.

## 1.3 Thesis Organization

The remainder of this thesis is organized as follows. Chapter 2 has extensive literature review about the research topic. Also, it describes the research gaps and how this thesis contributes to closing those gaps. Chapter 3 describes the optimal sizing of an

energy storage system to plan a microgrid for enhancing its reliability using deterministic and stochastic optimization approaches. The stochastic approach is considered when load uncertainty matters. Chapter 4 describes a technique to optimally size a storage system for microgrids connected to renewable energy sources. In this chapter, the optimal sizing is done under wind uncertainty. Chapter 5 describes the optimal allocation and distribution of the optimally sized storage system. Also, it discusses the optimal dispatch of the distributed generation units in the microgrid if a storage system exists in the system. Chapter 6 describes how to find the optimal power flow for microgrid connected to a storage system. Chapter 7 describes reliability modeling to assess the microgrid reliability using the reliability block diagram method. Finally, Chapter 8 concludes the thesis and has some recommendations and future works.

# CHAPTER 2

# LITERATURE REVIEW

## 2.1 Optimal Planning of Storage Systems

Traditional power systems are described as vertical and centralized systems [10] because their structure is vertical. Also, traditional power systems are unidirectional, and their stages are generation, transmission, and distribution stages. Those components are connected in order. So, the first stage is always a generation stage, and the last stage is always a distribution stage. On the other hand, centralized power systems such as microgrids have distributed generation units that are connected in the distribution level. Those units enhance the reliability of the system and reduce the total cost as well as ESSs. Another feature of microgrids is that they have controllable loads. All of those features make microgrids more efficient and flexible than traditional power systems.

Microgrids are small-scale intelligent power systems, and they are designed and built to mainly achieve the same purpose as large power systems, which is supplying power, electrical energy, to customers connected to them. Microgrids can be connected

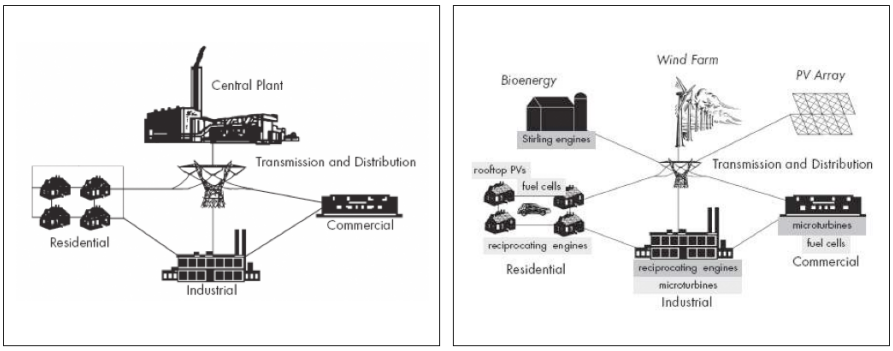


Figure 2.1: (a) Schematic of a centralized power system. (b) Schematic of a distributed power system [2]

.

to a main grid or islanded [10]. If a microgrid is connected to a main grid, it can exchange power through buying power from the main grid or selling to it. Microgrids have several features such as distributed generators, ESSs, and controllable loads. Those features make microgrids more flexible and efficient than traditional centralized power systems.

Figure 2.1 shows the difference between centralized power systems and distributed generation systems. Other reasons for building microgrids are lowering production cost, improving local reliability, reducing emissions, and enhancing power quality [11]. Being not centralized means that the reliability of a microgrid enhances because the different generation units are distributed within the microgrid. Also, microgrids are usually coupled with renewable energy sources, and those sources make the microgrid more economical than traditional power systems which depend on conventional generators. Integrating renewable energy sources with a microgrid reduces the production cost extremely because the operating cost of them are marginal and negligible compared with the conventional generators which cost regarding fuel cost. The renewable

energy sources are available without cost, but they only cost regarding investment and maintenance cost. [12] reviews the integration of renewable distributed generators into a distribution system. Another important component in a microgrid is the ESS. The storage technologies are improving, and their applications in microgrids are many [9]. For example, they contribute to support in case of an emergency load. Also, an ESS can provide the peak with energy in microgrids [13]. The ESSs are economic, and they reduce the cost as well as the renewable energy sources. Also, they charge energy in low-price periods and discharge in high-price periods [10]. This results in a more economical system for the suppliers. Incorporating renewable energy sources and ESSs enhance the reliability of a microgrid [14]. Smart Energy Management System (SEMS) is used to coordinate different components in a microgrid, such as renewable energy sources and ESS. The main objective of the SEMS is to generate and create appropriate set points for sources and storage systems to optimize power dispatch economically. Figure 2.5 represents a typical SEMS [15].

Smart grids are an intelligent type of microgrids, and they are bi-directional power and communication networks improving the reliability of an electric system. They have all stages found in a power system, and those stages are generation, transmission, and distribution stages. Also, they have energy storage systems (ESSs) which increase the reliability of a power system significantly. Also, an ESS decreases the total operating cost in a smart grid and saves a large portion of the fuel and maintenance costs. Smart grids could be small-scale or large-scale systems. Furthermore, smart grids are green, and they produce much fewer emissions than transitional power systems as well as microgrids.

The ESSs play important roles in microgrids as discussed. When thinking about integrating an ESS with a microgrid, sizing the ESS is firstly considered [13]. The optimal size of an ESS is the size that minimizes total cost of integrating an ESS in a microgrid. The total cost includes the investment cost and maintenance cost of an ESS, and the production and maintenance cost of the generation units. Also, if a microgrid is connected to a main grid, the cost and revenue of exchanged power are included. When the size of an ESS increases, the investment cost of ESS increases linearly and the operating cost of generation units in the same microgrid decreases exponentially [10]. The goal is to find the size costing the minimum cost [7]. Figure 2.2 shows how the size of an ESS vary with the investment and operating costs. Integrating an optimally sized ESS with a microgrid is so important. An oversized ESS results in a high capital cost whereas an undersized ESS may not be able to provide operational and economic benefits [10]. Optimal sizing of an ESS is done through one of the optimization methods. It can be sized using the mixed-integer linear programming (MILP) [13], mixed-integer non-linear programming (MINLP) [16], dynamic programming (DP) [17], particle swarm optimization (PSO) [18], two-stage stochastic programming [19], distributionally robust optimization [20], model predictive control (MPC) [21]. Optimization problems are either deterministic or probabilistic. If there is an uncertainty in the model, the optimization problem is called probabilistic, and the stochastic optimization or robust optimization could be used to find the optimal solution [19]. The heuristic algorithm is used to the optimal solution if there are uncertainties as well. [22] explains this algorithm and its application in finding the optimal operation of distributed generations in microgrids.

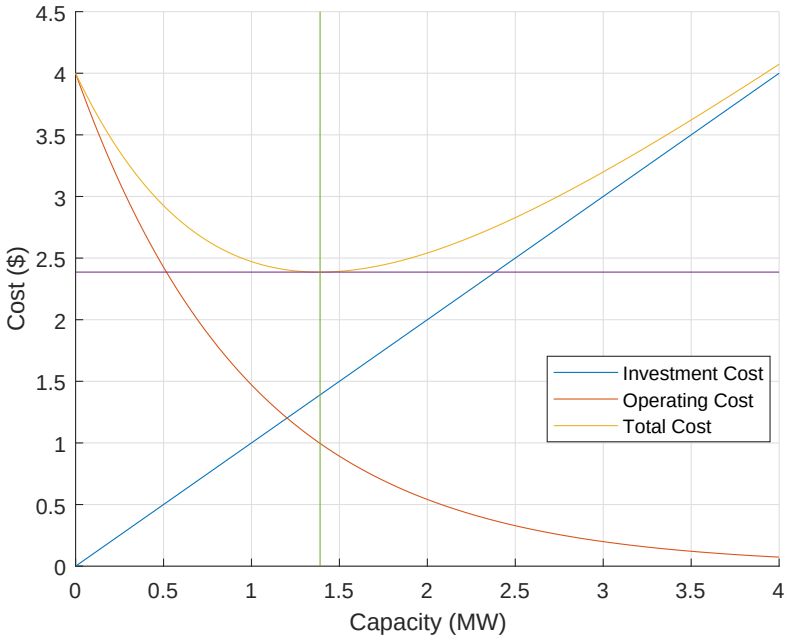


Figure 2.2: Cost vs ESS size

Moreover, the authors in [13] proposed an algorithm to size a battery energy battery system (BESS) in an islanded microgrid. The objective of this algorithm is the same objective in other optimization techniques, which is minimizing the cost. This algorithm is illustrated in details in [13] and Figure 2.3 illustrates this algorithm briefly.

The previously cited references have modeled systems that return the optimal size of an ESS regarding rated power and rated energy. In [23], a technique has been proposed to comprehensively size an ESS for microgrid applications, and this technique takes into account various factors. Those factors include distributed deployment and the number of charges and discharges cycles. This model returns the optimal size, technology, number, and the maximum limit for the depth of discharge. This model is solved using the MILP method after linearizing the model using the piecewise lin-

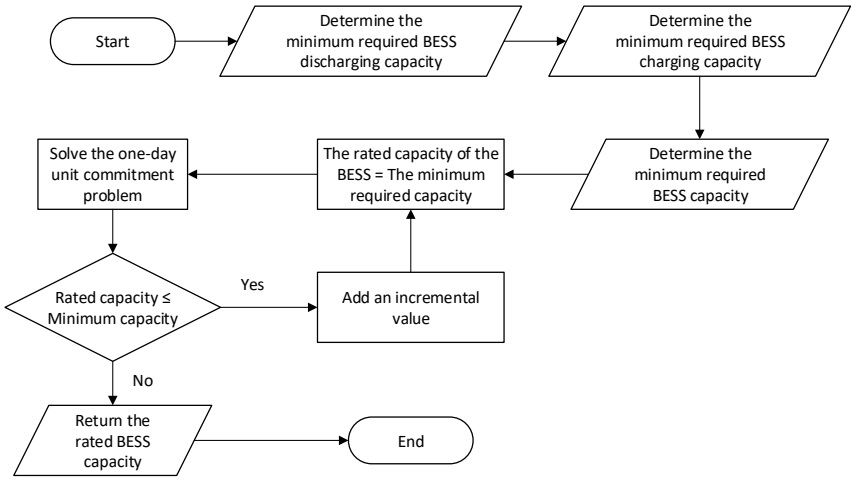


Figure 2.3: The flowchart of the proposed algorithm

earization technique. However, an essential factor is missing in this paper which is reliability, and this is what will be considered in this research.

The ESS is considered an attractive option to increase the flexibility of microgrid planning and operation. Also, as discussed, the ESSs absorb energy in case of low price or even excessive generation. Then, they return it during the high-price or low-generation periods [24]. There are many technologies related to the ESS. Some of them are superconducting magnetic energy storage system (SMES) [25], compressed air energy storage (CAES) [26], super-capacitor energy storage [27], pumped hydro storage [27], battery energy storage (BESS) [28], flywheel energy storage system [29], and power to gas storage method [30]. Furthermore, in power system optimization, there are many objective functions related to the ESS [24]. Some of the objective functions in ESS studies are compensate grid voltage fluctuations [25], overcome the destabilizing effect of instantaneous constant power loads in DC microgrids [27], prevention of transient under-frequency load shedding [31], reliability enhancement [32],

wind uncertainty management [33], fault ride through the support of grid-connected VSC HVDC-based offshore wind farms [29], phase balancing [34], wind curtailment reduction and congestion management [35], and active power loss payment minimization [36].

There are different types of ESS that have been developed, and some of them are available commercially. The other types are still under research and improvement. Those types differ in ESS technologies, and they have different characteristics. Figure 2.4 shows the power and discharge rate of the different ESS technologies. To compare those types with each other and select a specific ESS technology, there are several criteria. In [3], the authors compare the different characteristics as well as the advantages and disadvantages of the ESS technologies. The reliability a significant factor to judge a power system for both suppliers and customers. The reliability means the availability of electrical energy when it is needed at an economical cost. Many technologies have been developed to enhance the reliability of a power system. Integrating an ESS with a microgrid enhances its reliability [37] in addition to the other benefits that an ESS provides for a microgrid. ESSs increase the availability since they support in shaving the demand, especially at high peaks. Also, ESSs do not cost suppliers in production. Other reliability indices enhance as well with integrating an ESS with the microgrid. The reliability indices examined in this thesis are ASAI (Average System Availability Index), ASUI (Average System Unavailability Index), SAIFI (System Average Interruption Frequency Index), SAIDI (System Average Interruption Duration Index), and CAIDI (Customer Average Interruption Duration Index). There are other reliability indices considered in other papers, such as LOLE

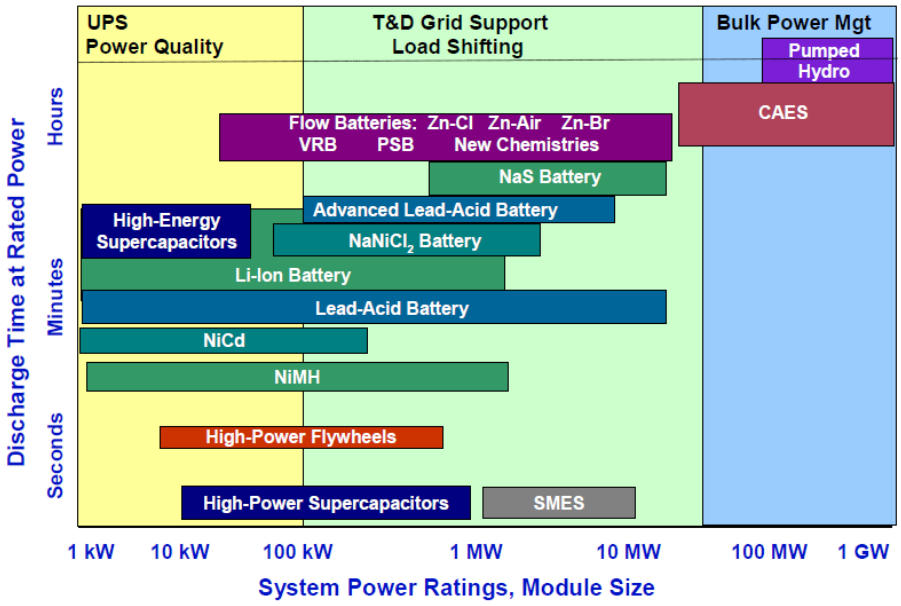


Figure 2.4: ESS technology comparison [3]

(Loss of Load Expectation) [38]. The missing gap in the previous research is that it did not study the impacts of integrating an optimally sized ESS with a microgrid on the reliability of that microgrid. However, it is mentioned in the literature that an ESS enhances the reliability without investigating and measuring this enhancement. Also, load uncertainty has not been considered previously in literature.

The technique used to solve the optimization problem is the MILP method. The purpose of this step is to calculate the rated power and rated energy of the needed ESS. Then, the unit commitment problem is solved to calculate the output power of each generation unit and the ESS to supply the load. Also, the total cost calculated in two cases for comparison. Those cases are (1) the microgrid without the ESS, and (2) the microgrid with the ESS. After that, the impacts of integrating the microgrid with the ESS on its reliability are analyzed. Also, load uncertainty is considered, and the optimization problem has been solved using two different approaches to optimally size

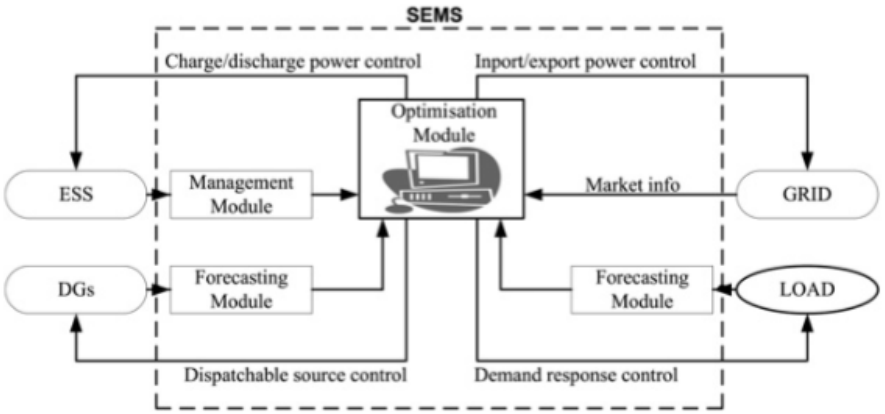


Figure 2.5: Schematic of inputs and outputs of SEMS

an ESS under load uncertainty. The most essential reliability indices are calculated in both cases for comparison and to investigate the results of integrating an ESS with a microgrid on its reliability. This thesis contributes to the literature by proposing a method to enhance the reliability of a power system by integrating an optimally sized ESS with it. This optimally sized ESS increases the availability of the power system and reduces the operating cost of it. So, the reliability of the power system enhances. This thesis aims to study and investigate the enhancement of microgrid reliability after integrating an optimally sized ESS with it. The reliability indices are calculated using the analytical method before and after integrating the ESS so that the reliability enhancement is investigated and measured. Moreover, load uncertainty has been included in the proposed model. This thesis aims to fill the research gap where this modeling has not been done. So, a power engineer could find out what technology or component can enhance the reliability of a power system more than the others depending on research case studies.

If there is an uncertainty in the model, the optimization problem is called proba-

bilistic, and the stochastic optimization or robust optimization could be used to find the optimal solution [19]. The heuristic algorithm is used to the optimal solution if there are uncertainties as well. [22] explains this algorithm and its application in finding the optimal operation of distributed generations in microgrids. Moreover, the authors in [13] proposed an algorithm to size a battery energy battery system (BESS) in an islanded microgrid. The objective of this algorithm is the same objective in other optimization techniques, which is minimizing the cost. This algorithm is illustrated in details in [13] and Figure 2.3 illustrates this algorithm briefly.

When renewable energy sources are integrated into a power system, the uncertainty matters because the output power from those sources cannot be determined accurately. Also, this depends mainly on forecasting which cannot be entirely accurate. Also, reliability gets more importance nowadays, and many technologies are being developed to enhance reliability. The missing gap in the literature is that there is no method to optimally size an ESS for a microgrid under wind uncertainties and reliability constraints. To find the optimal size of an ESS for a microgrid connected to renewable energy sources, the uncertainties must be taken into account. The problem, in this case, is called a probabilistic optimization problem which is different from deterministic optimization problems. Stochastic optimization and robust optimization are two methods used to optimize such problems. Stochastic programs are complicated and more difficult to formulate [39]. There are many solution approaches to solve stochastic optimization problems. Some of those approaches are decomposition, statistically based methods, stochastic decomposition, methods for multi-stage problems and computational illustration [39]. Another method to optimally size an ESS

connected to a system having renewable energy sources is generic sizing methodology using pinch analysis and design space [40].

This thesis discusses a technique to optimally size an ESS to be integrated into a microgrid connected to a main grid under wind uncertainties to enhance the microgrid reliability using the stochastic programming method. A lot of papers have been written about the optimal sizing of a storage system in a microgrid. However, sizing a storage system under generation uncertainties is missing. A new model has been proposed for optimal sizing of an energy storage system considering wind uncertainties in system modeling, which is critically essential in power systems containing intermittent renewable energy sources such as wind. Also, the proposed model is developed with an additional objective of enhancing system reliability particularly with the incorporation of reliability constraints. The reliability-constrained optimization problem under the influence of wind uncertainties is solved, and a comparison between two cases has been made to appreciate the effects of the optimally sized storage system on the microgrid reliability and to investigate how the microgrid reliability enhances.

## 2.2 Optimal Allocation of Storage Systems

The ESS is a necessary component in microgrids. A microgrid is a small-scale intelligent power system, and it is designed to function as a large power system, which is supplying electrical energy to customers. Microgrids can be connected to a main grid or islanded [10]. If a microgrid is connected to a main grid, it can exchange power by buying power from or selling to the main grid. Microgrids have several features

such as distributed generators, energy storage systems (ESS), and controllable loads. Those features make microgrids more flexible and efficient than traditional centralized power systems. Also, the existence of distributed renewable energy sources (RES), like solar photovoltaic or wind turbines, reduce the cost of energy delivered to customers, due to the high reduction in operation and maintenance cost.

For the stability and the effectiveness of microgrids, an ESS is critical. In the past few years, ESSs were improving, and their price was decreasing, and it is expected to continue due to the attention it is receiving from the industry and academia. ESSs provide the grid with so many benefits, such as improving control, load following, peak load management, power quality improvement, voltage and frequency stability, and reducing the effects of intermittency of solar photovoltaic and wind turbine. However, due to the relatively high cost of storage systems, the storage system capacity is optimally sized with the most accurate modeling to justify its economic viability and further prevent over or underutilization [9].

In the literature, the topic of ESS is regularly visited. Research regarding ESS integration to the power system has several applications. Several papers studied ESS in a buying-selling mode, where ESS is used for energy trading in all forms [41]–[43]. Another area of study is ESS providing auxiliary services. Lastly, ESS is integrated with renewable energy sources technologies transforming them to dispatchable and controllable generators capable of participating in the electricity market [44]–[46].

The authors in [7] reviewed the integration of renewable distributed generators into a distribution system, and how they lower the cost of supplying energy. They also discussed how renewable distributed generators are improving local reliability, power

quality, and system emission. In [46], the author proposes a probabilistic approach for sizing a battery storage system with the aim of mitigating the net load uncertainty associated with the off-grid wind power plant. A similar problem is solved in [44], the sizing and control strategy co-optimization for an existing IPV power plant is proposed and implemented. Global linear programming (LP) optimization algorithm is developed, where the optimal components sizing is computed directly in the same optimization as the operating management of the storage system. Furthermore, in [47], the objectives are tailored towards locating, sizing and operation of energy storage devices in distribution systems considering a typical load curve on a horizon of 24 hours is presented. Singh et al. [14] proposed that incorporating renewable energy sources and ESS's enhance the reliability of a microgrid. Also, an analytical approach to determine the reliability-constrained size of a backup storage unit in a power system is described in [48]. The backup could be in the form of electrical energy storage or fuel storage.

Based on the literature review, the knowledge gaps lie in the lack of models that correlate the DC optimal power flow and the required capacity and location of ESS. Also, there is a need for a long-term period of analysis taking into account ESS lifetime. Deriving this correlation will be an innovative tool to quantify the battery-to-wind plant's ratios that yield maximum system benefits.

This thesis proposes a methodology for accurately sizing and allocating an ESS in a microgrid. The novelty of the proposed approach is in developing a DC optimal power flow problem and solve it using mixed-integer linear programming (MILP) for a suggested test system with a wind turbine to optimally size and allocate an ESS,

which has not been tackled in the literature. This will enable the development of a more reliable microgrid. The ultimate contribution of this thesis is to maximize the benefits of integrating wind power in microgrid by sizing and allocating an ESS to accommodate all amounts of wind power and load fluctuations in hourly, daily, and seasonal horizons. The objective of the optimization problem is to minimize the total cost of the system which includes the investment cost of the storage system, and system operating and maintenance costs.

## 2.3 Optimal Power Flow of Microgrids

The increased penetration of renewable energy sources (RES) offers a sustainable future for the power system. However, the continuous increase in RES in microgrids (MG) and distribution systems as renewable distributed generation (RDG) poses great challenges for maintaining system stability and reliability due to the system reduced inertia. In addition, the intermittent nature of RES in general requires an increased amount of reserve as RES does not contribute to system reserve [49]. As a result, complete reliance of RES is infeasible and could increase the operational cost of a grid by requiring increased number of spinning-reserve generators. Therefore, requiring inefficient thermal generation units to pick up the load in case of sudden loss of generation. Consequently, if the requirement of adequate reserve in a power system with high RES penetration is not met, the risk of load shedding the blackouts increase significantly.

An increase in system reserve can be either supply-sided or demand-sided [50].

Demand-sided reserve could be interruptible loads. Supply-sided reserve could be thermal units in standby or energy storage systems (ESS). Increasing the number of thermal units in reserve means additional inefficient units that consume energy and money. Therefore, defeating the purpose of RES integration to the system. An emerging technology used to replace the requirement for spinning reserve is ESS. Adoption of this technology in a power grid facilitates increased integration of RES to a power system [51]. The integration of ESS to the grid requires optimally planning the operation to achieve full benefits of the system. In the planning phase, the optimal capacity and rating of ESS is determined. This study is based on long term variables and could be done without considering the power system technical constraints. An expansion of this study includes the placement of ESS in the grid. Furthermore, the optimal operation of ESS is achieved through two steps scheduling, day-ahead scheduling followed by real-time dispatch [52].

In the literature, the topic of ESS is frequently visited. Research regarding ESS integration to the power system has several applications. Several papers studied ESS in arbitrage mode, where ESS is used for energy trading in all forms. Another area of study for ESS integration is ESS providing ancillary services. Lastly, ESS is integrated with RES technologies transforming them to controllable generators capable of participating in the energy market.

[53] studied the applications of hybrid energy storage systems (HESS). In addition, it offered an overview of current ESS technologies. [51] researched the effects of RES penetration level of a power system relative to the ESS support needed. The study was done on distribution system and solved using stochastic mixed integer linear

programming. [54] proposed an operational scheme that will link between day-ahead planning and real-time operation to maximize the prosumer profit. The ESS system at hand operates in energy arbitrage mode [55]. [52] presented a single-step heuristic algorithm to solve optimal ESS scheduling and real-time dispatch. The method presented offered time-efficient simulations enabling the simulation of real-time dispatch. Another operation mode for ESS is frequency regulation and ancillary services presented in papers [56] and [57]. [58] studied the application of an ESS in a distribution network with high RES penetration to provide voltage regulation. The paper considered a coordinated control structure for ESS operation.

Generally, there are two main methods for optimal scheduling and operation of ESS present in the literature. Firstly, there are mathematical optimization techniques as opposed to heuristic optimization techniques. [59] presented optimal planning and operation of ESS using mixed integer second-order cone programming. The technique was applied on IEEE 34-bus distribution test feeder. [60] proposed a two-stage optimal dispatch strategy for ESS to manage RES generation fluctuation. The first stage is linked to day-ahead planning. It designed to counter RES generation fluctuation and increase the overall plant income. The second stage is linked to real-time dispatch. The second stage is designed to reduce the impact of forecast error on system operation.

[61] researched optimal scheduling of pumped hydro ESS. The research discussed the optimization problem with economy, reliability, emission, and water volume constraints. The problem model was provided then particles swarm optimization (PSO) was used in solving the optimization problem. [62] used grey wolf optimization (GWO) to solve a unit commitment problem without ESS. The research concluded that GWO

outperformed other methods in the literature. [55] used genetic algorithm (GA) to optimally allocate ESS in distribution networks for the purpose of load management. [63] used Cuckoo Search Algorithm for optimal allocation and sizing of DGs in the distribution system. the objective of the optimization problem was to minimize loss of load and improve the voltage profile in the system.

## 2.4 Reliability Assessment of Microgrids

With the increasing energy demands worldwide and the effects caused to the ecosystem of earth, such as Global warming and pollutions, by the traditional energy sources, such as oil, coal and nuclear, the need for the renewable energy sources increases. The increasing demands of energy worldwide, the capital cost reduction and the efficient renewable energy system were some of the motivations that help to propel the world to investigate, research and improve renewable energy to become more viable economic options. These renewable energy systems can be installed as an island, isolated from the grid, or integrated into the system but it can work independently as a microgrid [7]. There are many renewable energy sources that may be considered in a network to operate as distributed generation. The diversity of many sources of renewable energy can help improve the reliability of a system. Since the reliability of renewable energy sources due to the uncertainty of the availability in the energy sources, due to clouds in case of solar panels or reduction in wind speed in case of wind farm, were an issue in microgrid, introducing hybrid Energy Storage Systems (ESS) to microgrid can increase the efficiency and reliability of microgrid [9]. Energy storage systems came

as solutions to many issues faced the microgrid system reliability and cost-effective. Energy storage system can store the excess energy of microgrid during off-peak hours of the microgrid and provide it back to the microgrid when the energy source of renewable energy is unavailable or insufficient to cover the load demand. In which will result in the improvement of the reliability indices of the microgrid and reduce the loss of load probability, the loss of load expectation, and reduce the load shedding in which will help to reduce the losses of the microgrid. Also, the energy storage system can prolong the lifetime of the system by combining between high energy density system and high-power density system [64]. This will result in reducing the loading on the high energy density system in which will prolong the lifetime of an energy storage system and increases the reliability of a microgrid system. Also, it will reduce the costs of maintenance and operation of the system, which in turn affects the outcomes of the system and increase the benefits and the returns of the system. Also, it may help to meet the microgrid peak load and defer from the need of additional microgrid by stoning energy during off-peak hours of microgrid or from the networks during off-peak hours and provided it to the microgrid when it is required. In general, the optimum solution of the energy storage system in which will increase the reliability of the microgrid may not be the large and expensive one. By studying and analyzing a microgrid and its distributed generations either by installing renewable energy systems only or combined with traditional generation, an optimum energy storage system can be determined [65].

The number of microgrids is increasing, and their importance is increasing as well due to their operational and economic benefits. Some of the components of the

microgrids are distributed generations and storage systems. Some of the types of storage systems are battery energy storage systems (BESS) and supercapacitors [66]. The combination of more than one type of storage system is called a hybrid storage system. Distributed generations make a microgrid more reliable than a centralized power system. Also, storage systems enhance the reliability of microgrids regarding availability and costs. The purpose of this paper is to assess the reliability of a chosen microgrid that has distributed generations using the Reliability Block Diagram (RBD) and Monte Carlo simulation [17].

There are two approaches to assessing the reliability of a system; one is the direct analytical method, and the other is a simulation method. The behavior of a system in real time has a random nature. Therefore, the system will have different mean time to fail, mean time to repair and mean downtime to a certain degree. The reliability indices of a system can be estimated by collecting data on failure time and repair time. Monte Carlo method can mimic the failure time and repair time using the probability distribution of each component in the system to simulate the behavior of the entire system. Monte Carlo's method is a computer-based algorithm using random sampling to obtain a numerical result. The flowchart of this method is shown in Figure 2.6.

This thesis aims at:

- Assessing the reliability of a microgrid with distributed generations and hybrid storage Using RBD technique.
- Comparing the microgrid in three different cases.

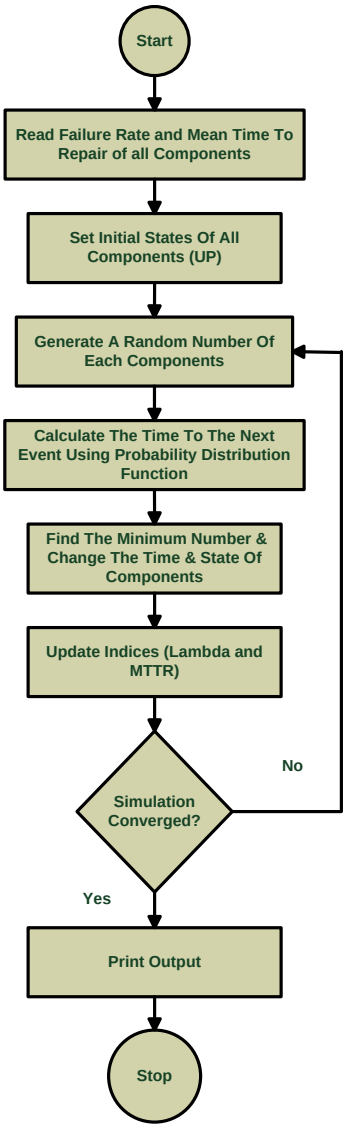


Figure 2.6: Flowchart of Monte Carlo's Simulation

# CHAPTER 3

# STORAGE SYSTEM PLANNING WITHOUT RENEWABLE ENERGY

## 3.1 Motivation

Reliability is one of the most important factors to judge a power system. So, assessing reliability is an important task in power system planning. Many techniques have been developed to enhance the reliability of a power system. Some of those techniques depend on integrating new components, and other techniques depend on changing some characteristics of existing components. One of the techniques depending on integrating new components is to integrate an energy storage system (ESS) with a power system. If the ESS is optimally sized to minimize the investment and operating cost, it enhances the reliability of the power system with a noticeable difference.

This chapter illustrates how to optimally size an ESS to be integrated with a grid-connected microgrid using the mixed-integer linear programming (MILP) method. Moreover, load uncertainty is considered, and the optimization problem is solved using two different approaches to size the ESS optimally. Simulation results depict the effectiveness of the proposed approach.

## 3.2 Problem Formulation

The problem in this chapter consists of two parts. Those parts are system modeling and optimal sizing of an ESS. In this section, the equations of both parts are formulated Subsection 3.2.1 and 3.2.2, respectively.

### 3.2.1 System Modeling

The system under study is an ESS, and it is modeled by some constraints. ESS constraints are the constraints limiting the charged and discharged power of the ESS. Also, they are used to model the ESS. The equation to calculate the stored energy at a specific hour is formulated in (3.1). The stored energy is called the state of charge, and there are methods developed to optimize it [67]. Also, the state of charge depends on the charging and discharging efficiencies. The charging or discharging powers might not be fully charged or discharged due to manufacturer limitations.

$$E_{ESS_t} = E_{ESS_{t-1}} + (P^c_{ESS_t}\eta_c - \frac{P^d_{ESS_t}}{\eta_d})\Delta_t \quad \forall t \in T \tag{3.1}$$

The first constraint is the limits of the power of the ESS. This power is limited by

the rated power of the ESS. Also, when the ESS charges, it is considered as a load and the power produced by the ESS is negative in this case. Moreover, when the ESS discharges, it is considered as a generation unit and the power produced by the ESS is positive in this case. This constraint is formulated in (3.2).

$$-P^R_{ESS} \leq P_{ESS_t} \leq P^R_{ESS} \quad \forall t \in T \tag{3.2}$$

The stored energy in the ESS is limited by its rated energy. Of course, the stored energy is always positive. This constraint is formulated in (3.3).

$$0 \leq E_{ESS_t} \leq E^R_{ESS} \quad \forall t \in T \tag{3.3}$$

In (3.3), $E_{ESS_t}$ is the energy stored in the ESS at hour $t$.

In (3.1), $P^c_{ESS_t}$ is the ESS charging power, $P^d_{ESS_t}$ is the ESS discharging power, $\eta_c$ and $\eta_d$ are the charging and discharging efficiencies, respectively.

The ESS output power is calculated as illustrated in (3.4).

$$P_{ESS_t} = P^c_{ESS_t} - P^d_{ESS_t} \quad \forall t \in T \tag{3.4}$$

### 3.2.2 Optimal Sizing of an ESS

The problem that this chapter aims to solve is the high operating costs in power systems and the interruptions which customers face. Many technologies have been developed to reduce operation costs and interruptions. One of them is the energy storage system. In this chapter, a method has been proposed to optimally size a stor-

age system under reliability constraints and load uncertainty to minimize the costs and enhance the reliability. As mentioned in the introduction, oversized ESSs cost more than needed while undersized ESSs might not be sufficient to provide the load. The optimally sized ESS has the minimum cost, and it is sufficient to provide the load. Regarding microgrid reliability, enhancing reliability leads to reducing the interruptions at the end of the day. The ESS is preferable over other systems capable of enhancing the microgrid reliability due to its relatively cheap investment cost compared with other systems. The optimal sizing problem is solved using the MILP technique. To model this problem, the unit commitment problem has to be modeled first. Then, the ESS constraints are added to the problem. The unit commitment problem is illustrated in [68] and [7], and the ESS constraints are illustrated in [7]. This optimization problem has been modeled and solved in GAMS (General Algebraic Modeling System). Modeling the problem in GAMS language is explained in [69] and [24].

**Objective Function**

The objective of the optimization problem is to minimize the total cost. The total cost of this problem includes the production cost of generating units, electricity cost and revenue from exchanging with the main grid, and the investment cost and of the ESS. The objective function of the optimal sizing of ESS for a given horizon is proposed in (3.5).

$$Min\ CMG_{units} + CMG_{ex} + IC_{ESS} \tag{3.5}$$

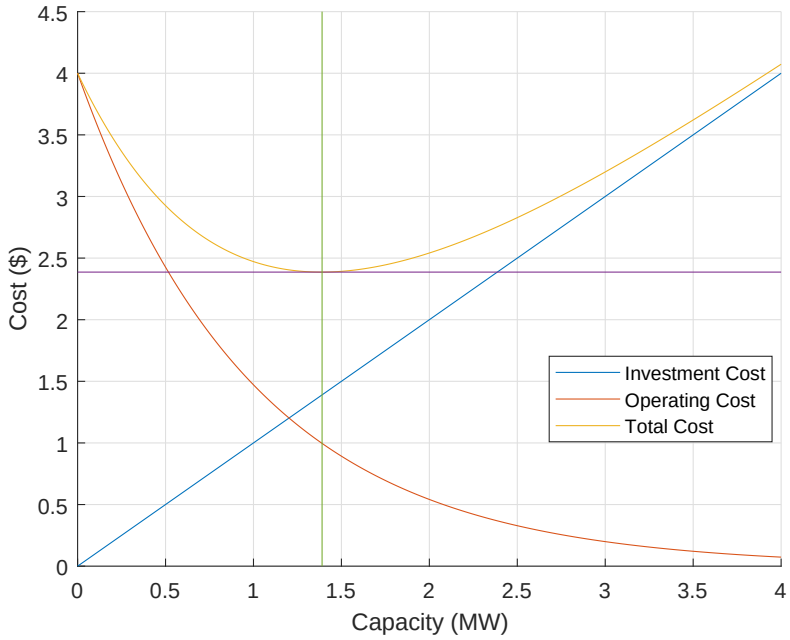


Figure 3.1: Cost vs ESS size

In (3.5), $CMG_{units}$ is the cost of microgrid related to its units, $CMG_{ex}$ is the cost of microgrid related to the exchanged power with the main grid, and $IC_{ESS}$ is the investment cost of the ESS.

The equation of cost related to the units in the microgrid is formulated in (3.6). The variables $u$, $y$, and $z$ are binary variables which can be either 1 or 0. These values indicate if the unit $i$ at hour $t$ is committed, started up, and shut down, respectively. This is why the integer constraint is needed in this problem. The fixed cost of unit $i$, $F$, is fixed if the unit $i$ is committed. On the other hand, the variable cost of unit $i$, $V$, is variable and it depends on the output power generated by the unit $i$. The cost function is assumed to be linear in this problem. Thus, the MILP is applicable here. There is no limitation in solving the linearized model. The same technique can be applied to the quadratic form of the cost function, and this model can be solved

using the mixed-integer non-linear programming (MINLP).

$$CMG_{units} = \sum_{t=1}^{NT} \sum_{i=1}^{NI} [F_i u_{i,t} + V_i P_{i,t} + SU_i y_{i,t} + SD_i z_{i,t}] \tag{3.6}$$

In (3.6), $i$ is the unit index, $NI$ is the number of units, $t$ is the hour index, $NT$ is the number of hours, $F_i$ is the fixed cost or no-load cost of unit $i$, $V_i$ is the variable cost of unit $i$ and it is related to the output power of unit $i$, $P_{i,t}$ is the output power of unit $i$ at hour $t$, $SU_i$ is the start up cost of unit $i$ and $SD_i$ is the shut down cost of unit $i$. $u_{i,t}$, $y_{i,t}$, and $z_{i,t}$ are binary variables represent the commitment state of unit $i$ at hour $t$, start up indicator of unit $i$ at hour $t$ and shut down indicator of unit $i$ at hour $t$, respectively.

The equation of cost related to the exchanged power between the microgrid and the main grid is formulated in (3.7). This cost is positive if the electricity is bought from the main grid, and it is negative if it is sold to the main grid.

$$CMG_{ex} = \sum_{t=1}^{NT} \rho P_{M_t} \tag{3.7}$$

In (3.7), $\rho$ is electricity price per one megawatt of power bought from or sold to the main grid and $P_{M_t}$ is the exchanged power between the microgrid and main grid at hour $t$. The sign convention in $P_{M_t}$ is that it is positive when the power flows from the main grid to the microgrid and it is negative when the power flows from the microgrid to the main grid.

The equation of investment cost of the ESS is formulated in (3.8). The unknowns

in this equation are the rated power of the ESS and the rated energy of it.

$$IC_{ESS} = PC_{ESS}\ P^{R}_{ESS} + EC_{ESS}\ E^{R}_{ESS} \tag{3.8}$$

In (3.8), $PC_{ESS}$ is the power cost of the ESS per one megawatt, $P^{R}_{ESS}$ is the rated power of the ESS, $EC_{ESS}$ is the energy cost of the ESS per one-megawatt hour, and $E^{R}_{ESS}$ is the rated energy of the ESS.

**System Constraints**

System constraints are the constraints related to the total output power in the microgrid, and they limit the output power. The main constraint among microgrid constraints is the balance equation. The total output power produced by the generating units, the ESS, and bought from the main grid must be at least equal to the demand at every hour. The reserve is usually added to the balance equation to overcome the continuous load variations so that the output power must be equal to the summation of demand and reserve at every hour. Also, the emissions constraint [70] is sometimes added as well in multi-objective unit commitment problems and the objectives of this kind of problems are to minimize both total costs of generated power and emissions produced by generation units [24]. In this chapter, the balance equation with demand is considered. This constraint is formulated in (3.9).

$$\sum_{i=1}^{NI}[P_{i,t} + P_{ESS_t} + P_{M_t}] = D_t \quad \forall t \in T \tag{3.9}$$

In (3.9), $P_{ESS_t}$ is the power stored to or produced bt the ESS at hour $t$, $D_t$ is the demand at hour $t$ and $T$ is the set of hours. The sign convention in $P_{ESS_t}$ is that it is positive when it is produced and negative when it is stored.

Another important constraint related to the microgrid is limiting the power exchanged between the main grid and microgrid. This power depends on the capacity of the transmission line connecting the microgrid to the main grid. The sign convention of the exchanged power is negative for the power exported to the main grid and positive for the power imported from the main grid. This constraint is formulated in (3.10).

$$-P_M^{max} \leq P_{M_t} \leq P_M^{max} \quad \forall t \in T \tag{3.10}$$

In (3.10), $P_M^{max}$ is the maximum capacity of the transmission line connecting between the microgrid and main grid.

**Generation Units Constraints**

Generation units constraints are the constraints that limit the output power of each generation unit, and they reflect its characteristics. Also, these constraints model the generation units. Each generation unit has a minimum limit of power to operate with stability. Also, each generation unit has a maximum limit that cannot be exceeded. This constraint is formulated in (3.11). Multiplying the minimum and maximum limits by the commitment state means that if a generation unit is OFF, the output power of this unit is zero.

$$P_i^{min} u_{i,t} \leq P_{i,t} \leq P_i^{max} u_{i,t} \quad \forall i \in I, \forall t \in T \tag{3.11}$$

In (3.11), $P_i^{min}$ is the minimum power that can be produced by unit $i$, $P_i^{max}$ is the maximum power that can be produced by unit $i$, and $I$ is the set of units.

Moreover, increasing or decreasing the output power of a generation unit are limited by two constant values which are the ramp up rate and ramp down rate, respectively. These constraints are formulated in (3.12) and (3.13), respectively.

$$P_{i,t} - P_{i,t-1} \leq RU_i \quad \forall i \in I, \forall t \in T \tag{3.12}$$

In (3.12), $RU_i$ is the ramp up rate of unit $i$.

$$P_{i,t-1} - P_{i,t} \leq RD_i \quad \forall i \in I, \forall t \in T \tag{3.13}$$

In (3.13), $RD_i$ is the ramp down rate of unit $i$.

When a generation unit starts up, it has to be ON for some time before it shuts down. This time is known as the minimum up time. Also, when a generation unit shuts down, it has to be OFF for some time before it starts up. This time is known as the minimum down time. These two constraints are formulated in (3.14) and (3.15), respectively.

$$T_{i,t}^{ON} \geq MUT_i[u_{i,t} - u_{i,t-1}] \quad \forall i \in I, \forall t \in T \tag{3.14}$$

In (3.14), $T_{i,t}^{ON}$ is the ON time of unit $i$ at hour $t$ and $MUT_i$ is the minimum up time of unit $i$.

$$T_{i,t}^{OFF} \geq MDT_i[u_{i,t-1} - u_{i,t}] \quad \forall i \in I, \forall t \in T \tag{3.15}$$

In (3.15), $T_{i,t}^{OFF}$ is the OFF time of unit $i$ at hour $t$ and $MDT_i$ is the minimum down time of unit $i$.

The generation unit cannot start up and shut down at the same time. This is a logic constraint and it is modeled in (3.16).

$$y_{i,t} - z_{i,t} = u_{i,t} - u_{i,t-1} \quad \forall i \in I, \forall t \in T \tag{3.16}$$

### 3.2.3 Reliability Constraints

Some reliability constraints are introduced to guarantee fewer interruptions and unavailability. In this chapter, the proposed reliability constraints are as illustrated in (3.17) and (3.18).

$$SAIFI \leq SAIFI_{Limit} \tag{3.17}$$

$$SAIDI \leq SAIDI_{Limit} \tag{3.18}$$

### 3.2.4 Uncertainty Modeling

To model the wind uncertainty, multiple load profiles will be considered. Different probabilities will be assigned to those profiles, and the summation of these probabilities must be equal to 1. Then, each probability will be multiplied with its corresponding load profile. The summation of those products will form a new profile that will be used in solving the optimal sizing problem. This solution will be compared to the

solution of each profile to justify solving the problem using this method when there are uncertainties in the optimization problem. The methodology of optimal sizing under wind uncertainty is illustrated and generalized in Algorithm 1.

**Algorithm 1** Proposed algorithm of optimal sizing of ESS

**function** SP_SIZING($n, S, P$) ▷ Where n - number of scenarios, S - array of all scenarios, P - vector of all scenario probabilities
    $n$ = number of scenarios
    **for** $i = 1$ to $n$ **do**
        $S[i]$ = scenario profile
        $P[i]$ = scenario probability
    **end for**
    **if** $\sum_{i=1}^{n} P[i] > 1$ **then**
        print: sum of probabilities is greater than 1
        Stop
    **else**
        $A = \sum_{i=1}^{n} P[i]S[i]$ ▷ Where A - vector of scenarios multiplied by their corresponding probabilities
    **end if**
    **for** $i = 1$ to $n$ **do**
        Optimally size $S[i]$
    **end for**
    Optimally size $A$
    Compare the results
**end function**

Another approach is used as well to calculate the optimal size of an ESS under load uncertainties. The algorithm of this method is shown in Algorithm 2. This method might give a more economic solution. Thus, the optimally sized ESS in this method might cost less than the previously proposed method.

**Algorithm 2** Another algorithm of optimal sizing of ESS

**function** SP_SIZING($n, S, Pr$) ▷ Where n - number of scenarios, S - array of all scenarios, Pr - vector of all scenario probabilities
    $n$ = number of scenarios
    **for** $i = 1$ to $n$ **do**
        $S[i]$ = scenario profile
        $Pr[i]$ = scenario probability
    **end for**
    **if** $\sum_{i=1}^{n} Pr[i] > 1$ **then**
        print: sum of probabilities is greater than 1
        Stop
    **else**
        Find $P_{ESS}[i]$ ▷ Where $P_{ESS}[i]$ - optimally sized ESS power for all scenarios separately
        Find $E_{ESS}[i]$ ▷ Where $E_{ESS}[i]$ - optimally sized ESS energy for all scenarios separately
        $P^{ESS} = \sum_{i=1}^{n} P_{ESS}[i]Pr[i]$ ▷ Where $P^{ESS}$ - normalized optimal size ESS power
        $E^{ESS} = \sum_{i=1}^{n} E_{ESS}[i]Pr[i]$ ▷ Where $E^{ESS}$ - normalized optimal size ESS energy
    **end if**
    **for** $i = 1$ to $n$ **do**
        Optimally size $S[i]$
    **end for**
    Compare the results
**end function**

## 3.3 A Case Study

A microgrid connected to a main grid is considered to perform a case study for the optimal sizing of an ESS. The case study is presented with its data. The results are introduced and discussed in Section 3.4. The system that will be studied consists of three generation units. The generation units in this case study are assumed to be distributed generators. All generators and load are assumed to be connected to the same bus without a transmission network for generalization. The effects of the transmission network are negligible. The unit commitment problem is solved for a scheduling horizon of two years. The load data has been taken from the IEEE Reliability Test System (RTS-96) [71] for the first year. For the second year, the load has increased by %5. The reserve and emission constraint are not considered in this case study. Table 3.1 shows the characteristics of the three generation units. The characteristics of the generation units except for the minimum up time and minimum down time are from [68]. The minimum up time and minimum down time are assumed to be unity in this case study. Table 3.2 represents the values of the other parameters used in this model. Figure 3.2 shows the load curve and load duration curve during the two years. The limits of SAIFI and SAIDI have been considered to be 1.00E-10. The ESS charging and discharging efficiencies are assumed to be unity.

The unit commitment problem of the microgrid is solved for a two-year horizon before and after integrating the ESS to calculate the output power of each generation unit, exchanged power with the main grid, and the power taking by the ESS or produced by it in the second case. Moreover, the probabilistic case is solved using the

Table 3.1: Characteristics of generation units

| Unit No. | Fixed Cost ($) | Variable Cost ($/MW) | Start Up Cost ($) | Shut Down Cost ($) | Min. Capacity (MW) |
|---|---|---|---|---|---|
| 1 | 9 | 20 | 40 | 20 | 5 |
| 2 | 7 | 18 | 30 | 20 | 3 |
| 3 | 5 | 15 | 20 | 20 | 2 |
| Unit No. | Max. Capacity (MW) | Ramp Down Rate (MW/h) | Ramp Up Rate (MW/h) | Min. Down Time (h) | Min. Up Time (h) |
| 1 | 20 | 15 | 15 | 1 | 1 |
| 2 | 30 | 15 | 15 | 1 | 1 |
| 3 | 40 | 20 | 20 | 1 | 1 |

Table 3.2: Values of other model parameters

| Parameter | $PC_{ESS}$ | $EC_{ESS}$ | $\rho$ | $P_M^{max}$ |
|---|---|---|---|---|
| Value | $1200 | $300 | $20 | 10 MW |

two algorithms proposed in 1 and 2 to illustrate how an ESS is optimally sized under load uncertainty. Three extra load profiles have been created by adding some noise to the RTS load. Figure 3.3 shows all load profiles during the first twenty-four hours. The probability of the RTS profile has been assumed to be 0.6, and the probability of each scenario of the other three scenarios is 0.2. The optimization problem has been written in GAMS (General Algebraic Modeling System) language [72] and has been simulated in the NEOS Server [73] which is a free internet-based service for solving numerical optimization problems.

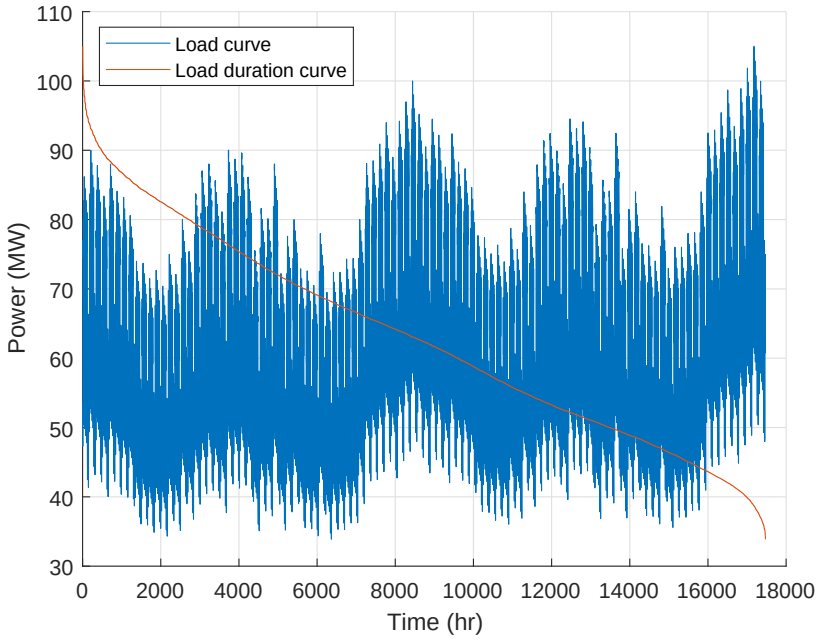


Figure 3.2: Load curve and load duration curve

## 3.4 Results and Discussions

The unit commitment problem has been solved using the MILP method to find the optimal size of the ESS which minimizes the total cost. The rated power of the ESS has been found to be 20 MW, and the rated energy is 214 MWh. The investment cost of the ESS is $88,200. For the first twenty-four hours, Figure 3.4 shows the solution of the unit commitment problem before integrating the microgrid with the ESS, and Figure 3.5 shows the solution of the unit commitment problem after calculating the optimal size of the ESS and integrating it with the microgrid. Those two figures represent the positive power only, which means that they do not represent the power in case of charging the ESS and in case of selling power to the main grid as well. The two variables related to the produced power from the ESS and exchanged power with the main grid are shown in Figure 3.6 with their negative values. The ESS acts like

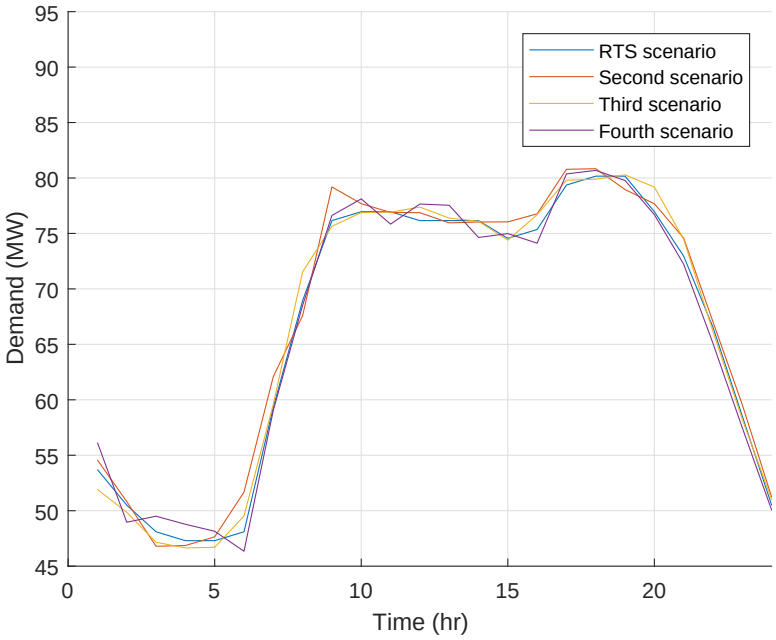


Figure 3.3: Load scenarios during the first twenty-four hours

a load when it charges and acts like a generator when it discharges. For the ESS to produce energy, it must have stored energy. Figure 3.7 shows the quantities of the stored energy during the first twenty-four hours.

The most expensive generation unit, which is Unit 1, is working at a low level when the ESS in not integrated as shown in Figure 3.4 and it is not working for most times when the ESS is integrated as shown in Figure 3.5. The ESS had made the microgrid more reliable economically and saved a portion of the production cost when it worked instead of Unit 1.

When uncertainty matters, stochastic optimization must be used to find the optimal size of an ESS. Algorithms 1 and 2 have been used as Approaches 1 and 2 in Table 3.3, respectively. In Approach 1, a new load profile has been formed, and the proposed method has been used to solve the optimization problem with this profile

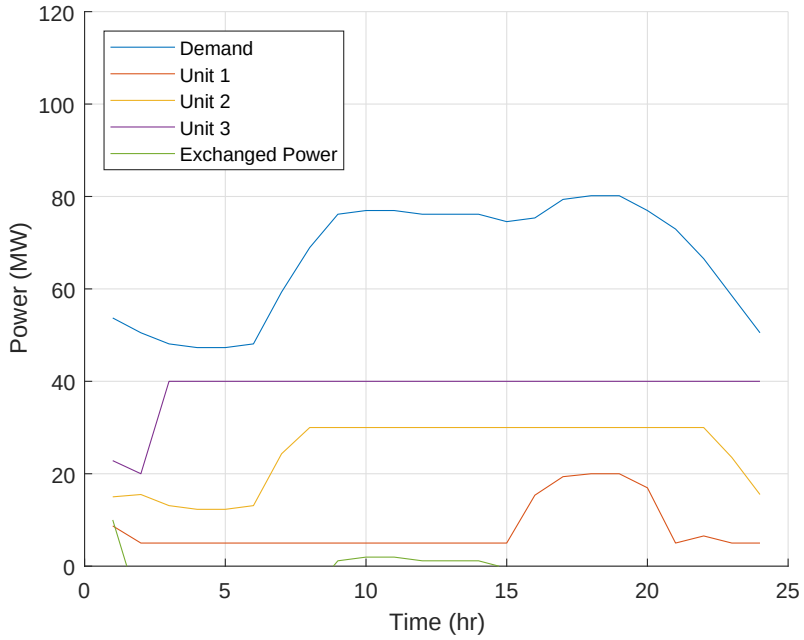


Figure 3.4: Economic dispatch without ESS

while all scenarios must be solved separately to form the decision variables later in Approach 2. The solution of Approach 2 is more economic, and the investment cost is less than Approach 1. This solution reflects many scenarios and is considered the optimal solution when uncertainty matters.

## 3.5 Summary

This chapter has presented a technique to optimally size a battery energy storage for a grid-connected microgrid subjected to practical reliability constraints. The unit commitment problem has been solved using the mixed-integer linear programming method. Moreover, load uncertainty has been considered, and stochastic optimization has been solved using two approaches. The purpose of integrating an optimally sized storage system with the microgrid is to enhance the reliability of the microgrid. Inte-

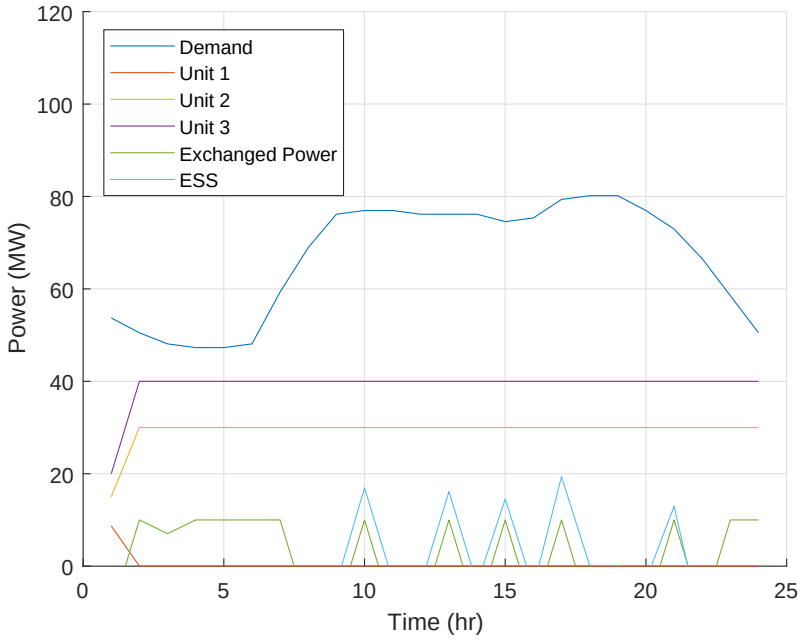


Figure 3.5: Economic dispatch with ESS

grating the ESS with the microgrid has decreased the net cost although this cost in the case of integrating the ESS includes the investment cost of building and establishing the ESS, which shows the economical feasibility of the system.

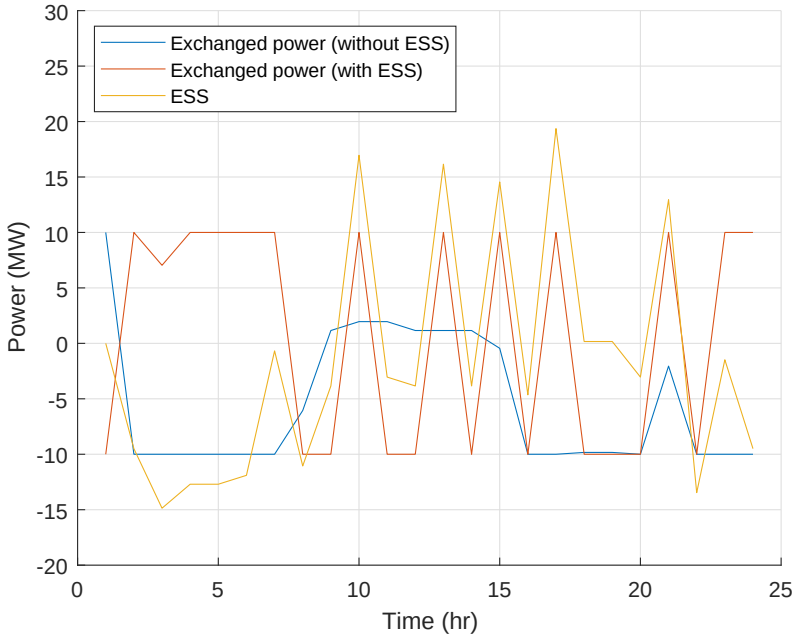


Figure 3.6: ESS power and exchanged power with negative values

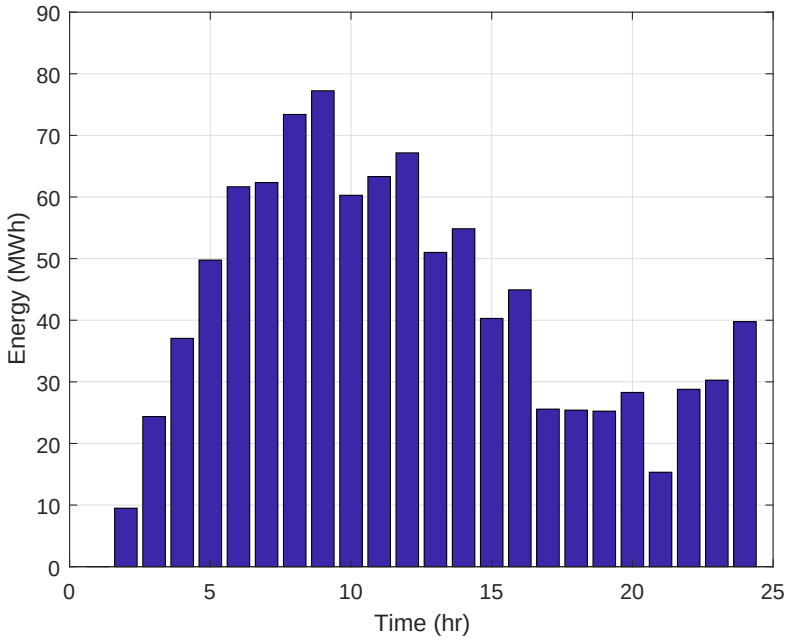


Figure 3.7: Stored energy in ESS

Table 3.3: Results of all scenarios solved separately

| Scenario | Total cost | $P_S^R$ (MW) | $E_S^R$ (MWh) |
|---|---|---|---|
| RTS | \$17,837,571.66 | 20.80 | 261.21 |
| S2 | \$17,844,093.52 | 21.85 | 280.12 |
| S3 | \$17,839,209.99 | 21.34 | 271.45 |
| S4 | \$17,828,819.84 | 24.12 | 183.78 |
| App 1 | \$17,860,781.23 | 23.32 | 352.57 |
| App 2 | \$17,837,453.34 | 21.78 | 251.55 |

# CHAPTER 4

# STORAGE SYSTEM PLANNING WITH RENEWABLE ENERGY

## 4.1 Motivation

In this chapter, a method for optimal sizing of battery energy storage systems (BESSs) under wind uncertainties is presented based on stochastic optimization approaches. The BESSs are becoming essential components in microgrids (MGs) due to significantly higher penetration of renewable energy sources. Integrating renewable energy sources coupled with BESSs in a power system enhances the power system reliability by increasing its availability and reducing its total cost of operation and maintenance. Also, the BESS connected to an MG should be optimally sized to be able to provide the necessary power and minimize the total cost of investment and operation. To optimally size a storage system, a constrained optimization problem is solved using an optimization method. This optimization problem could be deterministic or probabilistic. In case of optimizing the size of a BESS connected to a system

containing renewable energy sources, it is more effective to solve a probabilistic optimization problem because the forecast of their output power cannot be determined accurately. In this chapter, a probabilistic optimization problem is solved using the stochastic programming method to find the optimal size of a BESS to be connected to a grid-connected MG containing wind power generation. Then, a comparison is made to prove that solving the problem using stochastic programming gives better results. The simulation results prove the effectiveness of the proposed optimal sizing methodology.

## 4.2 Problem Formulation

The problem in this chapter consists of one part. This part is optimal sizing of an ESS. In this section, the equations of this part are formulated.

The optimal sizing problem is solved using the stochastic programming technique. To model this problem, the unit commitment problem has to be modeled first. Then, the ESS constraints are added to the problem. The unit commitment problem is illustrated in [68] and [7], and the ESS constraints are represented in [7]. This optimization problem has been modeled and solved in GAMS (General Algebraic Modeling System). Modeling the problem in GAMS language is explained in [69] and [24].

#### Objective Function

The objective of the optimization problem is to minimize the total cost. The total cost of this problem includes the production cost of generating units, electricity cost and

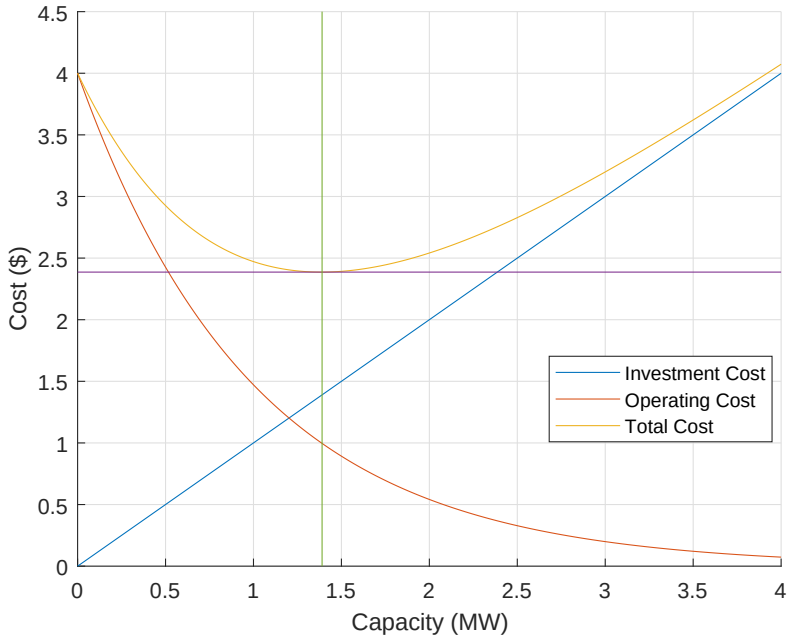


Figure 4.1: Cost vs ESS size

revenue from exchanging with the main grid, and the investment cost and of the ESS. The objective function of the optimal sizing of ESS for a given horizon is proposed in (4.1).

$$Min\ CMG_{units} + CMG_{ex} + IC_{ESS} \tag{4.1}$$

In (4.1), $CMG_{units}$ is the cost of microgrid related to its units, $CMG_{ex}$ is the cost of microgrid related to the exchanged power with the main grid, and $IC_{ESS}$ is the investment cost of the ESS.

The cost function is related to the units in the microgrid is formulated in (4.2). The variables $u$, $y$, and $z$ are binary variables which can be either 1 or 0. These values indicate if the unit $i$ at hour $t$ is committed, started up, and shut down, respectively. This is why the integer constraint is needed in this problem. The fixed cost of unit $i$, $F$, is fixed if the unit $i$ is committed. On the other hand, the variable cost of unit $i$,

$V$, is variable and it depends on the output power generated by the unit $i$.

$$CMG_{units} = \sum_{t=1}^{NT} \sum_{i=1}^{NI} [F_i u_{i,t} + V_i P_{i,t} + SU_i y_{i,t} + SD_i z_{i,t}] \tag{4.2}$$

In (4.2), $i$ is the unit index, $NI$ is the number of units, $t$ is the hour index, $NT$ is the number of hours, $F_i$ is the fixed cost or no-load cost of unit $i$, $V_i$ is the variable cost of unit $i$ and it is related to the output power of unit $i$, $P_{i,t}$ is the output power of unit $i$ at hour $t$, $SU_i$ is the start up cost of unit $i$ and $SD_i$ is the shut down cost of unit $i$. $u_{i,t}$, $y_{i,t}$, and $z_{i,t}$ are binary variables represent the commitment state of unit $i$ at hour $t$, start up indicator of unit $i$ at hour $t$ and shut down indicator of unit $i$ at hour $t$, respectively.

Note: In fact, the cost function is not linear, but a quadratic function. In (4.2), it has been linearized for simplicity.

The equation of cost related to the exchanged power between the microgrid and the main grid is formulated in (4.3). This cost is positive if the electricity is bought from the main grid, and it is negative if it is sold to the main grid.

$$CMG_{ex} = \sum_{t=1}^{NT} \gamma P_{M_t} \tag{4.3}$$

In (4.3), $\gamma$ is electricity price per one megawatt of power bought from or sold to the main grid and $P_{M_t}$ is the exchanged power between the microgrid and main grid at hour $t$. The sign convention in $P_{M_t}$ is that it is positive when the power flows from the main grid to the microgrid and it is negative when the power flows from the microgrid

to the main grid.

The equation of investment cost of the ESS is formulated in (4.4). The unknowns in this equation are the rated power of the ESS and the rated energy of it.

$$IC_{ESS} = PC_{ESS}\ P^{R}_{ESS} + EC_{ESS}\ E^{R}_{ESS} \tag{4.4}$$

In (4.4), $PC_{ESS}$ is the power cost of the ESS per one megawatt, $P^{R}_{ESS}$ is the rated power of the ESS, $EC_{ESS}$ is the energy cost of the ESS per one-megawatt hour, and $E^{R}_{ESS}$ is the rated energy of the ESS.

**System Constraints**

System constraints are the constraints related to the total output power in the microgrid, and they limit the output power. The main constraint among microgrid constraints is the balance equation. The total output power produced by the generating units, the ESS, and bought from the main grid must be at least equal to the demand at every hour. The reserve is usually added to the balance equation to overcome the continuous load variations so that the output power must be equal to the summation of demand and reserve at every hour. Also, the emissions constraint [70] is sometimes added as well in multi-objective unit commitment problems and the objectives of this kind of problems are to minimize both total costs of generated power and emissions produced by generation units [24]. In this chapter, the balance equation with demand

is considered. This constraint is formulated in (4.5).

$$\sum_{i=1}^{NI}[P_{i,t} + P_{ESS_t} + P_{M_t} - \sum_{s=1}^{NS}\rho_s P_{W_{t,s}}] = D_t \quad \forall t \in T, \forall s \in S \tag{4.5}$$

In (4.5), $s$ is the scenario index, $NS$ is the number of scenarios, $\rho_s$ is the probability of scenario $s$, $S$ is the set of scenarios, $P_{ESS_t}$ is the power stored to or produced by the ESS at hour $t$, $P_{W_t,s}$ is the wind power at hour $t$ in scenario $s$, $D_t$ is the demand at hour $t$ and $T$ is the set of hours. The sign convention in $P_{ESS_t}$ is that it is positive when it is produced and negative when it is stored.

Wind power is calculated from wind speed, and it is formulated in (4.6) [9].

$$P_{W_{t,s}} = \begin{cases} 0 & v_{t,s} < v_{CI} \text{ or } v_{t,s} \geq v_{CO} \\ P_W^{max}\frac{v_{t,s}-v_{CI}}{v_R-v_{CI}} & v_{CI} \leq v_{t,s} < v_R \\ P_W^{max} & v_R \leq v_{t,s} < v_{CO} \end{cases} \tag{4.6}$$

In (4.6), $P_W^{max}$ is the rated wind power, $v_{t,s}$ is the wind speed at hour $t$ in scenario $s$, $v_{CI}$ is the cut-in wind speed, $v_{CO}$ is the cut-out wind speed and $v_R$ is the rated wind speed. Figure 4.2 shows how the output wind power changes with wind speed [4].

Another important constraint related to the microgrid is limiting the power exchanged between the main grid and microgrid. This power depends on the capacity of the transmission line connecting the microgrid to the main grid. The sign convention of the exchanged power is negative for the power exported to the main grid and positive for the power imported from the main grid. This constraint is formulated in

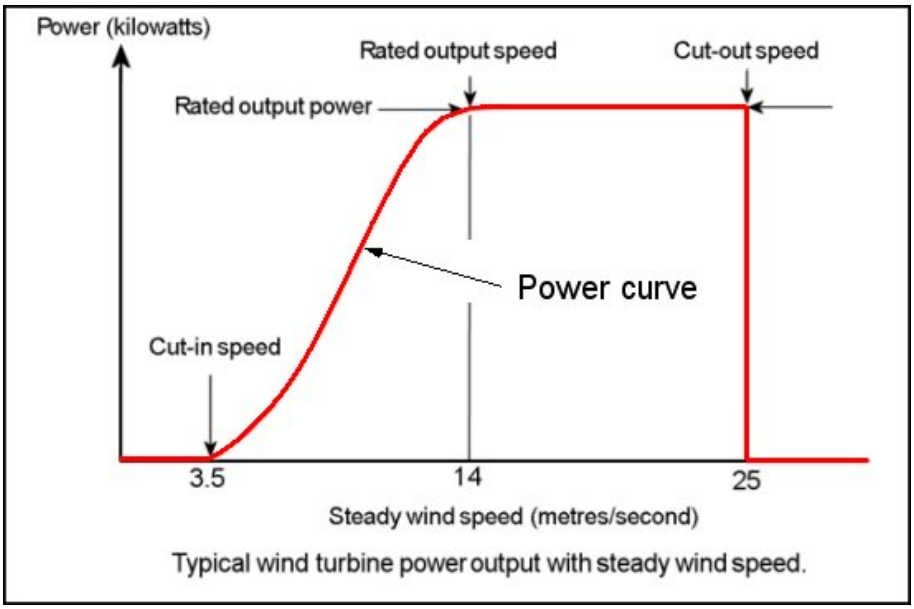


Figure 4.2: Wind power vs Wind speed [4]

(4.7).

$$-P_M^{max} \leq P_{M_t} \leq P_M^{max} \quad \forall t \in T \tag{4.7}$$

In (4.7), $P_M^{max}$ is the maximum capacity of the transmission line connecting between the microgrid and main grid.

### Generation Units Constraints

Generation units constraints are the constraints that limit the output power of each generation unit, and they reflect its characteristics. Also, these constraints model the generation units. Each generation unit has a minimum limit of power to operate with stability. Also, each generation unit has a maximum limit that cannot be exceeded. This constraint is formulated in (4.8). Multiplying the minimum and maximum limits by the commitment state means that if a generation unit is OFF, the output power

of this unit is zero.

$$P_i^{min} u_{i,t} \leq P_{i,t} \leq P_i^{max} u_{i,t} \quad \forall i \in I, \forall t \in T \tag{4.8}$$

In (4.8), $P_i^{min}$ is the minimum power that can be produced by unit $i$, $P_i^{max}$ is the maximum power that can be produced by unit $i$, and $I$ is the set of units.

Moreover, increasing or decreasing the output power of a generation unit are limited by two constant values which are the ramp up rate and ramp down rate, respectively. These constraints are formulated in (4.9) and (4.10), respectively.

$$P_{i,t} - P_{i,t-1} \leq RU_i \quad \forall i \in I, \forall t \in T \tag{4.9}$$

In (4.9), $RU_i$ is the ramp up rate of unit $i$.

$$P_{i,t-1} - P_{i,t} \leq RD_i \quad \forall i \in I, \forall t \in T \tag{4.10}$$

In (4.10), $RD_i$ is the ramp down rate of unit $i$.

When a generation unit starts up, it has to be ON for some time before it shuts down. This time is known as the minimum up time. Also, when a generation unit shuts down, it has to be OFF for some time before it starts up. This time is known as the minimum down time. These two constraints are formulated in (4.11) and (4.12), respectively.

$$T_{i,t}^{ON} \geq MUT_i[u_{i,t} - u_{i,t-1}] \quad \forall i \in I, \forall t \in T \tag{4.11}$$

In (4.11), $T_{i,t}^{ON}$ is the ON time of unit $i$ at hour $t$ and $MUT_i$ is the minimum up time of unit $i$.

$$T_{i,t}^{OFF} \geq MDT_i[u_{i,t-1} - u_{i,t}] \quad \forall i \in I, \forall t \in T \tag{4.12}$$

In (4.12), $T_{i,t}^{OFF}$ is the OFF time of unit $i$ at hour $t$ and $MDT_i$ is the minimum down time of unit $i$.

The generation unit cannot start up and shut down at the same time. This is a logic constraint and it is modeled in (4.13).

$$y_{i,t} - z_{i,t} = u_{i,t} - u_{i,t-1} \quad \forall i \in I, \forall t \in T \tag{4.13}$$

**Energy Storage System Constraints**

Energy storage system constraints are the constraints limiting the charged and discharged power of the ESS. Also, they are used to model the ESS. The first constraint is the limits of the power of the ESS. This power is limited by the rated power of the ESS. Also, when the ESS charges, it is considered as a load and the power produced by the ESS is negative in this case. Moreover, when the ESS discharges, it is considered as a generation unit and the power produced by the ESS is positive in this case. This constraint is formulated in (4.14).

$$-P_{ESS}^{R} \leq P_{ESS_t} \leq P_{ESS}^{R} \quad \forall t \in T \tag{4.14}$$

The stored energy in the ESS is limited by its rated energy. Of course, the stored energy is always positive. This constraint is formulated in (4.15).

$$0 \leq E_{ESS_t} \leq E_{ESS}^{R} \quad \forall t \in T \tag{4.15}$$

In (4.15), $E_{ESS_t}$ is the energy stored in the ESS at hour $t$.

The equation to calculate the stored energy at a specific hour is formulated in (4.16). The stored energy is called the state of charge and there are methods developed to optimize it [67].

$$E_{ESS_t} = E_{ESS_{t-1}} - P_{ESS_t} \quad \forall t \in T \tag{4.16}$$

### 4.2.1 Uncertainty Modeling

To model the wind uncertainty, multiple wind speed profiles will be generated. Different probabilities will be assigned to those profiles, and the summation of these probabilities must be equal to 1. Then, each probability will be multiplied with its corresponding wind speed profile. The summation of those products will form a new profile that will be used in solving the optimal sizing problem. This solution will be compared to the solution of each profile to justify solving the problem using this method when there are uncertainties in the optimization problem. The methodology of optimal sizing under wind uncertainty is illustrated and simplified in Algorithm 3.

Another approach is used as well to calculate the optimal size of an ESS under wind uncertainties. The algorithm of this method is shown in Algorithm 4. This method might give a more economic solution. Thus, the optimally sized ESS in this

**Algorithm 3** Proposed algorithm of optimal sizing of ESS

**function** SP_SIZING($n, S, P$) ▷ Where n - number of scenarios, S - array of all scenarios, P - vector of all scenario probabilities
    $n$ = number of scenarios
    **for** $i = 1$ to $n$ **do**
        $S[i]$ = scenario profile
        $P[i]$ = scenario probability
    **end for**
    **if** $\sum_{i=1}^{n} P[i] > 1$ **then**
        print: sum of probabilities is greater than 1
        Stop
    **else**
        $A = \sum_{i=1}^{n} P[i]S[i]$ ▷ Where A - vector of scenarios multiplied by their corresponding probabilities
    **end if**
    **for** $i = 1$ to $n$ **do**
        Optimally size $S[i]$
    **end for**
    Optimally size $A$
    Compare the results
**end function**

method might cost less than the previously proposed method.

**Algorithm 4** Another algorithm of optimal sizing of ESS

**function** SP_SIZING($n, S, Pr$) ▷ Where n - number of scenarios, S - array of all scenarios, Pr - vector of all scenario probabilities
    $n$ = number of scenarios
    **for** $i = 1$ to $n$ **do**
        $S[i]$ = scenario profile
        $Pr[i]$ = scenario probability
    **end for**
    **if** $\sum_{i=1}^{n} Pr[i] > 1$ **then**
        print: sum of probabilities is greater than 1
        Stop
    **else**
        Find $P_{ESS}[i]$ ▷ Where $P_{ESS}[i]$ - optimally sized ESS power for all scenarios separately
        Find $E_{ESS}[i]$ ▷ Where $E_{ESS}[i]$ - optimally sized ESS energy for all scenarios separately
        $P^{ESS} = \sum_{i=1}^{n} P_{ESS}[i]Pr[i]$ ▷ Where $P^{ESS}$ - normalized optimal size ESS power
        $E^{ESS} = \sum_{i=1}^{n} E_{ESS}[i]Pr[i]$ ▷ Where $E^{ESS}$ - normalized optimal size ESS energy
    **end if**
    **for** $i = 1$ to $n$ **do**
        Optimally size $S[i]$
    **end for**
    Compare the results
**end function**

### 4.2.2 Reliability Constraints

Some reliability constraints are introduced to guarantee fewer interruptions and unavailability. In this chapter, the proposed reliability constraints are as illustrated in (4.17) and (4.18).

$$SAIFI \leq SAIFI_{Limit} \tag{4.17}$$

$$SAIDI \leq SAIDI_{Limit} \tag{4.18}$$

## 4.3 A Case Study

A microgrid connected to a main grid is considered to perform a case study for the optimal sizing of an ESS under wind uncertainties. In this section, the case study is presented with its data. The results are introduced and discussed in Section 4.4. The system that will be studied consists of three thermal generators which are distributed generators in the microgrid. The unit commitment problem is solved using stochastic programming for a scheduling horizon of two years. The load data has been taken from the IEEE Reliability Test System (RTS-96) for the first year [71]. For the second year, the same load profile has been repeated with an increase of %5. The reserve and emission constraints are not considered in this case study. Ten scenarios of wind speed have been created randomly using the Weibull distribution parameters for monthly wind distribution calculated in Dhahran for 19 years [1]. Those parameters are shown in Table 4.1. In this table, $K$ represents the shape parameter, and $c$ represents the scale parameter. The probability density function of Weibull distribution used to calculate the wind speed at each hour is illustrated in (4.19). Those ten scenarios are assumed to be actual data taken from ten different years. The annual numerical values of $k$ and $c$ are 2.35 and 4.98, respectively. Figure 4.3 shows the Weibull distribution for annual wind speeds and wind frequency histogram for Dhahran [1] and Table 4.2 illustrates the average annual wind speeds in Dhahran for all scenarios. The probabilities of all

scenarios are equal, which means that $\rho_s$ is equal to 0.1 for all scenarios. The ten scenarios have been repeated twice to cover the horizon of two years.

$$f(t,c,k) = \begin{cases} \frac{k}{c}\left(\frac{t}{c}\right)^{k-1} e^{-\left(\frac{t}{c}\right)^k} & t \geq 0 \\ 0 & t < 0 \end{cases} \tag{4.19}$$

Table 4.3 shows the characteristics of the three generation units. The characteristics of the generation units except for the minimum up time and minimum down time are from [68]. Table 4.4 represents the values of the other parameters used in this model. Figure 4.4 shows the load curve and load duration curve during the two years. Figure 4.5 shows the ten scenarios of wind speed during the first year. They are represented in average daily speeds. The same scenarios have been repeated to cover the second year. Figure 4.6 illustrates the hourly speed for the ten scenarios during the first twenty-four hours.

The unit commitment problem of the microgrid is solved for a two-year horizon before and after integrating the ESS to calculate the output power of each generation unit, exchanged power with the main grid, and the power taken by the ESS or produced by it in the second case. The optimization problem of this system has been modeled in GAMS (General Algebraic Modeling System) language [72] and has been solved in the NEOS Server [73] which is a free online service for solving numerical optimization problems.

Table 4.1: Weibull parameters for monthly wind speed distribution in Dhahran [1]

| Month | $k$ | $c$ |
|---|---|---|
| JAN | 2.40 | 4.77 |
| FEB | 2.45 | 4.85 |
| MAR | 2.55 | 5.15 |
| APR | 2.40 | 5.06 |
| MAY | 2.40 | 5.52 |
| JUN | 2.60 | 6.51 |
| JUL | 2.50 | 5.54 |
| AUG | 2.30 | 4.91 |
| SEP | 2.20 | 4.18 |
| OCT | 2.05 | 4.09 |
| NOV | 2.20 | 4.38 |
| DEC | 2.00 | 4.68 |

Table 4.2: Average annual wind speeds in Dhahran for all scenarios

| Scenario | Wind speed (m/s) |
|---|---|
| Scenario 1 | 4.4446376 |
| Scenario 2 | 4.4169281 |
| Scenario 3 | 4.4102231 |
| Scenario 4 | 4.4032716 |
| Scenario 5 | 4.4007090 |
| Scenario 6 | 4.4340644 |
| Scenario 7 | 4.3894760 |
| Scenario 8 | 4.3762805 |
| Scenario 9 | 4.4285103 |
| Scenario 10 | 4.3670960 |

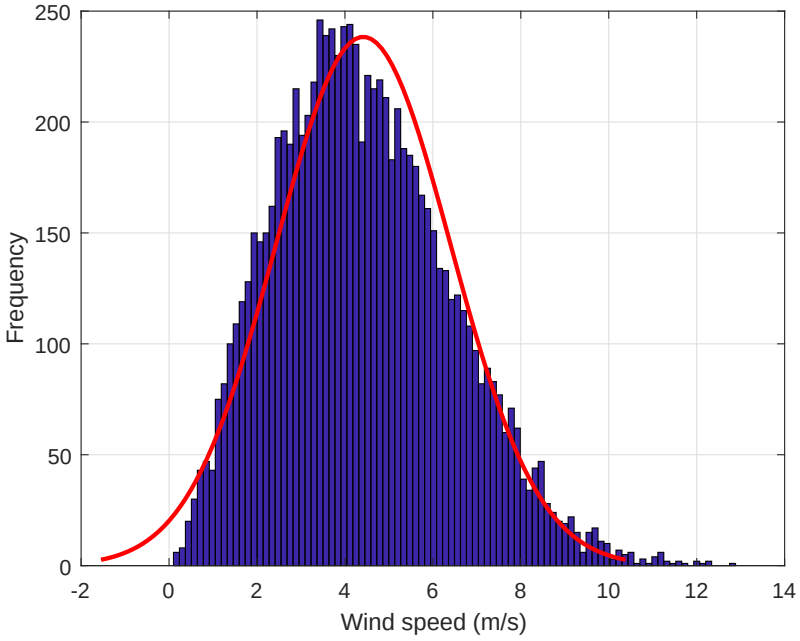


Figure 4.3: Wind frequency histogram and Weibull distribution for all wind speeds in Dhahran

Table 4.3: Characteristics of generation units

| Unit No. | Fixed Cost ($) | Variable Cost ($/MW) | Start Up Cost ($) | Shut Down Cost ($) | Min. Capacity (MW) |
|---|---|---|---|---|---|
| 1 | 9 | 20 | 40 | 20 | 5 |
| 2 | 7 | 18 | 30 | 20 | 3 |
| 3 | 5 | 15 | 20 | 20 | 2 |
| Unit No. | Max. Capacity (MW) | Ramp Down Rate (MW/h) | Ramp Up Rate (MW/h) | Min. Down Time (h) | Min. Up Time (h) |
| 1 | 20 | 15 | 15 | 1 | 1 |
| 2 | 30 | 15 | 15 | 1 | 1 |
| 3 | 40 | 20 | 20 | 1 | 1 |

Table 4.4: Values of other model parameters

| Parameter | $PC_{ESS}$ | $EC_{ESS}$ | $\gamma$ | $P_M^{max}$ | $SAIFI_{Limit}$ |
|---|---|---|---|---|---|
| Value | \$1200 | \$300 | \$20 | 10 MW | 1.00E-10 |
| Parameter | $P_W^{max}$ | $v_{CI}$ | $v_R$ | $v_{CO}$ | $SAIDI_{Limit}$ |
| Value | 15 MW | 1 m/s | 5 m/s | 11 m/s | 1.00E-10 |

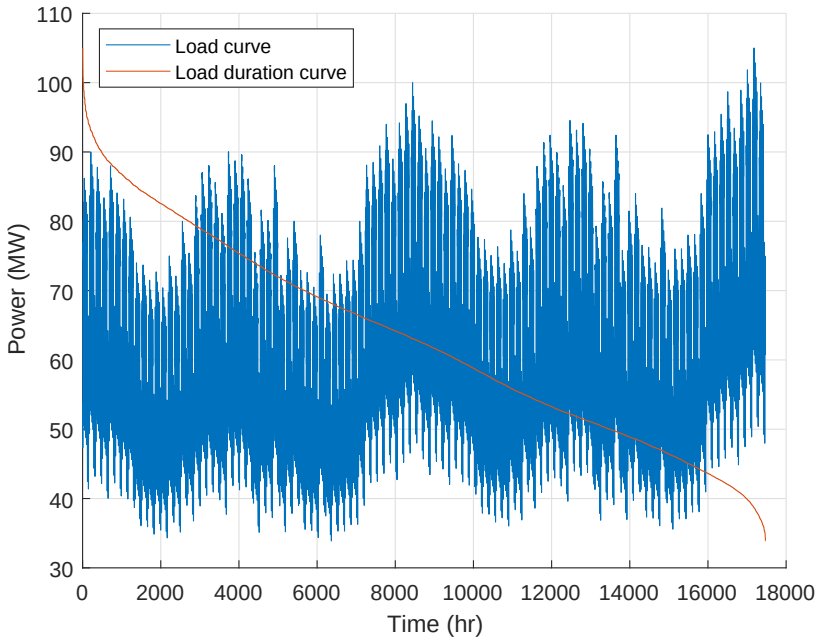


Figure 4.4: Load curve and load duration curve

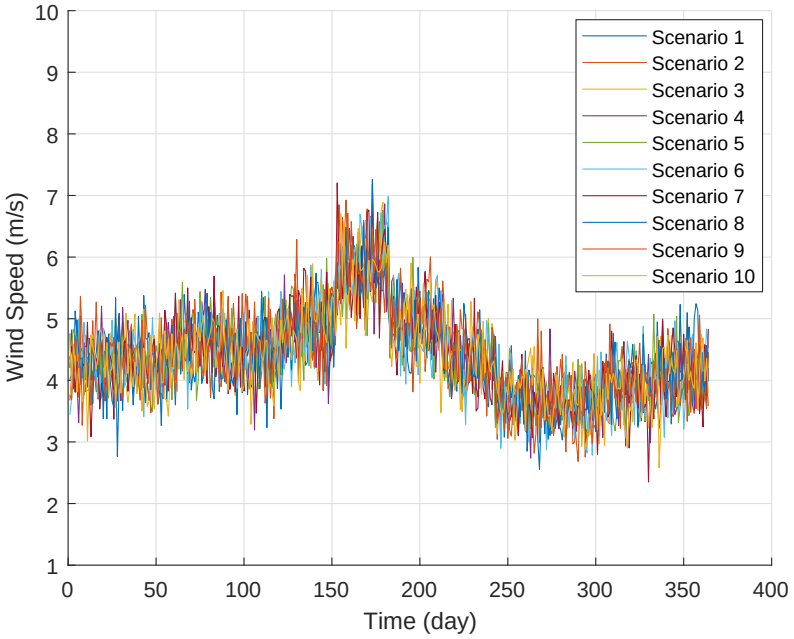


Figure 4.5: Average daily wind speeds of the ten scenarios

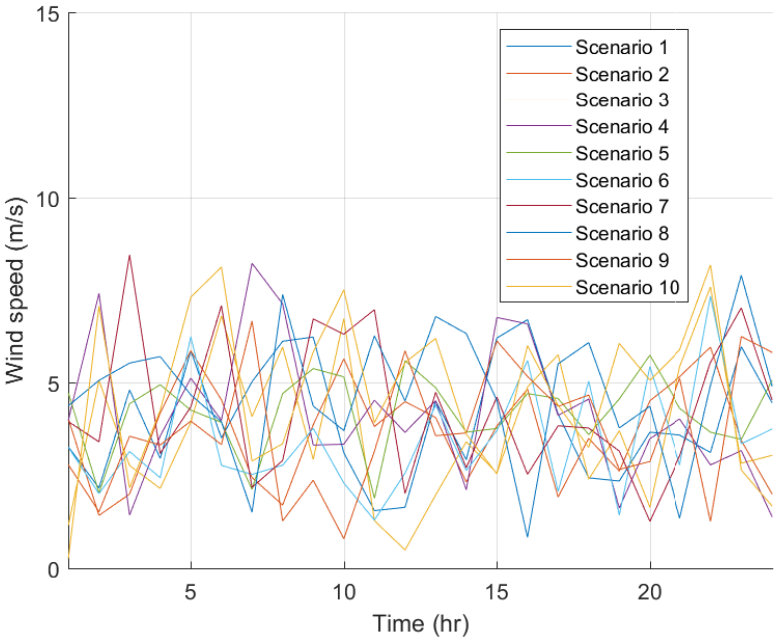


Figure 4.6: Hourly wind speeds during the first twenty-four hours of the ten scenarios

## 4.4 Results and Discussions

The unit commitment problem has been solved using the stochastic programming method to find the optimal size of the ESS which minimizes the total cost. The rated power of the ESS has been found to be 16.59 MW nd the rated energy is 128.84 MWh. The investment cost of the ESS is about $58,554. For the first twenty-four hours, Figure 4.7 shows the solution of the unit commitment problem before integrating the microgrid with the ESS, and Figure 4.8 shows the solution of the unit commitment problem after calculating the optimal size of the ESS and integrating it with the microgrid. Those two figures represent the positive power only, which means that they do not represent the power in case of charging the ESS and in case of selling power to the main grid as well. The two variables related to the produced power from the ESS and exchanged power with the main grid are shown in Figure 4.9 with their negative values. The ESS acts like a load when it charges and acts like a generator when it discharges. For the ESS to produce power, it must have stored energy. Figure 4.10 shows the quantities of the stored energy during the first twenty-four hours.

The most expensive generation unit, which is Unit 1, is working at a low level when the ESS in not integrated as shown in Figure 4.7 and it is not working for most hours when the ESS is integrated as shown in Figure 4.8. The ESS had made the microgrid more reliable economically and saved a portion of the production cost when it worked instead of Unit 1.

To prove that the solution of stochastic programming method is reasonably optimal, the ten scenarios, which are assumed previously as actual data for ten differ-

ent years, have been solved separately using the mixed-integer linear programming method. The results are shown in Table 4.5. They are compared to the solution of the stochastic programming method in Table 4.6. The solution of the probabilistic optimization method is the second optimal solution after the solution of Scenario 6. This shows that the probabilistic technique gives a reasonable solution compared to the deterministic technique of the ten scenarios. The stochastic programming technique is used when there is more than one scenario, and it gives better results as shown in Tables 4.5 and 4.6. Although the investment cost of the storage system in the stochastic programming solution is higher compared to other scenarios, the total cost is still lower. The objective is to minimize the total cost, not the investment cost. The solution of Scenario 6 is lower than the stochastic programming solution, but it reflects only one scenario instead of all scenarios. The results of deterministic and probabilistic optimization problems are illustrated also in Figures 4.11, 4.12 and 4.13 to be read and compared easily.

Moreover, using the other approach illustrated in Algorithm 4, the optimal size of an ESS has been calculated as well. As mentioned previously, this method might give more economic results. The investment cost in this method is less than the investment cost calculated in the first approach. The rated power of the optimally sized ESS in this technique is 15.87 MW, and the rated energy is 111.24 MWh. The investment cost of this ESS is about \$52,416. This cost is less than the investment cost in the first approach by 10.48%.

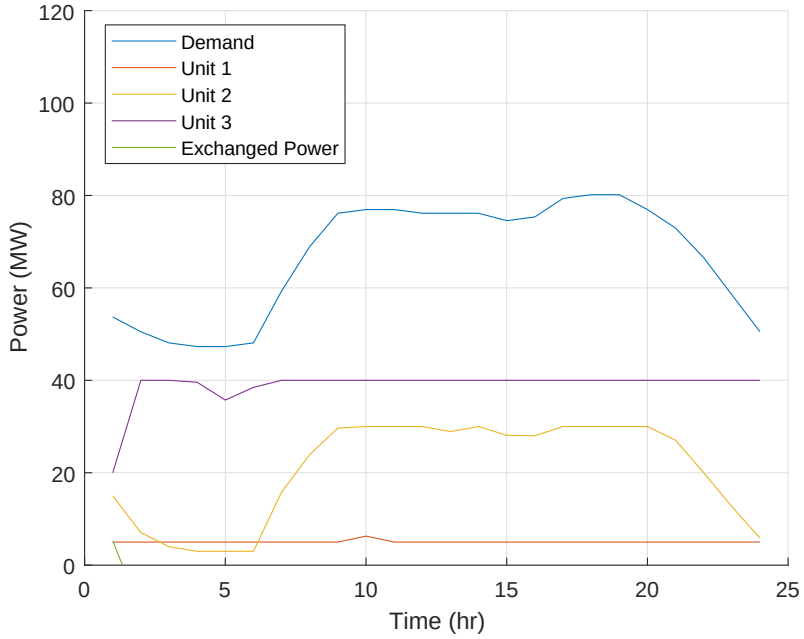


Figure 4.7: Economic dispatch without ESS

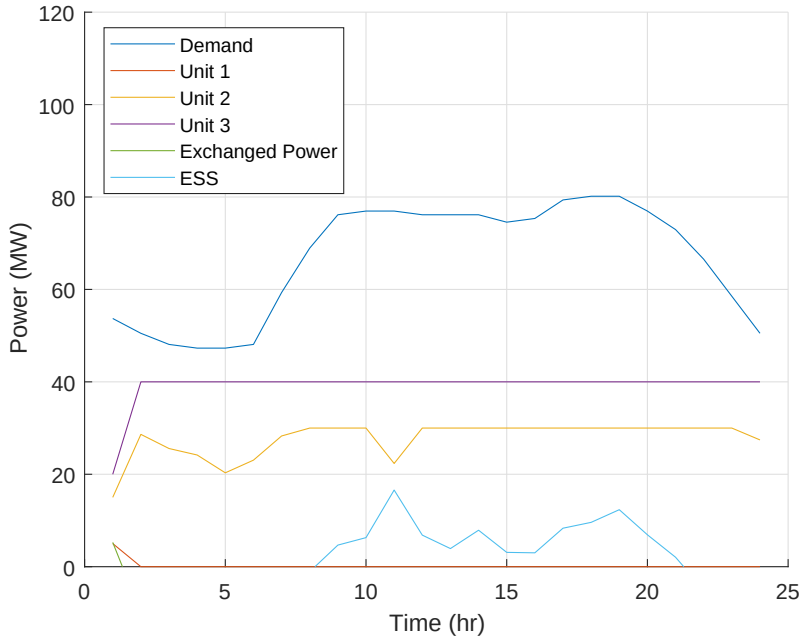


Figure 4.8: Economic dispatch with ESS

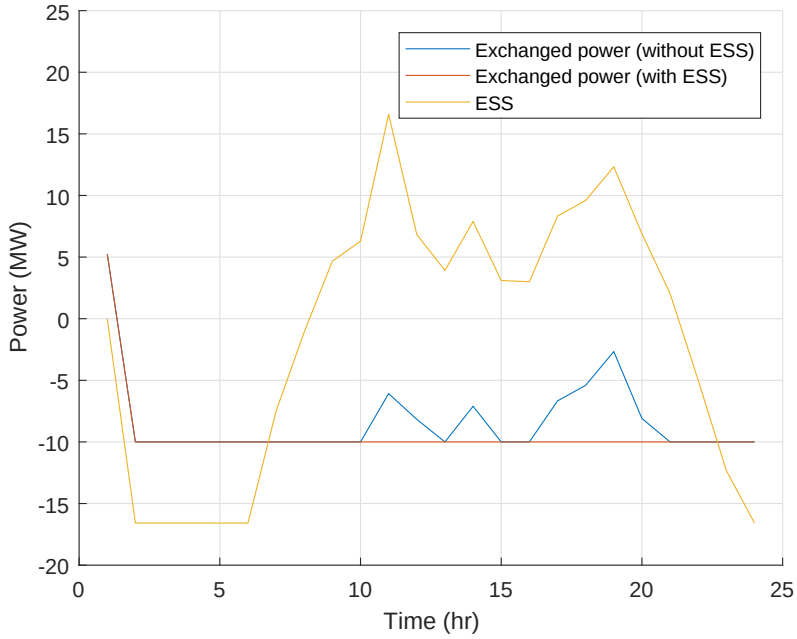


Figure 4.9: ESS power and exchanged power with negative values

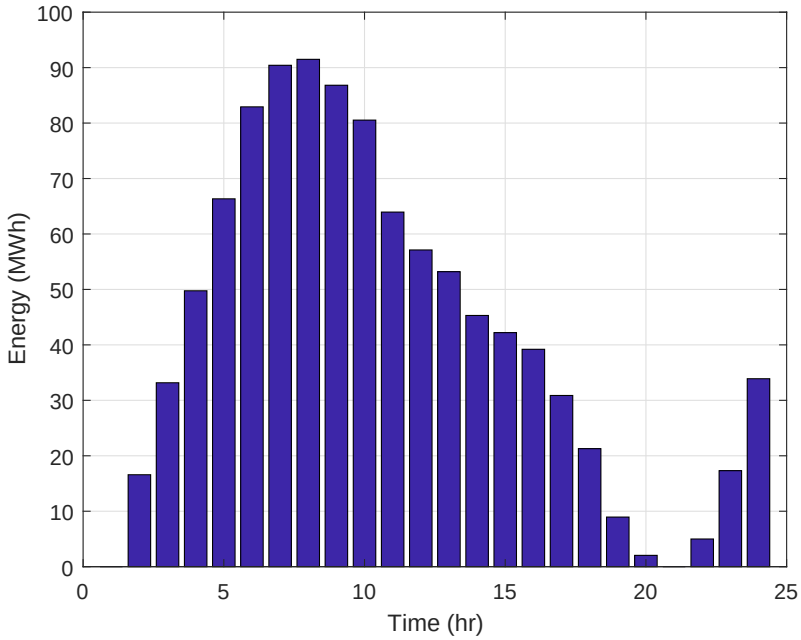


Figure 4.10: Stored energy in ESS

Table 4.5: Results of all scenarios solved separately

| Scenario | Total cost ($) | $P_S^R$ (MW) | $E_S^R$ (MWh) |
|---|---|---|---|
| S1 | 14,634,417.23 | 11.79 | 86.23 |
| S2 | 14,652,256.34 | 11.59 | 83.76 |
| S3 | 14,648,323.41 | 11.84 | 85.50 |
| S4 | 14,399,562.33 | 19.97 | 129.43 |
| S5 | 14,393,281.42 | 19.96 | 136.42 |
| S6 | 14,380,884.59 | 19.75 | 138.91 |
| S7 | 14,414,730.03 | 19.81 | 135.50 |
| S8 | 14,691,929.52 | 11.58 | 85.34 |
| S9 | 14,645,579.66 | 11.69 | 84.33 |
| S10 | 14,429,380.07 | 20.71 | 146.98 |
| SP | 14,392,584.15 | 16.59 | 128.84 |

Table 4.6: Comparison of results of all scenarios with SP solution

| Scenario | % Total cost | $\%P_S^R$ | $\%E_S^R$ |
|---|---|---|---|
| S1 | -1.6803% | 28.9064% | 33.0716% |
| S2 | -1.8042% | 30.1084% | 34.9909% |
| S3 | -1.7769% | 28.5996% | 33.6401% |
| S4 | -0.0485% | -20.4079% | -0.4634% |
| S5 | -0.0048% | -20.3461% | -5.8826% |
| S6 | 0.0813% | -19.0800% | -7.8221% |
| S7 | -0.1539% | -19.4598% | -5.1736% |
| S8 | -2.0799% | 30.1612% | 33.7609% |
| S9 | -1.7578% | 29.5432% | 34.5429% |
| S10 | -0.2557% | -24.8912% | -14.0825% |

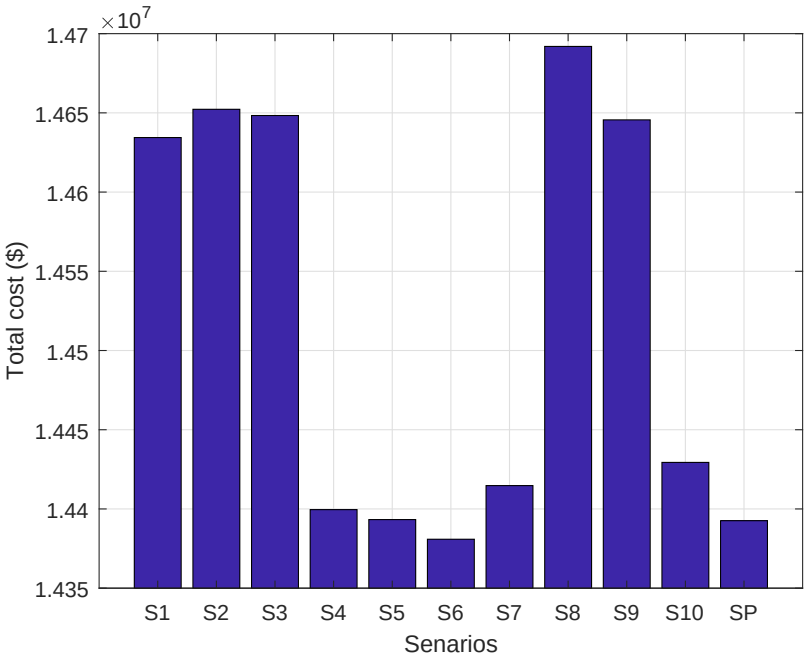


Figure 4.11: Total cost of all scenarios

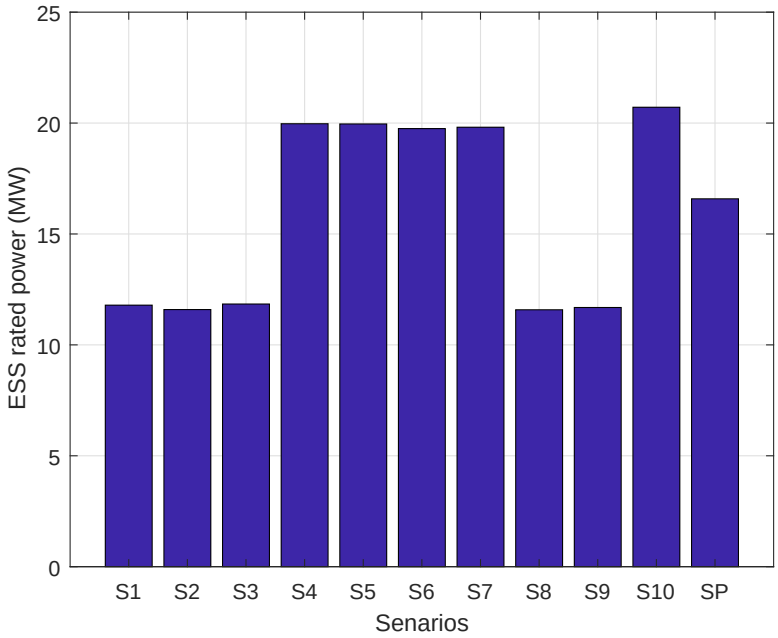


Figure 4.12: ESS rated power of all scenarios

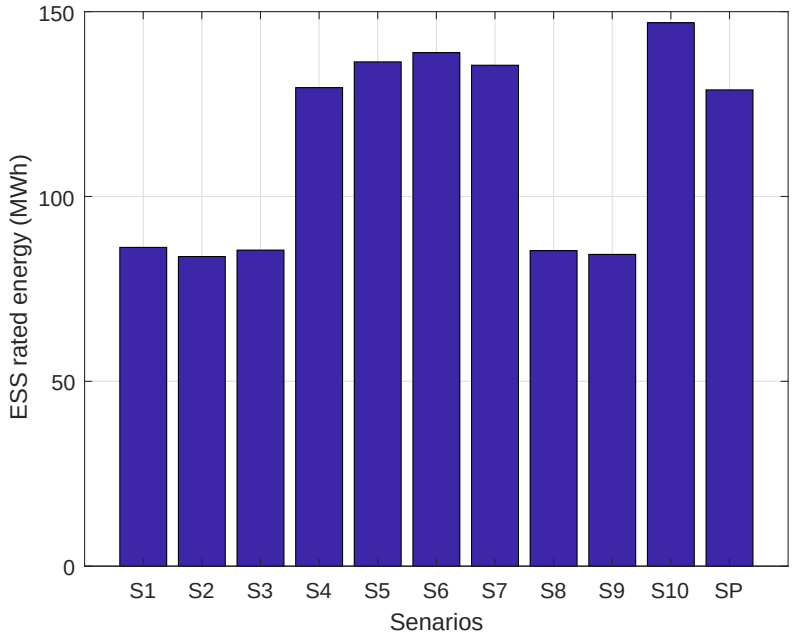


Figure 4.13: ESS rated energy of all scenarios

## 4.5 Summary

This chapter has presented a methodology to optimally size a BESS for a grid-connected MG under wind uncertainties using one of the probabilistic optimization techniques - stochastic programming. The results of the stochastic programming problem have been compared to the solutions of the deterministic optimization problems covering all possible scenarios to show that this solution is reasonably optimal and reflects all scenarios as well. One of the main purposes of integrating an optimally sized storage system with an MG is to enhance its reliability. It is proved that integrating the BESS with an MG has decreased the net cost although it includes the investment cost of building and establishing the BESS, which shows the economical feasibility of the system.

# CHAPTER 5

# OPTIMAL ALLOCATION OF STORAGE SYSTEMS

## 5.1 Motivation

In this chapter, a model for allocating and calculating the optimal size of an energy storage system (ESS) in a microgrid will be proposed. A larger ESS requires higher investment costs while reduces the microgrid operating cost. The optimal ESS sizing and allocating problem will be proposed which minimizes the total cost that includes investment cost of the ESS, as well as expected microgrid operating cost. Utilizing the ESS, generation shortage due to an outage of conventional units and intermittency of renewable units is handled. A practical model for ESS is utilized. Mixed-integer linear programming (MILP) will be utilized to solve the DC optimal power flow problem.

## 5.2 Problem Formulation

The objective of this chapter is to optimally size an ESS and solve the Optimal Power Flow (OPF) problem in a power system. The objectives of the OPF problem are to find the optimal dispatch of each generator and power flowing in branches connecting buses. Those results must be subjected to the transmission line limits and other constraints in the power system. So, the OPF problem includes the unit commitment problem which includes the economic dispatch problem. The OPF problem can be a single-period problem or multi-period problem. Also, it can be AC or DC. In this chapter, the multi-period DC OPF is formulated and solved. This section illustrates the formulation of this problem. This problem is a constrained optimization problem, and it is solved using linear programming. The equations are explained in [24].

The objective is to minimize the function which represents the total cost. The total cost includes the investment cost of the ESS, operating and maintenance cost. The objective function is formulated in (5.1).

$$OC = IC_{ESS} + \sum_{g,t} b_g \; P_{g,t} + \sum_{i,t} VOLL \times P_{i,t}^{LS} + VWC \times P_{i,t}^{wc} \tag{5.1}$$

In (5.1), $OC$ is the operating costs in dollars, $IC$ is the investment cost of the ESS, $g$ is the index of thermal generating units, $t$ is the index of time which is hour, $b_g$ is the fuel cost coefficient of thermal unit $g$, $P_{g,t}$ is the active power generated by thermal unit $g$ at time $t$ in MW, $VOLL$ is the value of loss of load in \$/MWh, $P_{i,t}^{LS}$ is the load shedding in bus $i$ at time $t$ in MW, $VWC$ is the value of loss of wind in \$/MWh and $P_{i,t}^{wc}$ is the curtailed power of wind turbine connected to bus $i$ at time $t$

in MW.

The equation of investment cost of the ESS is formulated in (5.2). The unknowns in this equation are the rated power of the ESS and the rated energy of it.

$$IC_{ESS} = PC_{ESS}\ P^{R}_{ESS} + EC_{ESS}\ E^{R}_{ESS} \tag{5.2}$$

In (5.2), $PC_{ESS}$ is the power cost of the ESS per one megawatt, $P^{R}_{ESS}$ is the rated power of the ESS, $EC_{ESS}$ is the energy cost of the ESS per one-megawatt hour, and $E^{R}_{ESS}$ is the rated energy of the ESS.

The nodal active and reactive power balances are constraints in this problem, and they are formulated in (5.3) and (5.4), respectively.

$$\sum_{g \in \Omega^{i}_{G}} P_{g,t} + P^{LS}_{i,t} + P^{w}_{i,t} - P^{L}_{i,t} - P^{c}_{i,t} + P^{d}_{i,t} = \sum_{j \in \Omega^{i}_{l}} P_{ij,t} \tag{5.3}$$

In (5.3), $\Omega^{i}_{G}$ is the set of all thermal generating units connected to bus $i$, $\Omega^{i}_{l}$ is the set of all buses connected to bus $i$, $i$ and $j$ are indices of network buses, $P_{g,t}$ is the active power generated by thermal unit $g$ at time $t$ in MW, $P^{w}_{i,t}$ is the active power generated by wind turbine connected to bus $i$ at time $t$ in MW, $P^{L}_{i,t}$ is the electric power demand in bus $i$ at time $t$ in MW, $P^{c}_{i,t}$ is the charging power of the ESS in bus $i$ at time $t$ in MW, $P^{d}_{i,t}$ is the discharging power of the ESS in bus $i$ at time $t$ in MW and $P_{ij,t}$ is the active power flow of branch connecting bus $i$ to bus $j$ at time $t$ in MW.

$$\sum_{g \in \Omega^{i}_{G}} Q_{g,t} + Q^{LS}_{i,t} + Q^{w}_{i,t} - Q^{L}_{i,t} - Q^{c}_{i,t} + Q^{d}_{i,t} = \sum_{j \in \Omega^{i}_{l}} Q_{ij,t} \tag{5.4}$$

In (5.4), $Q_{g,t}$ is the reactive power generated by thermal unit $g$ at time $t$ in Mvar, $Q^{w}_{i,t}$ is the reactive power generated by wind turbine connected to bus $i$ at time $t$ in Mvar, $Q^{L}_{i,t}$ is the reactive power demand in bus $i$ at time $t$ in Mvar, $Q^{c}_{i,t}$ is the reactive charging power of the ESS in bus $i$ at time $t$ in Mvar, $P^{d}_{i,t}$ is the reactive discharging power of the ESS in bus $i$ at time $t$ in Mvar and $Q_{ij,t}$ is the reactive power flow of branch connecting bus $i$ to bus $j$ at time $t$ in Mvar.

The current flowing in a branch connecting bus $i$ to bus $j$ at time $t$ is calculated in (5.5).

$$I_{ij,t} = \frac{V_{i,t}\angle\delta_{i,t} - V_{j,t}\angle\delta_{j,t}}{Z_{ij}\angle\theta_{ij}} + \frac{bV_{i,t}}{2}\angle\delta_{i,t} + \tfrac{\pi}{2} \tag{5.5}$$

In (5.5), $I_{ij,t}$ is the current flowing from bus $i$ to bus $j$ in A, $V_{i,t}$ and $V_{j,t}$ are the voltages at bus $i$ and bus $j$, respectively, at time $t$ in V, $\delta_{i,t}$ and $\delta_{j,t}$ are the voltage angles at bus $i$ and bus $j$, respectively, at time $t$ in radians, $Z_{ij}$ is the impedance of the branch connecting bus $i$ to bus $j$ in $\Omega$, $\theta_{ij}$ is the impedance angle of the branch connecting bus $i$ to bus $j$ in radians and $b$ is variable cost in dollars per MW.

The apparent power is the combination of active power and reactive power, and it is calculated using (5.6).

$$S_{ij,t} = (V_{i,t}\angle\delta_{i,t})I^{*}_{ij,t} \tag{5.6}$$

In (5.6), $S_{ij,t}$ is the apparent power in MVA and it is a complex number.

The active power and reactive power are calculated from the apparent power as formulated in (5.7) and (5.8), respectively.

$$P_{ij,t} = Real\{S_{ij,t}\} = \frac{V_{i,t}^2}{Z_{ij}} cos(\theta_{ij}) - \frac{V_{i,t}V_{j,t}}{Z_{ij}} cos(\delta_{i,t} - \delta_{j,t} + \theta_{ij}) \tag{5.7}$$

$$Q_{ij,t} = Img\{S_{ij,t}\} = \frac{V_{i,t}^2}{Z_{ij}} sin(\theta_{ij}) - \frac{V_{i,t}V_{j,t}}{Z_{ij}} sin(\delta_{i,t} - \delta_{j,t} + \theta_{ij}) - \frac{bV_{i,t}^2}{2} \tag{5.8}$$

The branch apparent power flow limits of each transmission line are formulated in (5.9).

$$-S_{ij}^{max} \leq S_{ij,t} \leq S_{ij}^{max} \tag{5.9}$$

In (5.9), $S_{ij}^{max}$ is the maximum apparent power flow limits of branch connecting bus $i$ to bus $j$ in MVA.

Every thermal unit has a minimum limit for operation with stability. Also, it has a maximum limit that cannot be exceeded. The operating limits of the thermal generating unit are modeled in (5.10) and (5.11).

$$P_g^{min} \leq P_{g,t} \leq P_g^{max} \tag{5.10}$$

In (5.10), $P_g^{min}$ is the minimum limit of active power generation of thermal unit $g$ in MW and $P_g^{max}$ is the maximum limit of active power generation of thermal unit $g$ in MW.

$$Q_g^{min} \leq Q_{g,t} \leq Q_g^{max} \tag{5.11}$$

In (5.11), $Q_g^{min}$ is the minimum limit of reactive power generation of thermal unit $g$ in Mvar and $Q_g^{max}$ is the maximum limit of reactive power generation of thermal unit $g$ in Mvar.

Every thermal unit has ramp rates. This means if the power is increasing, it is increasing according to a limited rate. This is happening if the power is decreasing as well. The ramp rates of thermal units are described in (5.12) and (5.13).

$$P_{g,t} - P_{g,t-1} \leq RU_g \tag{5.12}$$

In (5.12), $RU_g$ is the ramp-up rate of thermal unit $g$ in \$/MWh.

$$P_{g,t-1} - P_{g,t} \leq RD_g \tag{5.13}$$

In (5.13), $RD_g$ is the ramp-down rate of thermal unit $g$ in \$/MWh.

The load shedding is limited to the existing demand at the same bus as described in (5.14) and (5.15).

$$0 \leq P_{i,t}^{LS} \leq P_{i,t}^{L} \tag{5.14}$$

$$0 \leq Q_{i,t}^{LS} \leq Q_{i,t}^{L} \tag{5.15}$$

The wind power curtailment is formulated in (5.16).

$$P_{i,t}^{wc} = w_{i,t}\Lambda_i^w - P_{i,t}^w \tag{5.16}$$

In (5.16), $w_{i,t}$ is the availability of wind turbine connected to bus $i$ at time $t$ and $\Lambda_i^w$ is the capacity of wind turbine connected to bus $i$ in MW.

The amount of wind power depends on its availability and capacity as formulated in (5.17).

$$0 \leq P_{i,t}^w \leq w_{i,t}\Lambda_i^w \tag{5.17}$$

The state of charge of an ESS is calculated as described in (5.18). The state of charge of an ESS is the stored energy.

$$SOC_{i,t} = SOC_{i,t-1} + (P_{i,t}^c \eta_c - \frac{P_{i,t}^d}{\eta_d})\Delta_t \tag{5.18}$$

In (5.18), $SOC_{i,t}$ is the state of charge of ESS in bus $i$ at time $t$ in MWh, $\eta_c$ is the charging efficiency, $\eta_d$ is the discharging efficiency and $\Delta_t$ is time step in hours.

The charging and discharging powers of an ESS are limited as described in (5.19) and (5.20), respectively.

$$P_{i,min}^c \leq P_{i,t}^c \leq P_{i,max}^c \tag{5.19}$$

In (5.19), $P_{i,min}^c$ is the minimum charging power of ESS in bus $i$ in MW and $P_{i,max}^c$ is the maximum charging power of ESS in bus $i$ in MW.

$$P_{i,min}^d \leq P_{i,t}^d \leq P_{i,max}^d \tag{5.20}$$

In (5.20), $P_{i,min}^d$ is the minimum discharging power of ESS in bus $i$ in MW and

$P^d_{i,max}$ is the maximum discharging power of ESS in bus $i$ in MW.

The state of charge of an ESS is limited by its minimum and maximum as described in (5.21).

$$SOC_{i,min} \leq SOC_{i,t} \leq SOC_{i,max} \tag{5.21}$$

In (5.21), $SOC_{i,min}$ is the minimum state of charge of ESS in bus $i$ in MWh and $SOC_{i,max}$ is the maximum state of charge of ESS in bus $i$ in MWh.

## 5.3 Case Study

The system used for this case study is a 3-bus system that has three distributed generators. Each generator is connected to a different bus. Also, the proposed system has a wind farm located at Bus 2. The load is connected to Bus 2 as well. The proposed load profile has been taken from IEEE 24-bus RTS [71]. This load profile is for one year in the reference, but it has been extended for a second year with an increase of 5%. Figure 5.4 shows the load profile and load duration curve for the two years. The power flow in the system is modeled using DC optimal power flow and solved using MILP technique. The probability density function of Weibull distribution used to calculate the wind speed at each hour is illustrated in (5.22). By using Weibull distribution parameters for wind speed in Dhahran [1], a profile for wind turbines generated power was produced and used for this study. Table 5.1 shows the Weibull parameters for monthly wind speed distribution in Dhahran. In this table, $K$ represents the shape parameter, and $c$ represents the scale parameter. Figure 5.2

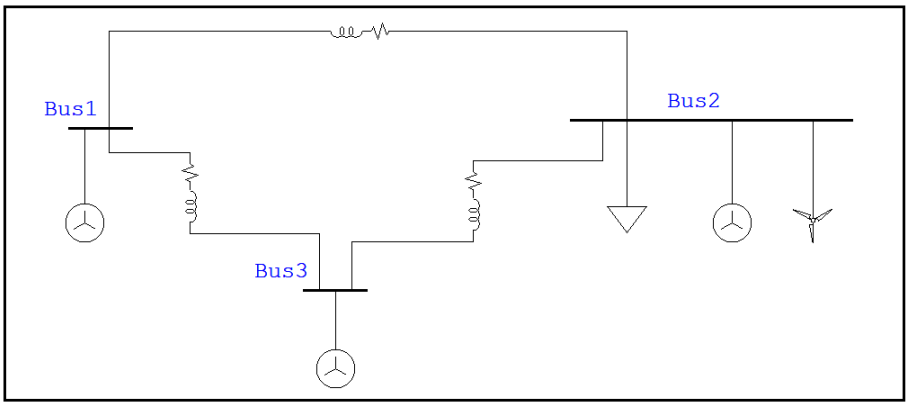


Figure 5.1: Proposed system

illustrates the wind frequency histogram and Weibull distribution for all wind speeds in Dhahran. The system is modeled using GAMS [24] and solved accordingly using MILP technique. Figure 5.3 illustrates the wind speed during the first twenty-four hours. Table 5.2 shows the characteristics of the generation units and Table 5.3 shows the characteristics of the transmission lines. Figure 5.4 shows the load profile of the IEEE 24-bus RTS during the first twenty-four hours.

$$f(t,c,k) = \begin{cases} \frac{k}{c}(\frac{t}{c})^{k-1} e^{-(\frac{t}{c})^k} & t \geq 0 \\ 0 & t < 0 \end{cases} \tag{5.22}$$

## 5.4 Results and Analysis

The system has been simulated to optimally size and allocates an ESS in a proposed microgrid. One of the impacts of integrating an ESS with a power system is reducing the total operating costs. It is proved that integrating an ESS with a microgrid enhances its reliability regarding increasing the availability and reducing the total

Table 5.1: Weibull parameters for monthly wind speed distribution in Dhahran [1]

| Month | $k$ | $c$ |
|---|---|---|
| JAN | 2.40 | 4.77 |
| FEB | 2.45 | 4.85 |
| MAR | 2.55 | 5.15 |
| APR | 2.40 | 5.06 |
| MAY | 2.40 | 5.52 |
| JUN | 2.60 | 6.51 |
| JUL | 2.50 | 5.54 |
| AUG | 2.30 | 4.91 |
| SEP | 2.20 | 4.18 |
| OCT | 2.05 | 4.09 |
| NOV | 2.20 | 4.38 |
| DEC | 2.00 | 4.68 |

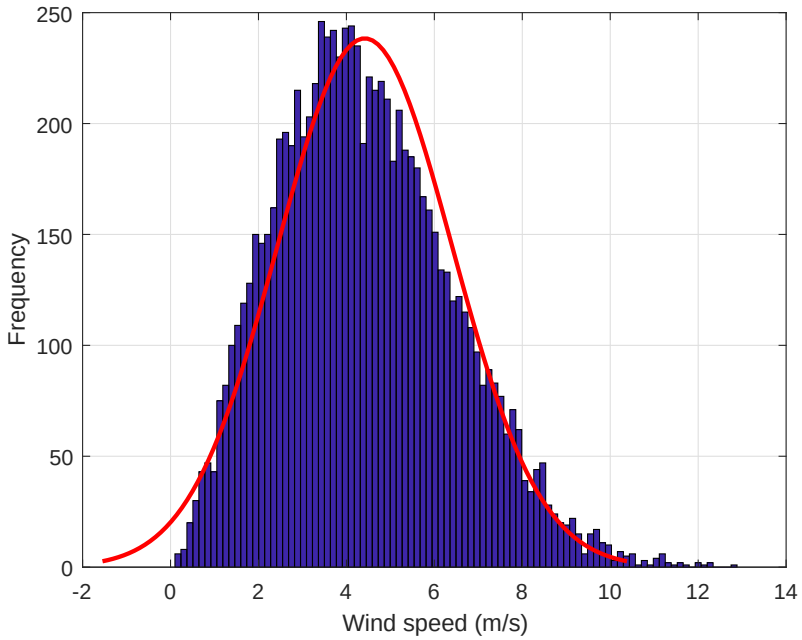


Figure 5.2: Wind frequency histogram and Weibull distribution for all wind speeds in Dhahran

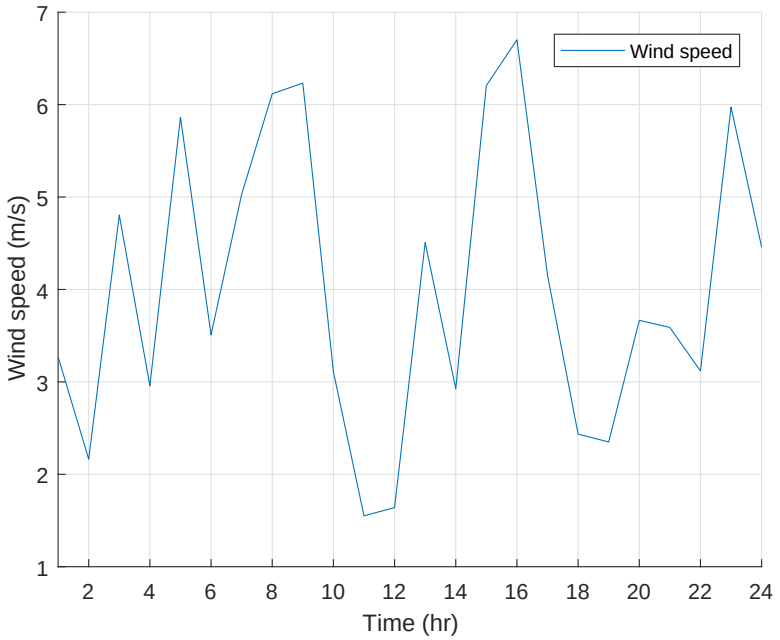


Figure 5.3: Wind speed during the first twenty-four hours

Table 5.2: Characteristics of generation units

| Unit No. | Fixed Cost ($) | Variable Cost ($/MW) | Start Up Cost ($) | Shut Down Cost ($) | Min. Capacity (MW) |
|---|---|---|---|---|---|
| 1 | 9 | 20 | 40 | 20 | 5 |
| 2 | 7 | 18 | 30 | 20 | 3 |
| 3 | 5 | 15 | 20 | 20 | 2 |
| Unit No. | Max. Capacity (MW) | Ramp Down Rate (MW/h) | Ramp Up Rate (MW/h) | Min. Down Time (h) | Min. Up Time (h) |
| 1 | 20 | 15 | 15 | 1 | 1 |
| 2 | 30 | 15 | 15 | 1 | 1 |
| 3 | 40 | 20 | 20 | 1 | 1 |

Table 5.3: Other parameters used in the model

| Parameter | $\eta_c$ | $\eta_d$ | $VOLL$ | $VWC$ |
|---|---|---|---|---|
| Value | 0.95 | 0.9 | 10,000 | 50 |

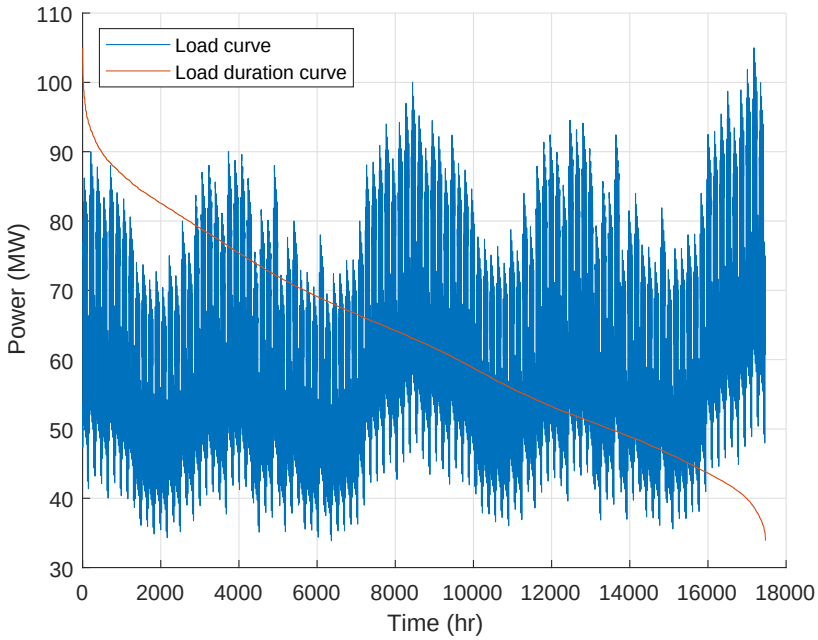


Figure 5.4: Load curve and load duration curve

cost of operation and maintenance. The total cost including the investment cost of the ESS is less than the total cost without investing in building the ESS. The results could be enhanced more if the planning is run for a longer horizon.

The optimal size of the ESS has been found to be 15.876 MW and 112.692 MWh. This means that the investment cost of ESS is $52,858.8. The optimal allocation of the ESS has been found to be 15.686 MW at Bus 2 and 0.189 MW at Bus 3. This is the optimal allocation that minimizes the operation cost to enhance the system reliability.

The DC optimal power flow assures that the input and output powers are equal at each bus. Also, a transmission line cannot carry the power that exceeds its limit. Losses calculation are ignored in DC optimal power flow, but they are considered in the AC optimal power flow problem. At each hour, the summation of the output power of all generation units, wind farm, and ESS is equal to the hourly demand. This equality is achieved with the minimum possible cost.

## 5.5 Summary

This chapter studies a technique to optimally size and allocates energy storage (ESS) system in a microgrid by solving the DC optimal power flow problem using mixed-integer linear programming (MILP) technique. The microgrid is a proposed 3-bus system integrated with a wind farm and an ESS. This chapter illustrates how a storage chapter, a 2-year horizon is considered. However, the results will get enhanced and improved in case of simulating a longer horizon. This helps in deciding on the size

and location of ESSs in a microgrid integrated with renewable energy or to build it in a power system in general.

# CHAPTER 6

# OPTIMAL POWER FLOW OF MICROGRIDS

## 6.1 Motivation

Optimal power flow (OPF) problem is the problem of calculating the optimal dispatch of each generator subject to transmission constraints. This problem is an optimization problem and could be solved using different optimization techniques. This chapter studies how to solve the DC OPF problem using linear programming of an IEEE test system integrated with wind farms and an energy storage system (ESS). Also, this chapter compares the power system before integrating the ESS and after integrating it regarding operating costs, load shedding and wind curtailment to investigate the impacts of integrating an ESS.

## 6.2 Problem Formulation

The objective of this chapter is to solve the optimal power flow (OPF) problem in a power system. The objectives of the OPF problem are to find the optimal dispatch of each generator and power flowing in branches connecting buses. So, the OPF problem includes the unit commitment problem which includes the economic dispatch problem. The OPF problem can be a single-period problem or multi-period problem. Also, it can be AC or DC. In this chapter, the multi-period DC OPF is formulated and solved. This section illustrates the formulation of this problem. This problem is a constrained optimization problem, and it is solved using linear programming. The equations are explained in [24].

The objective is to minimize the objective function which represents operating costs. The objective function is formulated in (6.1).

$$IC = PC * P_S^R + EC * E_S^R \tag{6.1}$$

$$OC = \sum_{g,t} b_g \ P_{g,t} + \sum_{i,t} VOLL \times LS_{i,t} + VWC \times P_{i,t}^{wc} \tag{6.2}$$

In (6.1), $OC$ is the operating costs in dollars, $g$ is the index of thermal generating units, $t$ is the index of time which is hour, $b_g$ is the fuel cost coefficient of thermal unit $g$, $P_{g,t}$ is the active power generated by thermal unit $g$ at time $t$ in MW, $VOLL$ is the value of loss of load in \$/MWh, $LS_{i,t}$ is the load shedding in bus $i$ at time $t$ in MW, $VWC$ is the value of loss of wind in \$/MWh and $P_{i,t}^{wc}$ is the curtailed power of wind

turbine connected to bus $i$ at time $t$ in MW.

The nodal power balance is a constraint in this problem, and it is formulated in (6.3).

$$\sum_{g \in \Omega_G^i} P_{g,t} + LS_{i,t} + P_{i,t}^w - L_{i,t} - P_{i,t}^c + P_{i,t}^d = \sum_{j \in \Omega_l^i} P_{ij,t} \tag{6.3}$$

In (6.3), $\Omega_G^i$ is the set of all thermal generating units connected to bus $i$, $\Omega_l^i$ is the set of all buses connected to bus $i$, $i$ and $j$ are indices of network buses, $P_{g,t}$ is the active power generated by thermal unit $g$ at time $t$ in MW, $P_{i,t}^w$ is the active power generated by wind turbine connected to bus $i$ at time $t$ in MW, $L_{i,t}$ is the electric power demand in bus $i$ at time $t$ in MW, $P_{i,t}^c$ is the charging power of the ESS in bus $i$ at time $t$ in MW, $P_{i,t}^d$ is the discharging power of the ESS in bus $i$ at time $t$ in MW and $P_{ij,t}$ is the active power flow of branch connecting bus $i$ to bus $j$ at time $t$ in MW.

The active flow in a branch connecting bus $i$ to bus $j$ is calculated in (6.4).

$$P_{ij,t} = \frac{\delta_{i,t} - \delta_{j,t}}{x_{ij}} \tag{6.4}$$

In (6.4), $\delta_{i,t}$ is the voltage angle at bus $i$ at time $t$ in radians and $x_{ij}$ is the reactance of branch connecting bus $i$ to bus $j$ in $\Omega$.

The branch flow limits of every branch is formulated in (6.5).

$$-P_{ij}^{max} \leq P_{ij,t} \leq P_{ij}^{max} \tag{6.5}$$

In (6.5), $P_{ij}^{max}$ is the maximum power flow limits of branch connecting bus $i$ to

bus $j$ in MW.

Every thermal unit has a minimum limit for operation with stability. Also, it has a maximum limit that cannot be exceeded. The operating limits of the thermal generating unit are modeled in (6.6).

$$P_g^{min} \leq P_{g,t} \leq P_g^{max} \tag{6.6}$$

In (6.6), $P_g^{min}$ is the minimum limit of power generation of thermal unit $g$ in MW and $P_g^{max}$ is the maximum limit of power generation of thermal unit $g$ in MW.

Every thermal unit has ramp rates. This means if the power is increasing, it is increasing according to a limited rate. This is happening if the power is decreasing as well. The ramp rates of thermal units are described in (6.7) and (6.8).

$$P_{g,t} - P_{g,t-1} \leq RU_g \tag{6.7}$$

In (6.7), $RU_g$ is the ramp-up rate of thermal unit $g$ in \$/MWh.

$$P_{g,t-1} - P_{g,t} \leq RD_g \tag{6.8}$$

In (6.8), $RD_g$ is the ramp-down rate of thermal unit $g$ in \$/MWh.

The load shedding is limited to the existing demand at the same bus as described in (6.9).

$$0 \leq LS_{i,t} \leq L_{i,t} \tag{6.9}$$

The wind power curtailment is formulated in (6.10).

$$P_{i,t}^{wc} = w_{i,t}\Lambda_i^w - P_{i,t}^w \tag{6.10}$$

In (6.10), $w_{i,t}$ is the availability of wind turbine connected to bus $i$ at time $t$ and $\Lambda_i^w$ is the capacity of wind turbine connected to bus $i$ in MW.

The amount of wind power depends on its availability and capacity as formulated in (6.11).

$$0 \leq P_{i,t}^w \leq w_{i,t}\Lambda_i^w \tag{6.11}$$

The state of charge of an ESS is calculated as described in (6.12). The state of charge of an ESS is the stored energy.

$$SOC_{i,t} = SOC_{i,t-1} + (P_{i,t}^c\eta_c - \frac{P_{i,t}^d}{\eta_d})\Delta_t \tag{6.12}$$

In (6.12), $SOC_{i,t}$ is the state of charge of ESS in bus $i$ at time $t$ in MWh, $\eta_c$ is the charging efficiency, $\eta_d$ is the discharging efficiency and $\Delta_t$ is time step in hours.

The charging and discharging powers of an ESS are limited as described in (6.12) and (6.13), respectively.

$$P_{i,min}^c \leq P_{i,t}^c \leq P_{i,max}^c \tag{6.13}$$

In (6.13), $P_{i,min}^c$ is the minimum charging power of ESS in bus $i$ in MW and $P_{i,max}^c$ is the maximum charging power of ESS in bus $i$ in MW.

$$P^d_{i,min} \leq P^d_{i,t} \leq P^d_{i,max} \tag{6.14}$$

In (6.14), $P^d_{i,min}$ is the minimum discharging power of ESS in bus $i$ in MW and $P^d_{i,max}$ is the maximum discharging power of ESS in bus $i$ in MW.

The state of charge of an ESS is limited by its minimum and maximum as described in (6.14).

$$SOC_{i,min} \leq SOC_{i,t} \leq SOC_{i,max} \tag{6.15}$$

In (6.15), $SOC_{i,min}$ is the minimum state of charge of ESS in bus $i$ in MWh and $SOC_{i,max}$ is the maximum state of charge of ESS in bus $i$ in MWh.

## 6.3 Case Study

The system used for this case study is a modified IEEE 24-bus RTS-1996 [74] with the same load profile, generation units, and branch data. The power flow in the system is modeled using DC power flow assumptions and constraints to be solved using linear programming. Four wind farms were added to the system at busses 3, 5, 7 and 16 as recommended by [74]. The capacities of those wind farms are 20% of the maximum load at each respective bus. By using Weibull distribution parameters for wind speed in Dhahran [1], a profile for wind turbines generated power was produced and used for this study. Since all busses selected are in a single area, the inter-bus variation of wind speed is ignored. Also, this study assumes that the capacity, rating, and location

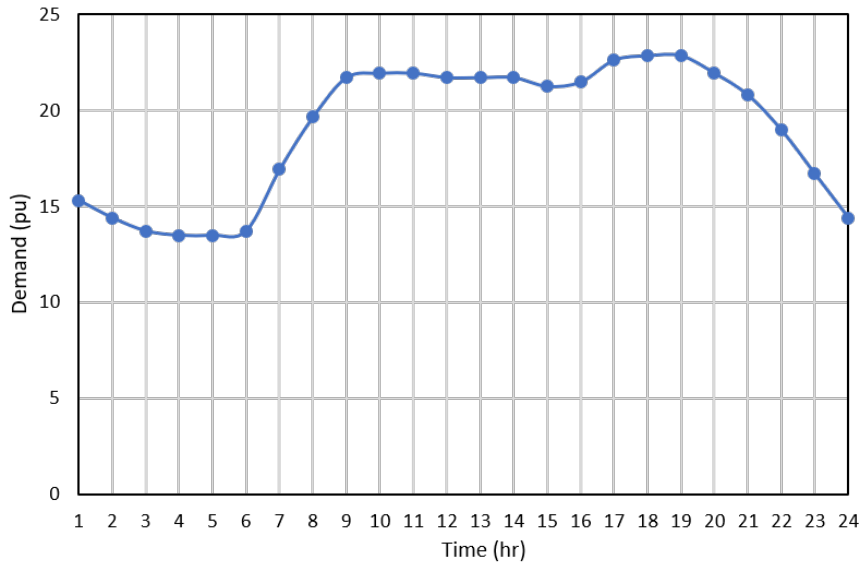


Figure 6.1: Load profile during the first twenty-four hours

of ESS have been determined in the planning phase. The industry recommends ESS capacity equate to 15-20% of total installed wind capacity [60]. The locations selected for placing ESS are busses 8 and 14. A base case without adding ESS to the system is considered first. Followed by the complete power system. In both cases, the system is modeled using GAMS [24] and solved accordingly using linear programming. Table 6.1 shows the capacities of wind farms and ESS and Table 6.2 shows other parameters used the model. Figure 6.1 shows the load profile of the IEEE test system during the first twenty-four hours.

## 6.4 Results and Analysis

The system has been simulated in two cases. The first case is simulating the system without an ESS and the second case includes the ESS. One of the impacts of integrating an ESS with a power system is reducing the total operating costs. Also, the

Table 6.1: Capacities of wind farms and ESS

| Type | Bus | Capacity (MW) |
|---|---|---|
| Wind farm | 3 | 36 |
| Wind farm | 5 | 14.2 |
| Wind farm | 7 | 25 |
| Wind farm | 16 | 20 |
| ESS | 8 | 9.52 |
| ESS | 14 | 9.52 |

Table 6.2: Other parameters used in the model

| Parameter | $\eta_c$ | $\eta_d$ | $VOLL$ | $VWC$ |
|---|---|---|---|---|
| Value | 0.95 | 0.9 | 10,000 | 50 |

ESS reduces the load shedding and wind curtailment. Table 6.3 shows the results of operating costs, load shedding and wind curtailment for both cases and Table 6.4 shows how these parameters have improved in Case 2 compared with Case 1. The improvement could be enhanced if the simulation is run for a longer horizon.

For the first twenty-four hours, Figure 6.2 shows the scheduling in the first case for all generating units. Figure 6.3 shows the wind power distribution in both cases. The wind power is the same in both cases because it is considered as a free energy source.

Table 6.3: Results of Case 1 and Case 2

| Item | Case 1 | Case 2 |
|---|---|---|
| Operating cost | \$143,005,573.55 | \$141,398,817.10 |
| Load shedding | 376.44 MW | 240.43 MW |
| Wind curtailment | 6,955.76 MW | 5,837.71 MW |

Table 6.4: Percentage difference of Case 1 and Case 2

| Item | Difference |
|---|---|
| Operating cost | 1.12% |
| Load shedding | 36.13% |
| Wind curtailment | 16.07% |

Figure 6.4 shows the total generation of thermal units and wind farms during the first twenty-four hours in Case 1. Figure 6.5 shows the scheduling in the second case for all generating units. Figure 6.6 shows the total generation of thermal units, wind farms and ESS during the first twenty-four hours in Case 2. Figure 6.7 shows Figure 6.6 after zooming in to show the ESS power. There is a difference in scheduling generating units between the two cases to achieve the minimum possible cost. Figure 6.8 illustrates how the ESS contributes to supplying energy and reducing generation costs. Storage systems charge in low-price periods and discharge in high-price periods [10] and this reduces the operating costs a lot. Also, Figure 6.8 shows the state of charge of the ESS, and this represents the energy stored in ESS at every hour.

## 6.5 Summary

This chapter studies a technique to solve the DC optimal power flow problem using linear programming of an IEEE test system integrated with wind farms and an energy storage system. This chapter illustrates how a storage system could reduce the operating costs of a power system, load shedding, and wind curtailment. Integrating an ESS with a power system makes it more reliable and economical. In the case study

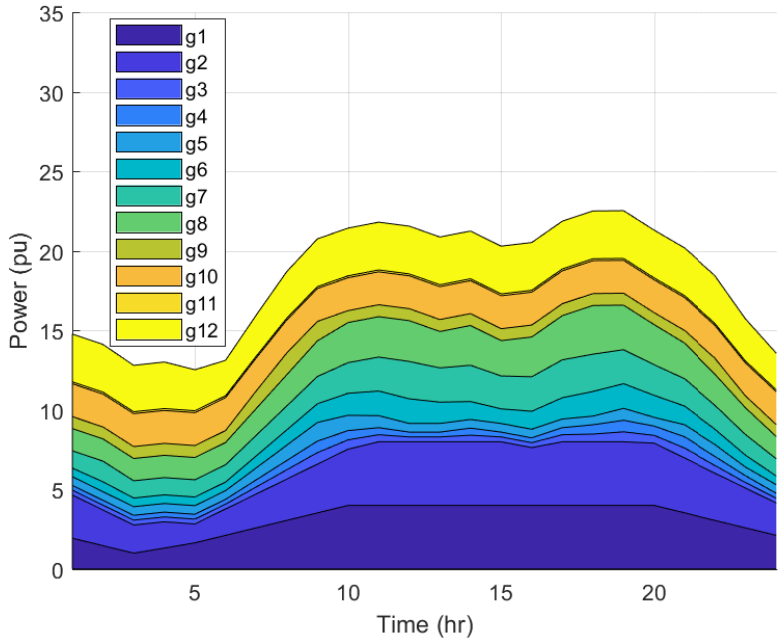


Figure 6.2: Generation units scheduling in Case 1 during the first twenty-four hours

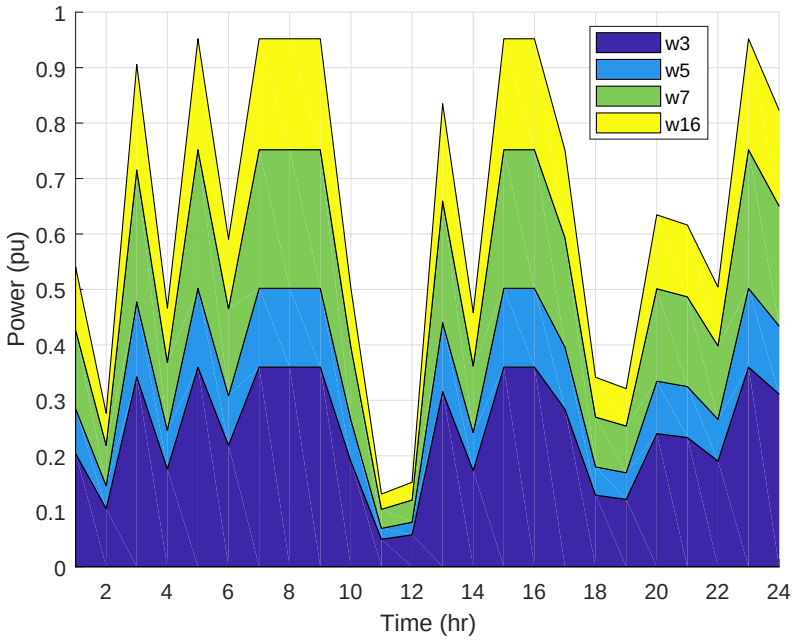


Figure 6.3: Wind power distribution in both cases during the first twenty-four hours

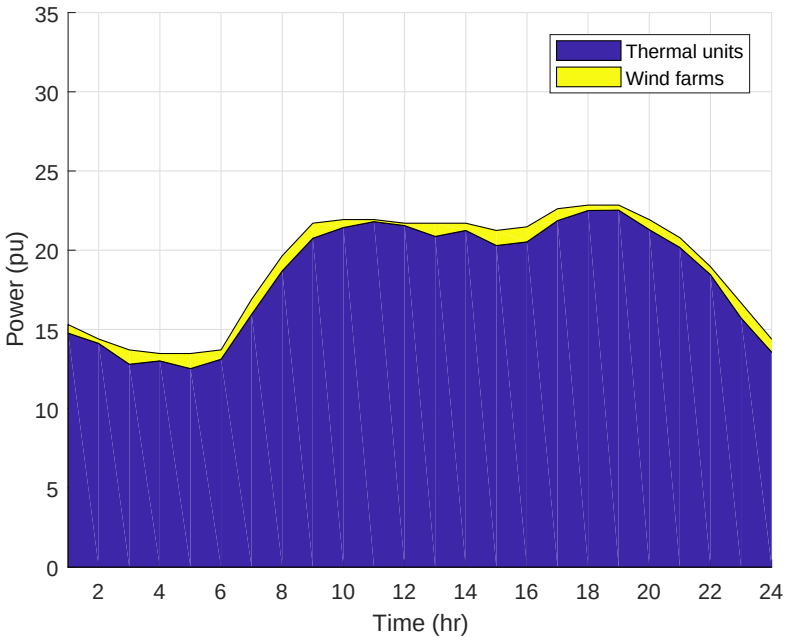


Figure 6.4: Total generation of units and wind in Case 1 during the first twenty-four hours

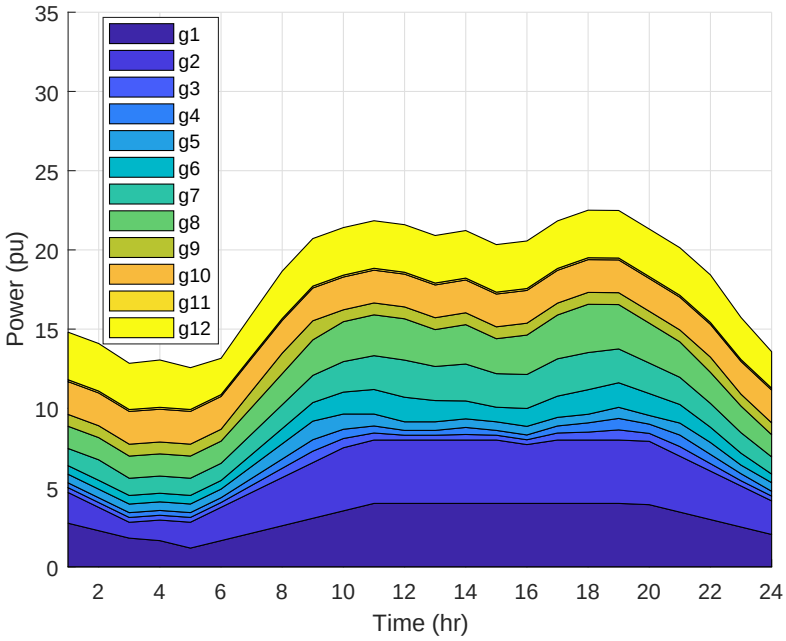


Figure 6.5: Generation units scheduling in Case 2 during the first twenty-four hours

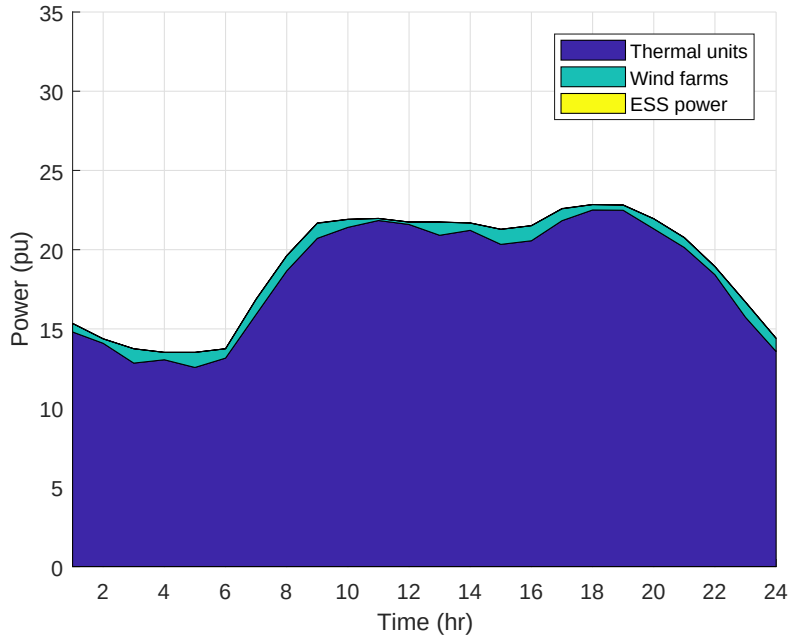


Figure 6.6: Total generation of units, wind and ESS in Case 2 during the first twenty-four hours

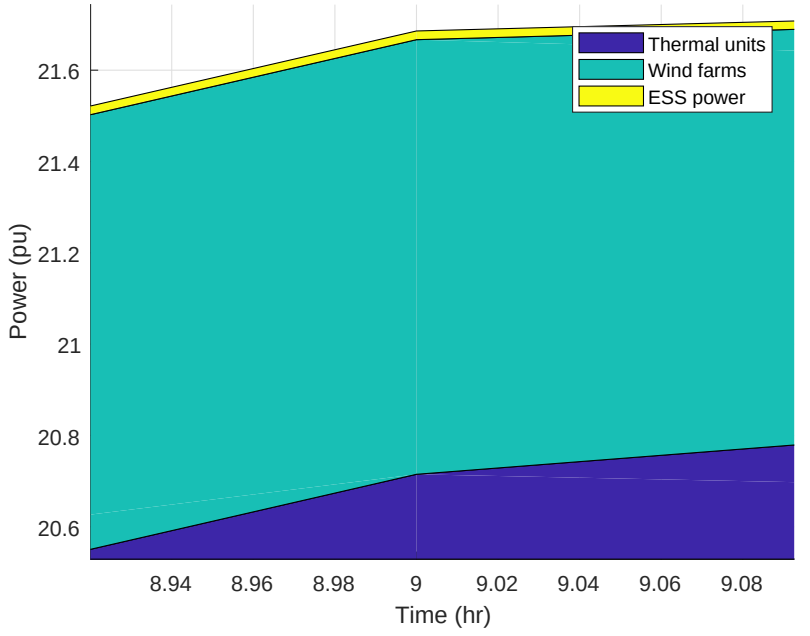


Figure 6.7: Total generation of units, wind and ESS in Case 2 during the a very small period

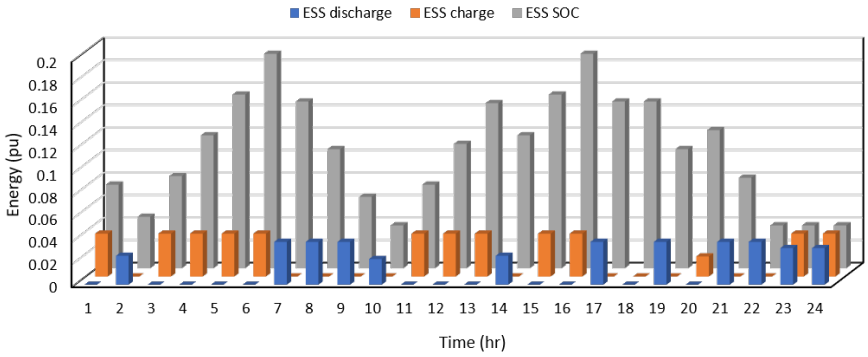


Figure 6.8: ESS output power in both cases during the first twenty-four hours

discussed in this chapter, the difference between the two cases is not very significant, especially regarding operating costs. However, this difference could be enhanced and improved in case of simulating a longer horizon. This helps in deciding on investing to build an ESS in a power system with wind generation and RES in general.

# CHAPTER 7

# RELIABILITY ASSESSMENT OF MICROGRIDS WITH RENEWABLE ENERGY SOURCES AND HYBRID STORAGE SYSTEMS

## 7.1 Motivation

Reliability assessment of power systems is one of the most important measurements to maintain continuous availability and evaluate suppliers' services. There are many techniques that have been developed to evaluate the reliability of a power system. Also, there are many ways and methods to enhance reliability. For example, inte-

grating renewable energy sources and energy storage systems with a power system enhances its reliability. This chapter presents a way to evaluate the reliability of a microgrid connected to the main grid and renewable energy sources. The method used in this chapter to evaluate the reliability is the reliability block diagram (RBD) method. Also, this chapter compares the reliability of the microgrid in different cases.

## 7.2 Problem Formulation

The availability of a component or system is the probability of the time that the component or system will be available during it, so the unavailability is the remaining probability as formulated in (7.1) [75], [76].

$$U = 1 - A \tag{7.1}$$

In (7.1), $U$ is the unavailability and $A$ is the availability.

The availability and unavailability are calculated from the mean time to fail of a component or system and the mean time to repair of a component or system as formulated in (7.2) and (7.3), respectively.

$$A = \frac{MTTF}{MTBF} \tag{7.2}$$

In (7.2), $MTTF$ is the mean time to fail and $MTBF$ is the mean time between failures.

$$U = \frac{MTTR}{MTBF} \tag{7.3}$$

In (7.3), $MTTR$ is the mean time to repair.

The mean time between failures of a component or system is calculated as formulated in (7.4).

$$MTBF = MTTF + MTTR \tag{7.4}$$

Also, the failure and repair rates can be used to calculate the availability and unavailability as formulated in (7.7) and (7.8), respectively.

$$\lambda = \frac{1}{MTTF} \tag{7.5}$$

In (7.5), $\lambda$ is the failure rate.

$$\mu = \frac{1}{MTTR} \tag{7.6}$$

In (7.6), $\mu$ is the repair rate.

These equations give (7.7) and (7.8).

$$A = \frac{\mu}{\lambda + \mu} \tag{7.7}$$

$$U = \frac{\lambda}{\lambda + \mu} \tag{7.8}$$

Components in a power system could be connected in parallel or series. There are different equations to calculate the overall reliability, and this difference depends on the connection type of components. In Sections 7.2.1 and 7.2.2, these equations are formulated for parallel and series components, respectively. It is assumed that the number of components is two. The equations can be derived for more than two com-

ponents in the same way. In Section 7.2.3, the equations of calculating the reliability indices are formulated.

### 7.2.1 Parallel Components

For components connected in parallel in a power system, the equivalent unavailability is equal to the product of all individual unavailabilities as formulated in (7.9).

$$U_{sys} = U_1 U_2 \tag{7.9}$$

So, the equivalent availability is calculated as formulated in (7.10).

$$A_{sys} = 1 - U_{sys} \tag{7.10}$$

$$A_{sys} = 1 - \frac{MTTR_1}{MTTF_1 + MTTR_1} \cdot \frac{MTTR_2}{MTTF_2 + MTTR_2} \tag{7.11}$$

Using the failure and repair rates:

$$\lambda_{sys} = \frac{(\mu_1 + \mu_2)\lambda_1\lambda_2}{\mu_1\mu_2 + \lambda_1\mu_2 + \lambda_2\mu_1} \tag{7.12}$$

The equivalent MTTF and MTTR are calculated simply as shown in (7.13) and (7.14).

$$MTTF_{sys} = \frac{1}{\lambda_{sys}} \tag{7.13}$$

$$MTTR_{sys} = \frac{1}{\mu_{sys}} \tag{7.14}$$

### 7.2.2 Series Components

For components connected in series in a power system, the equivalent availability is equal to the product of all individual availabilities as formulated in (7.15).

$$A_{sys} = A_1 A_2 \tag{7.15}$$

So, the equivalent unavailability is calculated as formulated in (7.16).

$$U_{sys} = 1 - A_{sys} \tag{7.16}$$

$$U_{sys} = 1 - \frac{MTTF_1}{MTTF_1 + MTTR_1} \cdot \frac{MTTF_2}{MTTF_2 + MTTR_2} \tag{7.17}$$

Using the failure and repair rates:

$$\mu_{sys} = \frac{(\lambda_1 + \lambda_2)\mu_1\mu_2}{\lambda_1\lambda_2 + \lambda_1\mu_2 + \lambda_2\mu_1} \tag{7.18}$$

The equivalent MTTF and MTTR are calculated simply as shown in (7.19) and (7.20).

$$MTTF_{sys} = \frac{1}{\lambda_{sys}} \tag{7.19}$$

$$MTTR_{sys} = \frac{1}{\mu_{sys}} \tag{7.20}$$

### 7.2.3 Reliability Indices

The reliability indices are calculated as illustrated in [77]:

$$SAIDI = \frac{Total\ duration\ of\ all\ interruptions}{Total\ number\ of\ customers\ connected} \tag{7.21}$$

$$SAIDI = \frac{\sum_{i=1}^{n} r_i N_i}{N_T} \tag{7.22}$$

$$SAIFI = \frac{Total\ number\ of\ all\ interruptions}{Total\ number\ of\ customers\ connected} \tag{7.23}$$

$$SAIFI = \frac{\sum_{i=1}^{n} N_i}{N_T} = \frac{\sum_{i=1}^{n} \lambda_{LP} N_{LP}}{N_T} \tag{7.24}$$

$$CAIDI = \frac{Total\ duration\ of\ all\ interruptions}{Total\ number\ of\ all\ interruptions} \tag{7.25}$$

$$CAIDI = \frac{\sum_{i=1}^{n} r_i N_i}{N_T} = \frac{SAIDI}{SAIFI} \tag{7.26}$$

## 7.3 Methodology

In this chapter, the proposed system for reliability assessment is shown in Figure 7.1. This system has two renewable energy sources, solar and wind, and a direct connection to the network (electric grid). To study the reliability of this system, all possible scenarios of the microgrid must be considered. For instance, if the energy storage system is fully charged, then it will be considered as a source. Otherwise it may be considered as a load, but it will not affect the actual load of the proposed system. RBD and Monte Carlo methods are used to determine all reliability indices for

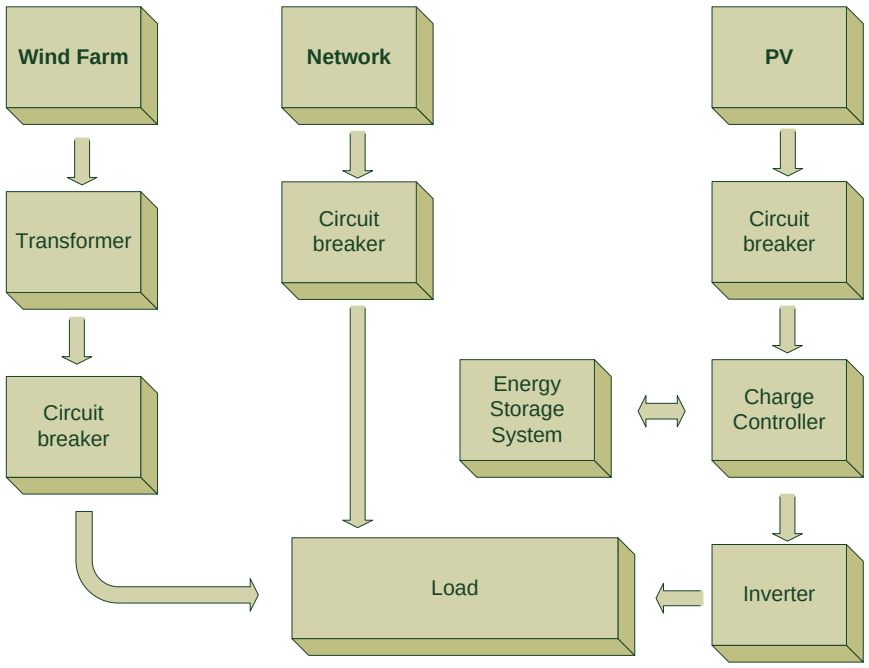


Figure 7.1: The proposed renewable energy microgrid system

the proposed system and compare it to the system when the load is directly connected to the network. The proposed cases to study the reliability indices are:

- The effect of losing PV on reliability indices of the load.
- The effect of losing Wind farm on reliability indices of the load.
- The effect of losing Network on reliability indices of the load.

## 7.4 Case Study

To study the system reliabilities indices, failure rate and mean time to repair must be identified for each component of the system. The breakdown of the proposed system

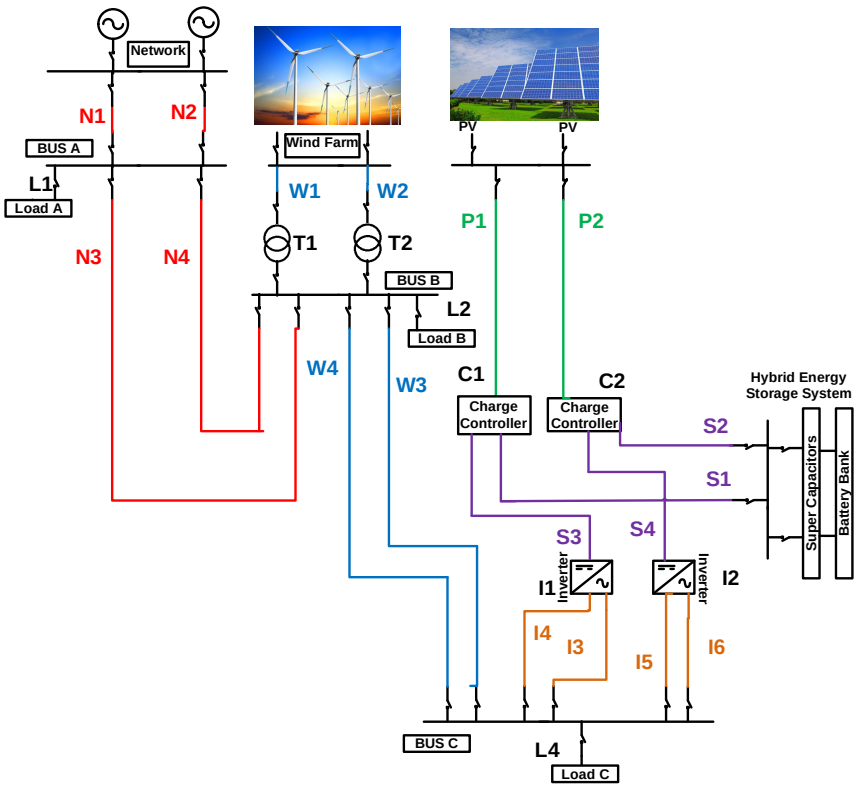


Figure 7.2: The proposed renewable energy microgrid system

components are shown in Figure 7.2 and Table 7.1. The microgrid is simplified in Figure 7.3 for easy modeling and calculation. For instance, N1 and N2 are two lines feeding the microgrid from the network, which are considered to be connected in parallel, can be modeled as F1 with equivalent mean time to repair and mean time to fail of both of the components.

To study the system reliabilities indices of load A, the system must be configured as seen from load A. Figure 7.3 shows the RBD of the system as seen from load A. As this figure shows, the RBD of Load A has many series and parallel components. To calculate the values of equivalent mean times to repair ($\mu$) and fail ($\lambda$) of load A using the RBD method, all components of the proposed microgrid have to be combined.

In this chapter three cases of a study carried out for each load point. The first case

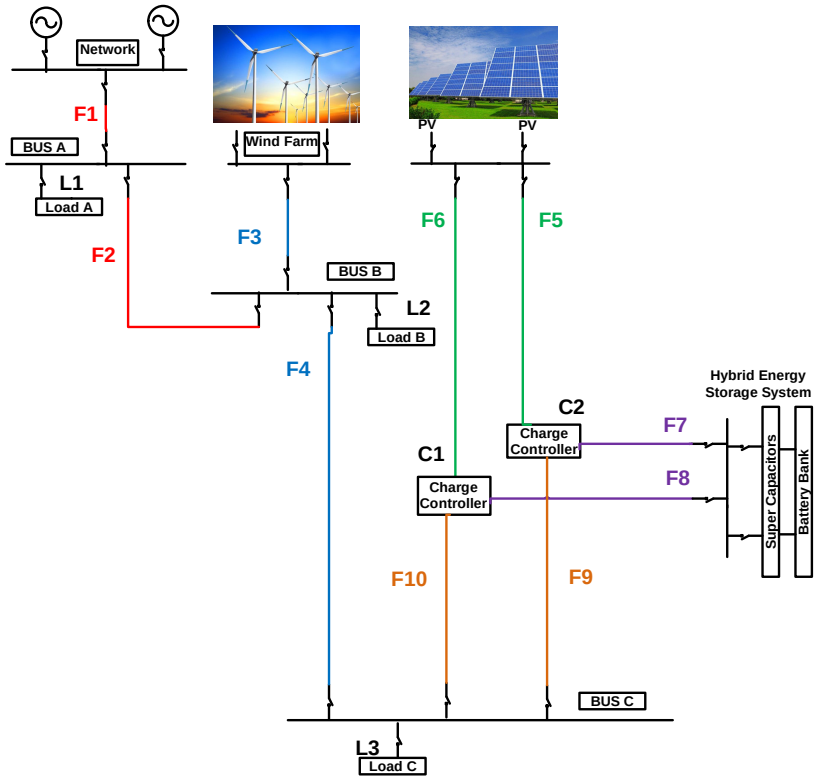


Figure 7.3: The simplified proposed renewable energy microgrid system

Table 7.1: System Components

| Component | Failure Rare $\lambda$ (failures/year) | MTTR (hr) |
|---|---|---|
| N | 0.2 | 4 |
| W | 0.3 | 3 |
| T | 0.1 | 4 |
| I | 0.3 | 3 |
| P | 0.35 | 3 |
| S | 0.35 | 2 |
| Load line | 0.4 | 1 |
| Inverter | 0.3 | 3 |
| Charge controller | 0.35 | 2 |

Table 7.2: Reduced system components

| Component | Failure Rare $\lambda$ (failures/year) | MTTR (hr) |
|---|---|---|
| F1 | 0.3077 | 2 |
| F2 | 0.3077 | 2 |
| F3 | 0.269 | 0.4875 |
| F4 | 0.4954 | 1.5 |
| F5 | 0.35 | 3 |
| F6 | 0.35 | 3 |
| F7 | 0.35 | 2 |
| F8 | 0.35 | 2 |
| F9 | 1.1454 | 0.758 |
| F10 | 1.1454 | 0.758 |
| C1 | 0.35 | 2 |
| C2 | 0.35 | 2 |
| L1 | 0.4 | 1 |
| L2 | 0.4 | 1 |
| L3 | 0.4 | 1 |
| L4 | 0.4 | 1 |

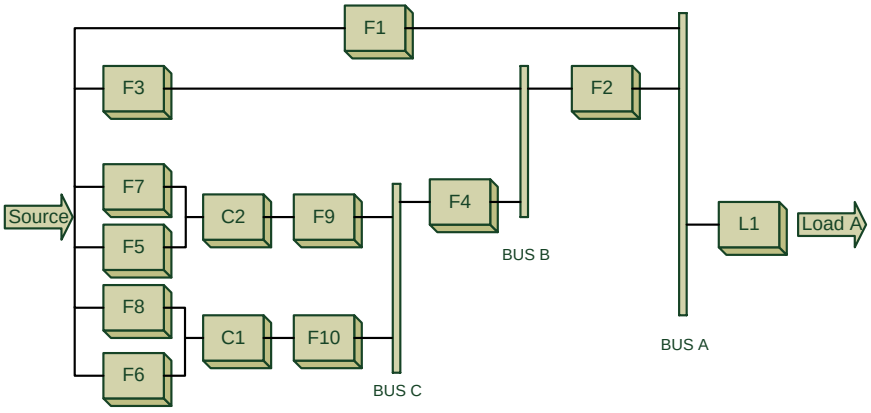


Figure 7.4: Load A RBD of the microgrid

where all the renewable energy sources and the network are working. The Reliability indices (SAIFI, SAIDI, CAIDI, ASAI, and ASUI) of this case are calculated Using RBD and Monte Carlo's simulation. This second case, the wind farm is assumed to be out and the whole system for load A is recalculated using both methods. The third case, losing the PV and energy storage system is assumed. After Calculating the reliability indices of the load A using Monte Carlo's method and RBD, a comparison is carried out to estimate the difference between both methods in identifying the reliability indices and the calculating the whole system reliability indices. The same methods are then carried out for both loads B and C, see Figure 7.4 and Figure 7.5.

## 7.5 Analysis and Results

In this chapter, the microgrid is presented to study the effects on renewable energy sources on the reliability indices, SAIFI, SAIDI, CAIDI, ASAI, and ASUI. Its already known that if the number of energy sources are increased the reliability indices will increase too, but by how much will effects the load reliability indices and how many

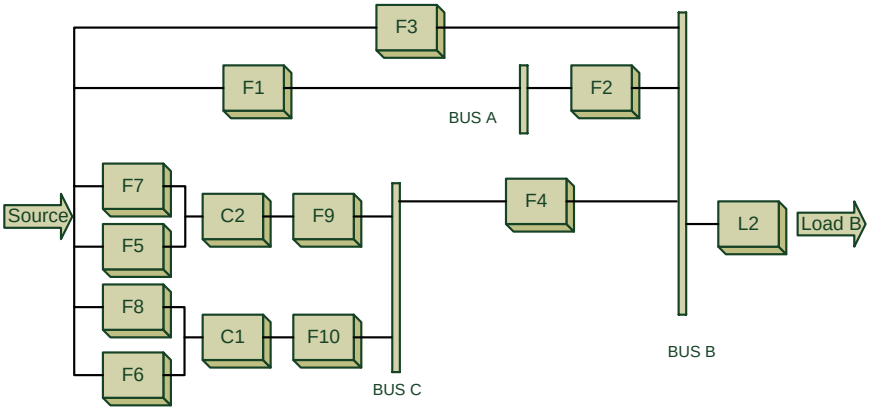


Figure 7.5: Load B RBD of the microgrid

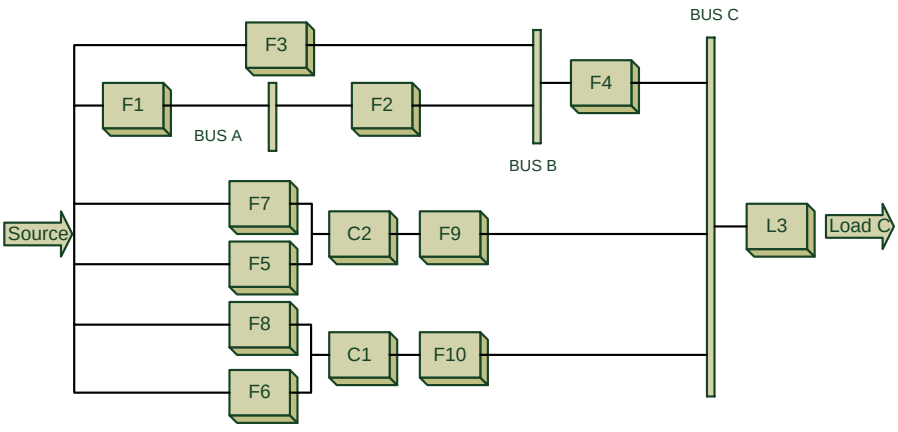


Figure 7.6: Load C RBD of the microgrid

of renewable energy sources will suffice to optimized the microgrid and where it is the best location of these renewable energy sources to be connected from the reliability point of view the.

In this section, the indices obtained from simulation are compared to those obtained analytically, using the RBD method. Since there are three different loads in different locations in the microgrid, the microgrid must be remodeled to each load point of view see Figures, 7.4, 7.5, and 7.6. Introducing the renewable energy sources will effect the reliability indices but where in the micro grid is best located for which load. To give a detailed study of each the load point, Figures 7.4, 7.5, and 7.6 are presented, which were driven from the main circuit shown in Figure 7.3, to simplify the model and calculate the total effects of each component on the system on the reliability indices of each load points. In addition, detail calculations and simplification of the system for each load point is shown in Table 7.7, 7.8, and 7.9. Furthermore, the effects of losing one of the energy sources wither the main network feeders, or one of the renewable energy sources are calculated and shown in detail for each load point and the system in general in Table 7.5.

Monte Carlo's method is used to simulate the system for each load point in each case for 1000 years as shown in Table 7.4. Since Monte Carlo's method is a computer algorithm based on sampling number, the results of the simulations are not a complete match to the analytical results of RBD. If the numbers of simulated years were increased, even more, the simulation result would come even closer to the actual analytical solution, but in the cost of simulation time.

Tables 7.4 and 7.5 shows the reliability indices of-of each load point in the microgrid

Table 7.3: Number of customers at each load point

| Load | $N_{costumers}$ |
|---|---|
| Load A | 50 |
| Load B | 30 |
| Load C | 20 |
| Total | 100 |

as well for the entire system. Case 1 in tables 7.4 and 7.5 shows the reliability indices of each load in case all the renewable energy sources and the network is working. This case study could be taken as the reference study for the presented microgrid and compared with the other cases. Case 2, study the effects of losing the wind farm to each of the loads and the microgrid reliability indices. Case 3 shows how losing the solar power will affect the reliability indices of each load and the entire microgrid.

Table 7.6 shows the reliability indices of the entire microgrid in case of losing one of the renewable energy sources. As shown, losing the solar energy source has a little effect on the reliability indices of the microgrid, while losing the wind farms will have huge effects the reliability indices of the microgrid. This is not due to lack of energy from the solar panel but where those renewable energy sources are connected in the microgrid and the load distribution as well.

## 7.6 Summary

In this chapter, the reliability indices of the microgrid were calculated using RBD and simulated using Monte Carlo's method. As it is shown that increasing the number of sampling using Monte Carlo's can yield an accurate result of the system, yet consume high computational time. Also, it shows that the reliability indices are affected by the

Table 7.4: Reliability indices of each load and the entire microgrid using Monte Carl's simulation

| Monte Carlo 1000 years | | | | |
|---|---|---|---|---|
| CASE 1 | | | | |
| | Load A | Load B | Load C | System |
| SAIFI | 0.695000 | 0.568000 | 0.618000 | 0.641500 |
| SAIDI | 0.177334 | 0.083796 | 0.107282 | 0.135262 |
| CAIDI | 0.255156 | 0.147528 | 0.173596 | 0.206556 |
| ASAI | 0.999979 | 0.999990 | 0.999987 | 0.999984 |
| ASUI | 0.000020 | 0.000009 | 0.000012 | 0.000015 |
| CASE 2 | | | | |
| | Load A | Load B | Load C | System |
| SAIFI | 1.456000 | 1.056000 | 0.956000 | 1.236000 |
| SAIDI | 0.649090 | 0.350903 | 0.263426 | 0.482501 |
| CAIDI | 0.445803 | 0.332294 | 0.275550 | 0.377700 |
| ASAI | 0.999925 | 0.999959 | 0.999969 | 0.999944 |
| ASUI | 0.000074 | 0.000040 | 0.000030 | 0.000055 |
| CASE 3 | | | | |
| | Load A | Load B | Load C | System |
| SAIFI | 0.738000 | 0.571000 | 0.583000 | 0.656900 |
| SAIDI | 0.170624 | 0.082764 | 0.091926 | 0.128527 |
| CAIDI | 0.231199 | 0.144946 | 0.157678 | 0.190619 |
| ASAI | 0.999980 | 0.999990 | 0.999989 | 0.999985 |
| ASUI | 0.000019 | 0.000009 | 0.000010 | 0.000014 |

Table 7.5: Reliability indices of each load and the entire microgrid using RBD

| CASE 1 | | | | |
|---|---|---|---|---|
| | Load A | Load B | Load C | System |
| SAIFI | 0.710110 | 0.566953 | 0.642793 | 0.653699 |
| SAIDI | 0.179177 | 0.079585 | 0.109211 | 0.135306 |
| CAIDI | 0.252323 | 0.140374 | 0.169901 | 0.206986 |
| ASAI | 0.999979 | 0.999990 | 0.999987 | 0.999984 |
| ASUI | 0.000020 | 0.000009 | 0.000012 | 0.000015 |
| CASE 2 | | | | |
| | Load A | Load B | Load C | System |
| SAIFI | 1.472759 | 1.060183 | 0.937820 | 1.241998 |
| SAIDI | 0.648939 | 0.347528 | 0.263400 | 0.481408 |
| CAIDI | 0.440628 | 0.327800 | 0.280865 | 0.387607 |
| ASAI | 0.999925 | 0.999960 | 0.999969 | 0.999945 |
| ASUI | 0.000074 | 0.000039 | 0.000030 | 0.000054 |
| CASE 3 | | | | |
| | Load A | Load B | Load C | System |
| SAIFI | 0.744106 | 0.571198 | 0.614295 | 0.666271 |
| SAIDI | 0.165171 | 0.081292 | 0.096086 | 0.126190 |
| CAIDI | 0.221972 | 0.142318 | 0.156418 | 0.189398 |
| ASAI | 0.999981 | 0.999990 | 0.999989 | 0.999985 |
| ASUI | 0.000018 | 0.000009 | 0.000010 | 0.000014 |

Table 7.6: Microgrid reliability indices comparison between all cases

| Comparison | | | |
|---|---|---|---|
| | Case 1 | Case 2 | Case 3 |
| SAIFI | 0.6536997197 | 1.2419989835 | 0.6662718558 |
| SAIDI | 0.1353068879 | 0.4814083521 | 0.1261907367 |
| CAIDI | 0.2069863025 | 0.3876076860 | 0.1893982698 |
| ASAI | 0.9999845540 | 0.9999450447 | 0.9999855946 |
| ASUI | 0.0000154459 | 0.0000549552 | 0.0000144053 |

Table 7.7: Case 1: Detailed RBD calculation of failure rate repair time of migrogrid when all sources are available

| CASE 1: ALL | | | |
|---|---|---|---|
| Load A | | $\lambda$ | r |
| F5//F7 | | 0.5456570 | 1.2000000 |
| C2+F9 | | 1.4954128 | 0.6744907 |
| (F5//F7)+C2+F9 | | 2.0410698 | 0.7233607 |
| ((F5//F7)+C2+F9) // ((F6//F8)+C1+F10) | A | 1.1666728 | 0.3616803 |
| A+F4 | | 1.6620856 | 0.5364063 |
| (A+F4)//F3 | | 0.3163214 | 0.2553925 |
| (A+F4)//F3+F2 | B | 0.6240137 | 0.2356425 |
| B//F1 | | 0.3601101 | 0.2108052 |
| B//F1+L1 | Total | 0.7101101 | 0.2523238 |
| | | | |
| Load B | | $\lambda$ | r |
| F5//F7 | | 0.5456570 | 1.2000000 |
| C2+F9 | | 1.4954128 | 0.6744907 |
| (F5//F7)+C2+F9 | | 2.0410698 | 0.7233607 |
| ((F5//F7)+C2+F9) // ((F6//F8)+C1+F10) | A | 1.1666728 | 0.3616803 |
| A+F4 | | 1.6620856 | 0.5364063 |
| (A+F4)//F3 | | 0.3163214 | 0.2553925 |
| F1+F2 | | 0.6153846 | 0.7692307 |
| ((A+F4)//F3)//(F1+F2) | | 0.1669534 | 0.1917346 |
| (((A+F4)//F3)//(F1+F2)) +L2 | Total | 0.5669534 | 0.1403742 |
| | | | |
| Load C | | $\lambda$ | r |
| F5//F7 | | 0.5456570 | 1.2000000 |
| C2+F9 | | 1.4954128 | 0.6744907 |
| (F5//F7)+C2+F9 | | 2.0410698 | 0.7233607 |
| ((F5//F7)+(C2+F9)) // ((F6//F8)+(C1+F10)) | A | 1.1666728 | 0.3616803 |
| F1+F2 | | 0.6153846 | 0.7692307 |
| (F1+F2)//F3 | | 0.1784706 | 0.2983932 |
| ((F1+F2)//F3)+F4 | B | 0.6738834 | 0.1899305 |
| A//B | | 0.2427930 | 0.1245336 |
| A//B+L3 | Total | 0.6427930 | 0.1699016 |

Table 7.8: Case 2: Detailed RBD calculation of failure rate repair time of migrogrid when the wind farm is not available

| CASE 2: WITHOUT WIND | | | |
|---|---|---|---|
| Load A | | $\lambda$ | r |
| F5//F7 | | 0.5456570 | 1.2000000 |
| C2+F9 | | 1.4954128 | 0.6744907 |
| (F5//F7)+C2+F9 | | 2.0410698 | 0.7233607 |
| ((F5//F7)+C2+F9) // ((F6//F8) +C1+F10) | A | 1.1666728 | 0.3616803 |
| A+F4 | | 1.6620856 | 0.5364063 |
| (A+F4)+F2 | | 2.1574985 | 0.6887369 |
| ((A+F4)+F2)//F1 | B | 1.0727596 | 0.5123126 |
| B+L1 | Total | 1.4727596 | 0.4406280 |
| | | | |
| | | | |
| Load B | | $\lambda$ | r |
| F5//F7 | | 0.5456570 | 1.2000000 |
| C2+F9 | | 1.4954128 | 0.6744907 |
| (F5//F7)+C2+F9 | | 2.0410698 | 0.7233607 |
| ((F5//F7)+C2+F9) // ((F6//F8) +C1+F10) | A | 1.1666728 | 0.3616803 |
| A+F4 | | 1.6620856 | 0.5364063 |
| F1+F2 | | 0.6153846 | 0.7692307 |
| (A+F4)//(F1+F2) | B | 0.6601838 | 0.3160298 |
| B+L2 | Total | 1.0601838 | 0.3278003 |
| | | | |
| Load C | | $\lambda$ | r |
| F5//F7 | | 0.5456570 | 1.2000000 |
| C2+F9 | | 1.4954128 | 0.6744907 |
| (F5//F7)+C2+F9 | | 2.0410698 | 0.7233607 |
| ((F5//F7)+C2+F9) // ((F6//F8) +C1+F10) | A | 1.1666728 | 0.3616803 |
| F1+F2 | | 0.6153846 | 0.7692307 |
| F1+F2+F4 | | 1.1107974 | 0.5911445 |
| (F1+F2+F4)//A | B | 0.5378201 | 0.2243910 |
| B+L3 | Total | 0.9378201 | 0.2808650 |

Table 7.9: Case 1 : Detailed RBD calculation of failure rate repair time of migrogrid when PV is not available

| CASE 3: WITHOUT PV | | | |
|---|---|---|---|
| Load A | | $\lambda$ | r |
| C2+F9 | | 1.4954128 | 0.6744907 |
| C2+F9+F7 | | 1.8454128 | 0.6662162 |
| (C2+F9+F7) // (C1+F10+F8) | A | 1.0299883 | 0.3331081 |
| A+F4 | | 1.5254011 | 0.5016593 |
| (A+F4)//F3 | | 0.2877673 | 0.2472391 |
| ((A+F4)//F3) +F2 | B | 0.5954596 | 0.2222262 |
| B//F1 | | 0.3441060 | 0.2000032 |
| B//F1+L1 | Total | 0.7441060 | 0.2219728 |
| | | | |
| Load B | | $\lambda$ | r |
| C2+F9 | | 1.4954128 | 0.6744907 |
| C2+F9+F7 | | 1.8454128 | 0.6662162 |
| (C2+F9+F7) // (C1+F10+F8) | A | 1.0299883 | 0.3331081 |
| A+F4 | | 1.5254011 | 0.5016593 |
| F1+F2 | | 0.6153846 | 0.7692307 |
| (F1+F2)//F3 | B | 0.1784706 | 0.2983932 |
| (A+F4)//B | | 0.1711987 | 0.1871024 |
| ((A+F4)//B) +L2 | Total | 0.5711987 | 0.1423185 |
| | | | |
| Load C | | $\lambda$ | r |
| C2+F9 | | 1.4954128 | 0.6744907 |
| C2+F9+F7 | | 1.8454128 | 0.6662162 |
| (C2+F9+F7) // (C1+F10+F8) | A | 1.0299883 | 0.3331081 |
| F1+F2 | | 0.6153846 | 0.7692307 |
| (F1+F2)//F3 | | 0.1784706 | 0.2983932 |
| ((F1+F2)//F3) +F4 | B | 0.6738834 | 0.1899305 |
| A//B | | 0.2142959 | 0.1209612 |
| A//B+L3 | Total | 0.6142959 | 0.1564180 |

location of the renewable energy sources on the microgrid as much as their numbers. Also, the load distribution of a microgrid has an impact on the reliability indices. In summary, each microgrid must be studied carefully to optimize its reliability indices and to identified the best location of installing the renewable energy source.

# CHAPTER 8

# CONCLUSION

This thesis has presented a technique to optimally size a battery energy storage for a grid-connected microgrid subjected to practical reliability constraints. The unit commitment problem has been solved using the mixed-integer linear programming method. Moreover, load and wind uncertainties have been considered, and stochastic optimization has been solved using two approaches. The purpose of integrating an optimally sized storage system with the microgrid is to enhance the reliability of the microgrid. Also, a technique to optimally allocate the storage system has been presented. Also, optimal dispatch and power flow have been calculated for a microgrid connected to a storage system. Finally, reliability indices of a microgrid have been calculated to illustrate the impact of the ESS on the reliability indices. Integrating the ESS with the microgrid has decreased the net cost although this cost in the case of integrating the ESS includes the investment cost of building and establishing the ESS, which shows the economical feasibility of the system.

## 8.1 Future Work

This work can be extended and applied to a system consisting of multiple microgrids for generalization. Also, more renewable energy sources can be integrated.

# REFERENCES


[1] S. Rehman, T. Halawani, and T. Husain, "Weibull parameters for wind speed distribution in saudi arabia," *Solar Energy*, vol. 53, no. 6, pp. 473–479, 1994.

[2] "Ontario electricity policy," Oct 2017. [Online]. Available: https://en.wikipedia.org/wiki/Ontario_electricity_policy

[3] E. DOE, "Electricity storage handbook in collaboration with nreca," *EPRI, Albuquerque*, 2013.

[4] [Online]. Available: http://www.wind-power-program.com/popups/powercurve.htm

[5] C. M. Rangel, D. Mascarella, and G. Joos, "Real-time implementation & evaluation of grid-connected microgrid energy management systems," in *Electrical Power and Energy Conference (EPEC), 2016 IEEE*. IEEE, 2016, pp. 1–6.

[6] H. Marzooghi, G. Verbic, and D. J. Hill, "Aggregated effect of demand response on performance of future grid scenarios," in *PowerTech Conference*. IEEE. The Journal's web site is located at http://ieeexplore. ieee. org/xpl/conhome. jsp? punumber= 1000589, 2015.

[7] S. Bahramirad and H. Daneshi, "Optimal sizing of smart grid storage management system in a microgrid," 2012.

[8] S. Conti, R. Nicolosi, S. Rizzo, and H. Zeineldin, "Optimal dispatching of distributed generators and storage systems for mv islanded microgrids," *IEEE Transactions on Power Delivery*, vol. 27, no. 3, pp. 1243–1251, 2012.

[9] S. Bahramirad, W. Reder, and A. Khodaei, "Reliability-constrained optimal sizing of energy storage system in a microgrid," *perspectives*, vol. 1, p. 3, 2012.

[10] D. W. Gao, *Energy storage for sustainable microgrid*. Academic Press, 2015.

[11] S. Bahramirad and E. Camm, "Practical modeling of smart grid sms™ storage management system in a microgrid," in *PES T D 2012*, May 2012, pp. 1–7.

[12] T. Adefarati and R. Bansal, "Integration of renewable distributed generators into the distribution system: a review," *IET Renewable Power Generation*, vol. 10, no. 7, pp. 873–884, 2016.

[13] S. Chen, H. B. Gooi, and M. Wang, "Sizing of energy storage for microgrids," *IEEE Transactions on Smart Grid*, vol. 3, no. 1, pp. 142–151, 2012.

[14] S. Singh, M. Singh, and S. C. Kaushik, "Optimal power scheduling of renewable energy systems in microgrids using distributed energy storage system," *IET Renewable Power Generation*, vol. 10, no. 9, pp. 1328–1339, 2016.

[15] C. Chen, S. Duan, T. Cai, B. Liu, and G. Hu, "Smart energy management system for optimal microgrid economic operation," *IET renewable power generation*, vol. 5, no. 3, pp. 258–267, 2011.

[16] P. P. Gupta, P. Jain, S. Sharma, and R. Bhakar, "Reliability-security constrained unit commitment based on benders decomposition and mixed integer non-linear programming," in *Computer, Communications and Electronics (Comptelix), 2017 International Conference on*. IEEE, 2017, pp. 328–333.

[17] T. A. Nguyen, M. L. Crow, and A. C. Elmore, "Optimal sizing of a vanadium redox battery system for microgrid systems," *IEEE transactions on sustainable energy*, vol. 6, no. 3, pp. 729–737, 2015.

[18] T. Kerdphol, Y. Qudaih, and Y. Mitani, "Battery energy storage system size optimization in microgrid using particle swarm optimization," in *Innovative Smart Grid Technologies Conference Europe (ISGT-Europe), 2014 IEEE PES*. IEEE, 2014, pp. 1–6.

[19] Y. Huang, P. M. Pardalos, and Q. P. Zheng, *Electrical power unit commitment: deterministic and two-stage stochastic programming models and algorithms*. Springer, 2017.

[20] P. Xiong, P. Jirutitijaroen, and C. Singh, "A distributionally robust optimization model for unit commitment considering uncertain wind power generation," *IEEE Transactions on Power Systems*, vol. 32, no. 1, pp. 39–49, 2017.

[21] N. T. Mbungu, R. Naidoo, R. C. Bansal, and M. Bipath, "Optimisation of grid connected hybrid photovoltaic–wind–battery system using model predictive control design," *IET Renewable Power Generation*, vol. 11, no. 14, pp. 1760–1768, 2017.

[22] N. Nikmehr and S. Najafi-Ravadanegh, "Optimal operation of distributed generations in micro-grids under uncertainties in load and renewable power generation using heuristic algorithm," *IET Renewable Power Generation*, vol. 9, no. 8, pp. 982–990, 2015.

[23] I. Alsaidan, A. Khodaei, and W. Gao, "A comprehensive battery energy storage optimal sizing model for microgrid applications," *IEEE Transactions on Power Systems*, vol. 33, no. 4, pp. 3968–3980, 2018.

[24] A. Soroudi, *Power System Optimization Modeling in GAMS*. Springer, 2017.

[25] A. M. Gee, F. Robinson, and W. Yuan, "A superconducting magnetic energy storage-emulator/battery supported dynamic voltage restorer," *IEEE Transactions on Energy Conversion*, vol. 32, no. 1, pp. 55–64, 2017.

[26] C. Krupke, J. Wang, J. Clarke, and X. Luo, "Modeling and experimental study of a wind turbine system in hybrid connection with compressed air energy storage," *IEEE Transactions on Energy Conversion*, vol. 32, no. 1, pp. 137–145, 2017.

[27] X. Chang, Y. Li, X. Li, and X. Chen, "An active damping method based on a supercapacitor energy storage system to overcome the destabilizing effect of

instantaneous constant power loads in dc microgrids," *IEEE Transactions on Energy Conversion*, vol. 32, no. 1, pp. 36–47, 2017.

[28] J. M. Lujano-Rojas, R. Dufo-López, J. L. Bernal-Agustín, and J. P. Catalão, "Optimizing daily operation of battery energy storage systems under real-time pricing schemes." *IEEE Trans. Smart Grid*, vol. 8, no. 1, pp. 316–330, 2017.

[29] M. I. Daoud, A. M. Massoud, A. S. Abdel-Khalik, A. Elserougi, and S. Ahmed, "A flywheel energy storage system for fault ride through support of grid-connected vsc hvdc-based offshore wind farms," *IEEE Transactions on Power Systems*, vol. 31, no. 3, pp. 1671–1680, 2016.

[30] C. Park, R. Sedundo, V. Knazkins, and P. Korbakorba, "Feasibility analysis of the power-to-gas concept in the future swiss power system," 2016.

[31] S. Pulendran and J. E. Tate, "Energy storage system control for prevention of transient under-frequency load shedding," *IEEE Transactions on Smart Grid*, vol. 8, no. 2, pp. 927–936, 2017.

[32] C. L. Borges and D. M. Falcao, "Optimal distributed generation allocation for reliability, losses, and voltage improvement," *International Journal of Electrical Power & Energy Systems*, vol. 28, no. 6, pp. 413–420, 2006.

[33] P. Maghouli, A. Soroudi, and A. Keane, "Robust computational framework for mid-term techno-economical assessment of energy storage," *IET Generation, Transmission & Distribution*, vol. 10, no. 3, pp. 822–831, 2016.

[34] S. Sun, B. Liang, M. Dong, and J. A. Taylor, "Phase balancing using energy storage in power grids under uncertainty," *IEEE Transactions on Power Systems*, vol. 31, no. 5, pp. 3891–3903, 2016.

[35] L. S. Vargas, G. Bustos-Turu, and F. Larraín, "Wind power curtailment and energy storage in transmission congestion management considering power plants ramp rates," *IEEE Trans. Power Syst*, vol. 30, no. 5, pp. 2498–2506, 2015.

[36] A. Soroudi, P. Siano, and A. Keane, "Optimal dr and ess scheduling for distribution losses payments minimization under electricity price uncertainty," *IEEE Transactions on smart grid*, vol. 7, no. 1, pp. 261–272, 2016.

[37] Y. Chen, Y. Zheng, F. Luo, J. Wen, and Z. Xu, "Reliability evaluation of distribution systems with mobile energy storage systems," *IET Renewable Power Generation*, vol. 10, no. 10, pp. 1562–1569, 2016.

[38] F. Bhuiyan and A. Yazdani, "Reliability assessment of a wind-power system with integrated energy storage," *IET Renewable Power Generation*, vol. 4, no. 3, pp. 211–220, 2010.

[39] J. L. Higle, "Stochastic programming: optimization when uncertainty matters," in *Emerging Theory, Methods, and Applications*. Informs, 2005, pp. 30–53.

[40] S. Bandyopadhyay, "Design and optimization of isolated energy systems through pinch analysis," *Asia-Pacific Journal of Chemical Engineering*, vol. 6, no. 3, pp. 518–526, 2011.

[41] C. A. Correa-Florez, A. Gerossier, A. Michiorri, R. Girard, and G. Kariniotakis, "Residential electrical and thermal storage optimisation in a market environment," *CIRED-Open Access Proceedings Journal*, vol. 2017, no. 1, pp. 1967–1970, 2017.

[42] E. Nasrolahpour, J. Kazempour, H. Zareipour, and W. D. Rosehart, "A bilevel model for participation of a storage system in energy and reserve markets," *IEEE Transactions on Sustainable Energy*, vol. 9, no. 2, pp. 582–598, 2018.

[43] A. Masoumzadeh, E. Nekouei, T. Alpcan, and D. Chattopadhyay, "Impact of optimal storage allocation on price volatility in energy-only electricity markets," *IEEE Transactions on Power Systems*, vol. 33, no. 2, pp. 1903–1914, 2018.

[44] A. Saez-de Ibarra, A. Milo, H. Gaztañaga, V. Debusschere, and S. Bacha, "Co-optimization of storage system sizing and control strategy for intelligent photovoltaic power plants market integration," *IEEE Transactions on Sustainable Energy*, vol. 7, no. 4, pp. 1749–1761, 2016.

[45] Y. Niu and S. Santoso, "Sizing and coordinating fast-and slow-response energy storage systems to mitigate hourly wind power variations," *IEEE Transactions on Smart Grid*, vol. 9, no. 2, pp. 1107–1117, 2018.

[46] T. M. Masaud, O. Oyebanjo, and P. Sen, "Sizing of large-scale battery storage for off-grid wind power plant considering a flexible wind supply–demand balance," *IET Renewable Power Generation*, vol. 11, no. 13, pp. 1625–1632, 2017.

[47] L. F. Grisales, A. Grajales, O. D. Montoya, R. A. Hincapie, M. Granada, and C. A. Castro, "Optimal location, sizing and operation of energy storage in distribution systems using multi-objective approach," *IEEE Latin America Transactions*, vol. 15, no. 6, pp. 1084–1090, 2017.

[48] J. Mitra, "Reliability-based sizing of backup storage," *IEEE Transactions on Power Systems*, vol. 25, no. 2, pp. 1198–1199, 2010.

[49] D. A. Halamay, T. K. Brekken, A. Simmons, and S. McArthur, "Reserve requirement impacts of large-scale integration of wind, solar, and ocean wave power generation," *IEEE Transactions on Sustainable Energy*, vol. 2, no. 3, pp. 321–328, 2011.

[50] B. Kladnik, G. Artac, T. Stokelj, R. Golob, and A. F. Gubina, "Demand-side participation in system reserve provision in a stochastic market model with high wind penetration," in *Power System Technology (POWERCON), 2012 IEEE International Conference on*. IEEE, 2012, pp. 1–5.

[51] L. H. Macedo, J. F. Franco, R. Romero, M. A. Ortega-Vazquez, and M. J. Rider, "Increasing the hosting capacity for renewable energy in distribution networks," in *Power & Energy Society Innovative Smart Grid Technologies Conference (ISGT), 2017 IEEE*. IEEE, 2017, pp. 1–5.

[52] Z. Zhang, J. Wang, T. Ding, and X. Wang, "A two-layer model for microgrid real-time dispatch based on energy storage system charging/discharging hidden costs," *IEEE Transactions on Sustainable Energy*, vol. 8, no. 1, pp. 33–42, 2017.

[53] A. Mamen and U. Supatti, "A survey of hybrid energy storage systems applied for intermittent renewable energy systems," in *Electrical Engineering/Electronics, Computer, Telecommunications and Information Technology (ECTI-CON), 2017 14th International Conference on.* IEEE, 2017, pp. 729–732.

[54] S. Choi and S.-W. Min, "Optimal scheduling and operation of the ess for prosumer market environment in grid-connected industrial complex," *IEEE Transactions on Industry Applications*, vol. 54, no. 3, pp. 1949–1957, 2018.

[55] A. S. Awad, T. H. El-Fouly, and M. M. Salama, "Optimal ess allocation for load management application," *IEEE Transactions on Power Systems*, vol. 30, no. 1, pp. 327–336, 2015.

[56] A. Klem, K. Dehghanpour, and H. Nehrir, "Primary frequency regulation in islandec microgrids through droop-based generation and demand control," in *Intelligent System Application to Power Systems (ISAP), 2017 19th International Conference on.* IEEE, 2017, pp. 1–6.

[57] T. K. Chau, S. S. Yu, T. Fernando, and H. H.-C. Iu, "Demand-side regulation provision from industrial loads integrated with solar pv panels and energy storage system for ancillary services," *IEEE Transactions on Industrial Informatics*, 2017.

[58] Y. Wang, K. Tan, X. Y. Peng, and P. L. So, "Coordinated control of distributed energy-storage systems for voltage regulation in distribution networks," *IEEE Transactions on Power Delivery*, vol. 31, no. 3, pp. 1132–1141, 2016.

[59] M. Qin, K. W. Chan, C. Y. Chung, X. Luo, and T. Wu, "Optimal planning and operation of energy storage systems in radial networks for wind power integration with reserve support," *IET Generation, Transmission & Distribution*, vol. 10, no. 8, pp. 2019–2025, 2016.

[60] Z. Zhang, Y. Zhang, and W.-J. Lee, "Energy storage based optimal dispatch scheme for financial improvement and fluctuation mitigation on wind power generation," in *Industry Applications Society Annual Meeting, 2017 IEEE.* IEEE, 2017, pp. 1–7.

[61] S. Nag and K. Y. Lee, "Optimal scheduling and dispatch of pumped hydro—thermal—wind systems," in *Power Symposium (NAPS), 2017 North American.* IEEE, 2017, pp. 1–6.

[62] J. Rameshkumar, S. Ganesan, M. Abirami, and S. Subramanian, "Cost, emission and reserve pondered pre-dispatch of thermal power generating units coordinated with real coded grey wolf optimisation," *IET Generation, Transmission & Distribution*, vol. 10, no. 4, pp. 972–985, 2016.

[63] M. Majidi, A. Ozdemir, and O. Ceylan, "Optimal dg allocation and sizing in radial distribution networks by cuckoo search algorithm," in *Intelligent System Application to Power Systems (ISAP), 2017 19th International Conference on.* IEEE, 2017, pp. 1–6.

[64] R. Billinton and R. N. Allan, "Power-system reliability in perspective," *Electronics and Power*, vol. 30, no. 3, pp. 231–236, 1984.

[65] J. P. Fossati, A. Galarza, A. Martín-Villate, and L. Fontán, "A method for optimal sizing energy storage systems for microgrids," *Renewable Energy*, vol. 77, pp. 539–549, 2015.

[66] R. Allan, "Power system reliability assessment—a conceptual and historical review," *Reliability Engineering & System Safety*, vol. 46, no. 1, pp. 3–13, 1994.

[67] J. Zou, C. Peng, J. Shi, X. Xin, and Z. Zhang, "State-of-charge optimising control approach of battery energy storage system for wind farm," *IET Renewable Power Generation*, vol. 9, no. 6, pp. 647–652, 2015.

[68] E. Castillo, A. J. Conejo, P. Pedregal, R. Garcia, and N. Alguacil, *Building and solving mathematical programming models in engineering and science*. John Wiley & Sons, 2011, vol. 62.

[69] D. Chattopadhyay, "Application of general algebraic modeling system to power system optimization," *IEEE Transactions on Power Systems*, vol. 14, no. 1, pp. 15–22, 1999.

[70] D. Simopoulos, Y. Giannakopoulos, S. Kavatza, and C. Vournas, "Effect of emission constraints on short-term unit commitment," in *Electrotechnical Conference, 2006. MELECON 2006. IEEE Mediterranean*. IEEE, 2006, pp. 973–977.

[71] R. T. Force, "The ieee reliability test system-1996," *IEEE Trans. Power Syst*, vol. 14, no. 3, pp. 1010–1020, 1999.

[72] [Online]. Available: https://www.gams.com/

[73] [Online]. Available: https://neos-server.org/neos/

[74] C. Grigg, P. Wong, P. Albrecht, R. Allan, M. Bhavaraju, R. Billinton, Q. Chen, C. Fong, S. Haddad, S. Kuruganty *et al.*, "The ieee reliability test system-1996. a report prepared by the reliability test system task force of the application of probability methods subcommittee," *IEEE Transactions on power systems*, vol. 14, no. 3, pp. 1010–1020, 1999.

[75] P. M. Subcommittee, "Ieee reliability test system," *IEEE Transactions on power apparatus and systems*, no. 6, pp. 2047–2054, 1979.

[76] R. Allan and R. Billinton, "Power system reliability and its assessment. iii. distribution systems and economic considerations," *Power Engineering Journal*, vol. 7, no. 4, pp. 185–192, 1993.

[77] R. Billinton and S. Jonnavithula, "A test system for teaching overall power system reliability assessment," *IEEE transactions on Power Systems*, vol. 11, no. 4, pp. 1670–1676, 1996.

# VITAE

- Name: Mohammed Atta Ahmed Abdulgalil
- Nationality: Sudanese
- Date of Birth: July 5, 1993
- Email: *mohd.atta.galil@gmail.com*
- Permenant Address: Khartoum, Sudan

- Master of Science in Electrical Engineering, College of Engineering, King Fahd University of Petroleum & Minerals, Dhahran, Saudi Arabia, May 2018.
- Bachelor of Science in Electrical Engineering, College of Engineering, King Fahd University of Petroleum & Minerals, Dhahran, Saudi Arabia, May 2016.